

# For Reference

---

NOT TO BE TAKEN FROM THIS ROOM

## For Reference

---

NOT TO BE TAKEN FROM THIS ROOM

---

Ex LIBRIS  
UNIVERSITATIS  
ALBERTAENSIS





Digitized by the Internet Archive  
in 2018 with funding from  
University of Alberta Libraries

<https://archive.org/details/Pandit1963>









3 (F)  
72

THE UNIVERSITY OF ALBERTA

TORSION IN CONCRETE SECTIONS

by

GANPAT SHANKAR PANDIT

A THESIS

SUBMITTED TO THE FACULTY OF GRADUATE STUDIES  
IN PARTIAL FULFILMENT OF THE REQUIREMENTS FOR THE DEGREE  
OF MASTER OF SCIENCE

DEPARTMENT OF CIVIL ENGINEERING

EDMONTON, ALBERTA

SEPTEMBER, 1963



## ABSTRACT

The object of the investigation was to study the behaviour of the plain and reinforced sections in pure torsion. The study was especially directed to the controversial issues and some of the variables not examined previously.

A simple set up for testing the specimens in pure torsion was developed and fabricated. The twistmeters for measuring the angle of twist were also developed and fabricated.

Thirty specimens, having the following as variables, were tested in pure torsion:

- (i) Percentage of the longitudinal steel.
- (ii) Percentage of the transverse steel.
- (iii) Position and size of the longitudinal steel.
- (iv) Bar size and spacing of the ties.
- (v) Two different overlaps for the ties, and
- (vi) The steel strength.

All specimens were 4" x 4" in cross-section and 4' 6" long. Three different grades of steel were used. The concrete strength, as determined by control specimens, varied from 3335 to 4190 psi.

The tests indicated that the behaviour of the specimen up to the cracking torque was not affected by the reinforcement. The torque-rotation curve was almost linear and practically the same for all specimens in this region. The shape of the curve beyond the cracking torque depended primarily on the reinforcement.

Though the concrete behaved practically as an elastic material at low torques, there was significant plastic deformation at and beyond



the cracking torque. The elastic theory under-estimated and the plastic theory over-estimated the strength of the concrete section.

While the cracking torque was unaffected, the ultimate torque was increased substantially by an adequate combination of longitudinal and transverse steel. When suitably combined, either reinforcement could be stressed to the yield point. The ultimate strength increased in proportion to the percentage of transverse steel but for higher percentages, the rate of increase of strength decreased. There appeared to be a limit to which the ultimate strength could be increased by providing reinforcement.

For same percentages, smaller size of bar or closer spacing gave higher strength. Longitudinal bars remote from the axis of twist were more effective. The ties of higher strength steel gave higher ultimate torque. An adequate overlap in the ties was necessary for full effectiveness.





## ACKNOWLEDGMENTS

The project was carried out as a part of the investigation of concrete in torsion. The investigation was made possible through the financial assistance provided by the National Research Council of Canada. The Canadian Commonwealth Scholarship and Fellowship Committee provided scholarship aid for carrying out the graduate program at the University of Alberta.

The investigation was guided by Dr. J. Warwaruk, Associate Professor in the Department of Civil Engineering. His assistance in planning the tests and his helpful comments in preparing this report are gratefully acknowledged.

The author also wishes to express his sincere appreciation to the following:

Mr. R. McDonald and the staff of the machine shop for fabrication of the torsion testing rig.

Mr. A.L. Ekman for fabrication of the twistmeters.

Messrs. R. Sandhu, H. Panse and B. Aves for the assistance in casting the specimens and testing them.

Miss H. Doerksen for typing the final manuscript.

Mr. G.T. Wormsbecker for the assistance in preparation of the drawings.

The author is also indebted to his wife for her assistance and moral support during the entire program.



## TABLE OF CONTENTS

	PAGE
Title page	i
Approval sheet	ii
Abstract	iii
Acknowledgments	v
Table of Contents	vi
List of Tables	ix
List of Figures	xi
 CHAPTER I     INTRODUCTION	
1-1     Introductory Remarks	1
1-2     Object	3
1-3     Scope	3
1-4     Notations	4
 CHAPTER II    REVIEW OF PREVIOUS WORK	
2-1     Introduction	7
2-2     Tests on Plain Concrete	8
2-3     Tests on Reinforced Concrete	9
2-4     Tests on Prestressed Concrete	11
2-5     Combined Stresses	12
 CHAPTER III   DESCRIPTION OF TESTING EQUIPMENT	
3-1     Torsion Testing Rig	14
3-2     Twistmeter	17

CHAPTER IV

The first part of the chapter is devoted to a discussion of the various methods of determining the rate of reaction. The second part is devoted to a discussion of the various factors which influence the rate of reaction. The third part is devoted to a discussion of the various factors which influence the equilibrium constant. The fourth part is devoted to a discussion of the various factors which influence the activation energy of a reaction.

THE RATE OF REACTION

The rate of reaction is defined as the change in concentration of a reactant or product per unit time. It can be determined by measuring the change in concentration of a reactant or product over a known period of time. The rate of reaction can be affected by various factors, such as temperature, concentration, and the presence of a catalyst.

EQUILIBRIUM CONSTANT

The equilibrium constant is a measure of the extent to which a reaction proceeds. It is defined as the ratio of the concentrations of the products to the concentrations of the reactants, each raised to the power of its stoichiometric coefficient. The equilibrium constant is a function of temperature and is independent of the initial concentrations of the reactants and products.

ACTIVATION ENERGY

The activation energy is the minimum energy required for a reaction to occur. It is a measure of the energy barrier that must be overcome for a reaction to proceed. The activation energy can be determined by measuring the rate of reaction at different temperatures.

## TABLE OF CONTENTS (continued)

	PAGE
CHAPTER IV DESCRIPTION OF MATERIALS, FABRICATION AND TEST SPECIMENS	
4-1 Materials	27
4-2 Electrical Strain Gages	30
4-3 Moulds	33
4-4 Casting and Curing	35
4-5 Control Specimens	35
4-6 Description of Test Specimens	39
CHAPTER V PRESENTATION OF TEST RESULTS	
5-1 The Testing Procedure	45
5-2 Test Results	47
5-3 General Behaviour	83
CHAPTER VI DISCUSSION OF TEST RESULTS	
6-1 Tensile Strength of Concrete	88
6-2 Cracking Torque	90
6-3 Torsional Strength	95
6-4 Torsional Stiffness	102
6-5 Effect of Longitudinal Reinforcement Only	103
6-6 Effect of Varying Lateral Steel	104
6-7 Effect of Position and Size of Longitudinal Bars	104
6-8 Effect of Bar Size of Transverse Steel	105
6-9 Effectiveness of Ties	105
6-10 Effect of Steel Strength	106
6-11 Steel Stresses	106

THE HISTORY OF THE

REIGN OF THE

EMPEROR

OF THE

WESTERN

EMPIRE

FROM THE

DEATH OF

THE

EMPEROR

OF THE

EASTERN

EMPIRE

TO THE

PRESENT

TIME

OF

THE

REIGN

OF

THE

## TABLE OF CONTENTS (continued)

	PAGE
CHAPTER VII SUMMARY AND CONCLUSIONS	
7-1 Summary	108
7-2 Conclusions	108
BIBLIOGRAPHY	
APPENDIX A ELASTIC THEORY	
A-1 Circular Section	A 1
A-2 Non-circular Section	A 2
A-3 Membrane Analogy	A 13
A-4 Rectangular Section	A 15
APPENDIX B PLASTIC THEORY	
B-1 Circular Section	B 1
B-2 Non-circular Section	B 2
B-3 Sand Heap Analogy	B 3

# MEMORANDUM FOR THE RECORD

DATE:

SUBJECT: [Illegible]

TO:

[Illegible]

FROM:

[Illegible]

[Illegible]

[Illegible]

[Illegible]

[Illegible]

[Illegible]

[Illegible]

[Illegible]

[Illegible]

[Illegible]

[Illegible]

[Illegible]

[Illegible]



# LIST OF TABLES

TABLE		PAGE
IV-1	Physical Properties of Sand	27
IV-2	Sieve Analysis of Sand	28
IV-3	Physical Properties of Coarse Aggregate	28
IV-4	Sieve Analysis of Coarse Aggregate	29
IV-5	Strength Properties of Reinforcement	30
IV-6	Test Results of Control Specimens (28 Day Tests)	38
IV-7	Details of Specimens	43
V-1	Co-relation Between Staff Reading and Lever Arm	47
V-2	Specimen A.1	48
V-3	" A.2	49
V-4	" A.3	49
V-5	" B.1	51
V-6	" B.2	51
V-7	" C.1	53
V-8	" C.2	53
V-9	" D.1	55
V-10	" D.2	55
V-11	" E.1	57
V-12	" E.2	57
V-13	" F.1	59
V-14	" F.2	59
V-15	" G.1	61
V-16	" G.2	61

Table of Contents

1	Introduction	1
2	Chapter 1: The History of the Book	2
3	Chapter 2: The Book in the Middle Ages	3
4	Chapter 3: The Book in the Renaissance	4
5	Chapter 4: The Book in the 17th and 18th Centuries	5
6	Chapter 5: The Book in the 19th Century	6
7	Chapter 6: The Book in the 20th Century	7
8	Chapter 7: The Book in the 21st Century	8
9	Chapter 8: The Book in the Future	9
10	Conclusion	10
11	Bibliography	11
12	Index	12
13	Appendix A	13
14	Appendix B	14
15	Appendix C	15
16	Appendix D	16
17	Appendix E	17
18	Appendix F	18
19	Appendix G	19
20	Appendix H	20
21	Appendix I	21
22	Appendix J	22
23	Appendix K	23
24	Appendix L	24
25	Appendix M	25
26	Appendix N	26
27	Appendix O	27
28	Appendix P	28
29	Appendix Q	29
30	Appendix R	30
31	Appendix S	31
32	Appendix T	32
33	Appendix U	33
34	Appendix V	34
35	Appendix W	35
36	Appendix X	36
37	Appendix Y	37
38	Appendix Z	38
39	Appendix AA	39
40	Appendix AB	40
41	Appendix AC	41
42	Appendix AD	42
43	Appendix AE	43
44	Appendix AF	44
45	Appendix AG	45
46	Appendix AH	46
47	Appendix AI	47
48	Appendix AJ	48
49	Appendix AK	49
50	Appendix AL	50
51	Appendix AM	51
52	Appendix AN	52
53	Appendix AO	53
54	Appendix AP	54
55	Appendix AQ	55
56	Appendix AR	56
57	Appendix AS	57
58	Appendix AT	58
59	Appendix AU	59
60	Appendix AV	60
61	Appendix AW	61
62	Appendix AX	62
63	Appendix AY	63
64	Appendix AZ	64
65	Appendix BA	65
66	Appendix BB	66
67	Appendix BC	67
68	Appendix BD	68
69	Appendix BE	69
70	Appendix BF	70
71	Appendix BG	71
72	Appendix BH	72
73	Appendix BI	73
74	Appendix BJ	74
75	Appendix BK	75
76	Appendix BL	76
77	Appendix BM	77
78	Appendix BN	78
79	Appendix BO	79
80	Appendix BP	80
81	Appendix BQ	81
82	Appendix BR	82
83	Appendix BS	83
84	Appendix BT	84
85	Appendix BU	85
86	Appendix BV	86
87	Appendix BW	87
88	Appendix BX	88
89	Appendix BY	89
90	Appendix BZ	90
91	Appendix CA	91
92	Appendix CB	92
93	Appendix CC	93
94	Appendix CD	94
95	Appendix CE	95
96	Appendix CF	96
97	Appendix CG	97
98	Appendix CH	98
99	Appendix CI	99
100	Appendix CJ	100
101	Appendix CK	101
102	Appendix CL	102
103	Appendix CM	103
104	Appendix CN	104
105	Appendix CO	105
106	Appendix CP	106
107	Appendix CQ	107
108	Appendix CR	108
109	Appendix CS	109
110	Appendix CT	110
111	Appendix CU	111
112	Appendix CV	112
113	Appendix CW	113
114	Appendix CX	114
115	Appendix CY	115
116	Appendix CZ	116
117	Appendix DA	117
118	Appendix DB	118
119	Appendix DC	119
120	Appendix DD	120
121	Appendix DE	121
122	Appendix DF	122
123	Appendix DG	123
124	Appendix DH	124
125	Appendix DI	125
126	Appendix DJ	126
127	Appendix DK	127
128	Appendix DL	128
129	Appendix DM	129
130	Appendix DN	130
131	Appendix DO	131
132	Appendix DP	132
133	Appendix DQ	133
134	Appendix DR	134
135	Appendix DS	135
136	Appendix DT	136
137	Appendix DU	137
138	Appendix DV	138
139	Appendix DW	139
140	Appendix DX	140
141	Appendix DY	141
142	Appendix DZ	142
143	Appendix EA	143
144	Appendix EB	144
145	Appendix EC	145
146	Appendix ED	146
147	Appendix EE	147
148	Appendix EF	148
149	Appendix EG	149
150	Appendix EH	150
151	Appendix EI	151
152	Appendix EJ	152
153	Appendix EK	153
154	Appendix EL	154
155	Appendix EM	155
156	Appendix EN	156
157	Appendix EO	157
158	Appendix EP	158
159	Appendix EQ	159
160	Appendix ER	160
161	Appendix ES	161
162	Appendix ET	162
163	Appendix EU	163
164	Appendix EV	164
165	Appendix EW	165
166	Appendix EX	166
167	Appendix EY	167
168	Appendix EZ	168
169	Appendix FA	169
170	Appendix FB	170
171	Appendix FC	171
172	Appendix FD	172
173	Appendix FE	173
174	Appendix FF	174
175	Appendix FG	175
176	Appendix FH	176
177	Appendix FI	177
178	Appendix FJ	178
179	Appendix FK	179
180	Appendix FL	180
181	Appendix FM	181
182	Appendix FN	182
183	Appendix FO	183
184	Appendix FP	184
185	Appendix FQ	185
186	Appendix FR	186
187	Appendix FS	187
188	Appendix FT	188
189	Appendix FU	189
190	Appendix FV	190
191	Appendix FW	191
192	Appendix FX	192
193	Appendix FY	193
194	Appendix FZ	194
195	Appendix GA	195
196	Appendix GB	196
197	Appendix GC	197
198	Appendix GD	198
199	Appendix GE	199
200	Appendix GF	200
201	Appendix GG	201
202	Appendix GH	202
203	Appendix GI	203
204	Appendix GJ	204
205	Appendix GK	205
206	Appendix GL	206
207	Appendix GM	207
208	Appendix GN	208
209	Appendix GO	209
210	Appendix GP	210
211	Appendix GQ	211
212	Appendix GR	212
213	Appendix GS	213
214	Appendix GT	214
215	Appendix GU	215
216	Appendix GV	216
217	Appendix GW	217
218	Appendix GX	218
219	Appendix GY	219
220	Appendix GZ	220
221	Appendix HA	221
222	Appendix HB	222
223	Appendix HC	223
224	Appendix HD	224
225	Appendix HE	225
226	Appendix HF	226
227	Appendix HG	227
228	Appendix HH	228
229	Appendix HI	229
230	Appendix HJ	230
231	Appendix HK	231
232	Appendix HL	232
233	Appendix HM	233
234	Appendix HN	234
235	Appendix HO	235
236	Appendix HP	236
237	Appendix HQ	237
238	Appendix HR	238
239	Appendix HS	239
240	Appendix HT	240
241	Appendix HU	241
242	Appendix HV	242
243	Appendix HW	243
244	Appendix HX	244
245	Appendix HY	245
246	Appendix HZ	246
247	Appendix IA	247
248	Appendix IB	248
249	Appendix IC	249
250	Appendix ID	250
251	Appendix IE	251
252	Appendix IF	252
253	Appendix IG	253
254	Appendix IH	254
255	Appendix II	255
256	Appendix IJ	256
257	Appendix IK	257
258	Appendix IL	258
259	Appendix IM	259
260	Appendix IN	260
261	Appendix IO	261
262	Appendix IP	262
263	Appendix IQ	263
264	Appendix IR	264
265	Appendix IS	265
266	Appendix IT	266
267	Appendix IU	267
268	Appendix IV	268
269	Appendix IW	269
270	Appendix IX	270
271	Appendix IY	271
272	Appendix IZ	272
273	Appendix JA	273
274	Appendix JB	274
275	Appendix JC	275
276	Appendix JD	276
277	Appendix JE	277
278	Appendix JF	278
279	Appendix JG	279
280	Appendix JH	280
281	Appendix JI	281
282	Appendix JJ	282
283	Appendix JK	283
284	Appendix JL	284
285	Appendix JM	285
286	Appendix JN	286
287	Appendix JO	287
288	Appendix JP	288
289	Appendix JQ	289
290	Appendix JR	290
291	Appendix JS	291
292	Appendix JT	292
293	Appendix JU	293
294	Appendix JV	294
295	Appendix JW	295
296	Appendix JX	296
297	Appendix JY	297
298	Appendix JZ	298
299	Appendix KA	299
300	Appendix KB	300
301	Appendix KC	301
302	Appendix KD	302
303	Appendix KE	303
304	Appendix KF	304
305	Appendix KG	305
306	Appendix KH	306
307	Appendix KI	307
308	Appendix KJ	308
309	Appendix KK	309
310	Appendix KL	310
311	Appendix KM	311
312	Appendix KN	312
313	Appendix KO	313
314	Appendix KP	314
315	Appendix KQ	315
316	Appendix KR	316
317	Appendix KS	317
318	Appendix KT	318
319	Appendix KU	319
320	Appendix KV	320
321	Appendix KW	321
322	Appendix KX	322
323	Appendix KY	323
324	Appendix KZ	324
325	Appendix LA	325
326	Appendix LB	326
327	Appendix LC	327
328	Appendix LD	328
329	Appendix LE	329
330	Appendix LF	330
331	Appendix LG	331
332	Appendix LH	332
333	Appendix LI	333
334	Appendix LJ	334
335	Appendix LK	335
336	Appendix LL	336
337	Appendix LM	337
338	Appendix LN	338
339	Appendix LO	339
340	Appendix LP	340
341	Appendix LQ	341
342	Appendix LR	342
343	Appendix LS	343
344	Appendix LT	344
345	Appendix LU	345
346	Appendix LV	346
347	Appendix LW	347
348	Appendix LX	348
349	Appendix LY	349
350	Appendix LZ	350
351	Appendix MA	351
352	Appendix MB	352
353	Appendix MC	353
354	Appendix MD	354
355	Appendix ME	355
356	Appendix MF	356
357	Appendix MG	357
358	Appendix MH	358
359	Appendix MI	359
360	Appendix MJ	360
361	Appendix MK	361
362	Appendix ML	362
363	Appendix MM	363
364	Appendix MN	364
365	Appendix MO	365
366	Appendix MP	366
367	Appendix MQ	367
368	Appendix MR	368
369	Appendix MS	369
370	Appendix MT	370
371	Appendix MU	371
372	Appendix MV	372
373	Appendix MW	373
374	Appendix MX	374
375	Appendix MY	375
376	Appendix MZ	376
377	Appendix NA	377
378	Appendix NB	378
379	Appendix NC	379
380	Appendix ND	380
381	Appendix NE	381
382	Appendix NF	382
383	Appendix NG	383
384	Appendix NH	384
385	Appendix NI	385
386	Appendix NJ	386
387	Appendix NK	387
388	Appendix NL	388
389	Appendix NM	389
390	Appendix NN	390
391	Appendix NO	391
392	Appendix NP	392
393	Appendix NQ	393
394	Appendix NR	394
395	Appendix NS	395
396	Appendix NT	396
397	Appendix NU	397
398	Appendix NV	398
399	Appendix NW	399
400	Appendix NX	400
401	Appendix NY	401
402	Appendix NZ	402
403	Appendix OA	403
404	Appendix OB	404
405	Appendix OC	405
406	Appendix OD	406
407	Appendix OE	407
408	Appendix OF	408
409	Appendix OG	409
410	Appendix OH	410
411	Appendix OI	411
412	Appendix OJ	412
413	Appendix OK	413
414	Appendix OL	414
415	Appendix OM	415
416	Appendix ON	416
417	Appendix OO	417
418	Appendix OP	418
419	Appendix OQ	419
420	Appendix OR	420
421	Appendix OS	421
422	Appendix OT	422
423	Appendix OU	423
424	Appendix OV	424
425	Appendix OW	425
426	Appendix OX	426
427	Appendix OY	427
428	Appendix OZ	428
429	Appendix PA	429
430	Appendix PB	430
431	Appendix PC	431
432	Appendix PD	432
433	Appendix PE	433
434	Appendix PF	434
435	Appendix PG	435
436	Appendix PH	436
437	Appendix PI	437
438	Appendix PJ	438
439	Appendix PK	439
440	Appendix PL	440
441	Appendix PM	441
442	Appendix PN	442
443	Appendix PO	443
444	Appendix PP	4

## LIST OF TABLES (continued)

TABLE		PAGE
V-17	Specimen H.1	63
V-18	" H.2	63
V-19	" I.1	65
V-20	" I.2	65
V-21	" J.1	67
V-22	" J.2	67
V-23	" K.1	69
V-24	" K.2	69
V-25	" L.1	71
V-26	" L.2	71
V-27	" M.1	73
V-28	" M.2	74
V-29	" N.1	79
V-30	" N.2	80
V-31	" N.3	81
VI-1	Overall Average Values of the Compressive Strength, The Tensile Strength and the Modulus of Rupture	91
VI-2	Weighted Average Values of Tensile Strength	92
VI-3	Rotations, Cracking Torques and Ultimate Torques of Specimens	96
VI-4	Contribution of Steel to the Ultimate Torque	99
VII-1	Principal Test Results	109
A-1	Table of Constants	A 19
B-1	Ratio of Elasto-Plastic to Plastic Resisting Torque for Various Values of Plasticity Ratio	B 2



## LIST OF FIGURES

FIGURE		PAGE
3.1(a)	Torsion Testing Rig.Elevation Showing General Arrangement	19
3.1(b)	Plan Showing General Arrangement of Torsion Testing Rig	20
3.1(c)	General View of Testing Rig from West Side	21
3.1(d)	General View of Testing Rig from East Side	21
3.2	Details of Grip and Support S	22
3.3	Loading Arrangement and Movable Cross-arm Details	23
3.4	Details of Pedestal B and Support S	24
3.5(a)	Details of Twistmeter	25
3.5(b)	Front View of Twistmeter	26
3.5(c)	Cose-up of Twistmeter	26
4.1	Tension Tests on Reinforcement	31
4.2	Tension Tests on Reinforcement	32
4.3	Tension Tests on Reinforcement	32
4.4	Details of Mould	34
4.5	Variation of Concrete Compressive Strength With Time	37
4.6	Variation of Concrete Tensile Strength With Time	37
4.7	Reinforcement Details	44
5.1	Co-relation between Staff Reading and Lever Arm	46
5.2	Torque-Rotation Curves - Specimens A	50
5.3	Torque-Rotation and Torque-Steel Stress Curves - Specimens B	52

# INDEX

1	1
2	2
3	3
4	4
5	5
6	6
7	7
8	8
9	9
10	10
11	11
12	12
13	13
14	14
15	15
16	16
17	17
18	18
19	19
20	20
21	21
22	22
23	23
24	24
25	25
26	26
27	27
28	28
29	29
30	30
31	31
32	32
33	33
34	34
35	35
36	36
37	37
38	38
39	39
40	40
41	41
42	42
43	43
44	44
45	45
46	46
47	47
48	48
49	49
50	50
51	51
52	52
53	53
54	54
55	55
56	56
57	57
58	58
59	59
60	60
61	61
62	62
63	63
64	64
65	65
66	66
67	67
68	68
69	69
70	70
71	71
72	72
73	73
74	74
75	75
76	76
77	77
78	78
79	79
80	80
81	81
82	82
83	83
84	84
85	85
86	86
87	87
88	88
89	89
90	90
91	91
92	92
93	93
94	94
95	95
96	96
97	97
98	98
99	99
100	100

## LIST OF FIGURES (continued)

FIGURE		PAGE
5.4	Torque-Rotation and Torque-Steel Stress Curves - Specimens C	54
5.5	Torque Rotation Curves - Specimens D	56
5.6	Torque Rotation Curves - Specimens E	58
5.7	Torque Rotation and Torque-Steel Stress Curves - Specimens F	60
5.8	Torque-Rotation Curves - Specimens G	62
5.9	Torque-Rotation and Torque-Steel Stress Curves - Specimens H	64
5.10	Torque-Rotation and Torque-Steel Stress Curves - Specimens I	66
5.11	Torque-Rotation and Torque-Steel Stress Curves - Specimens J	68
5.12	Torque-Rotation and Torque-Steel Stress Curves - Specimens K	70
5.13	Torque-Rotation and Torque-Steel Stress Curves - Specimens L	72
5.14	Torque-Rotation and Torque-Steel Stress Curves - Specimens M	75
5.15	Test Specimen M.1 at Effective Twisting Moment of 7030 Pound Inches	76
5.16	Test Specimen M.1 at Effective Twisting Moment of 8100 Pound Inches	76
5.17	Test Specimen M.1 Seen from East Side after Collapse	77
5.18	Test Specimen M.1 Seen from West Side after Collapse	77
5.19	Test Specimen M.2 Seen from West Side after Collapse	78
5.20	Test Specimen M.2 Seen from East Side after Collapse	78

# THE HISTORY OF THE

1	THE HISTORY OF THE	1711
2	THE HISTORY OF THE	1712
3	THE HISTORY OF THE	1713
4	THE HISTORY OF THE	1714
5	THE HISTORY OF THE	1715
6	THE HISTORY OF THE	1716
7	THE HISTORY OF THE	1717
8	THE HISTORY OF THE	1718
9	THE HISTORY OF THE	1719
10	THE HISTORY OF THE	1720
11	THE HISTORY OF THE	1721
12	THE HISTORY OF THE	1722
13	THE HISTORY OF THE	1723
14	THE HISTORY OF THE	1724
15	THE HISTORY OF THE	1725
16	THE HISTORY OF THE	1726
17	THE HISTORY OF THE	1727
18	THE HISTORY OF THE	1728
19	THE HISTORY OF THE	1729
20	THE HISTORY OF THE	1730
21	THE HISTORY OF THE	1731
22	THE HISTORY OF THE	1732
23	THE HISTORY OF THE	1733
24	THE HISTORY OF THE	1734
25	THE HISTORY OF THE	1735
26	THE HISTORY OF THE	1736
27	THE HISTORY OF THE	1737
28	THE HISTORY OF THE	1738
29	THE HISTORY OF THE	1739
30	THE HISTORY OF THE	1740
31	THE HISTORY OF THE	1741
32	THE HISTORY OF THE	1742
33	THE HISTORY OF THE	1743
34	THE HISTORY OF THE	1744
35	THE HISTORY OF THE	1745
36	THE HISTORY OF THE	1746
37	THE HISTORY OF THE	1747
38	THE HISTORY OF THE	1748
39	THE HISTORY OF THE	1749
40	THE HISTORY OF THE	1750
41	THE HISTORY OF THE	1751
42	THE HISTORY OF THE	1752
43	THE HISTORY OF THE	1753
44	THE HISTORY OF THE	1754
45	THE HISTORY OF THE	1755
46	THE HISTORY OF THE	1756
47	THE HISTORY OF THE	1757
48	THE HISTORY OF THE	1758
49	THE HISTORY OF THE	1759
50	THE HISTORY OF THE	1760
51	THE HISTORY OF THE	1761
52	THE HISTORY OF THE	1762
53	THE HISTORY OF THE	1763
54	THE HISTORY OF THE	1764
55	THE HISTORY OF THE	1765
56	THE HISTORY OF THE	1766
57	THE HISTORY OF THE	1767
58	THE HISTORY OF THE	1768
59	THE HISTORY OF THE	1769
60	THE HISTORY OF THE	1770
61	THE HISTORY OF THE	1771
62	THE HISTORY OF THE	1772
63	THE HISTORY OF THE	1773
64	THE HISTORY OF THE	1774
65	THE HISTORY OF THE	1775
66	THE HISTORY OF THE	1776
67	THE HISTORY OF THE	1777
68	THE HISTORY OF THE	1778
69	THE HISTORY OF THE	1779
70	THE HISTORY OF THE	1780
71	THE HISTORY OF THE	1781
72	THE HISTORY OF THE	1782
73	THE HISTORY OF THE	1783
74	THE HISTORY OF THE	1784
75	THE HISTORY OF THE	1785
76	THE HISTORY OF THE	1786
77	THE HISTORY OF THE	1787
78	THE HISTORY OF THE	1788
79	THE HISTORY OF THE	1789
80	THE HISTORY OF THE	1790
81	THE HISTORY OF THE	1791
82	THE HISTORY OF THE	1792
83	THE HISTORY OF THE	1793
84	THE HISTORY OF THE	1794
85	THE HISTORY OF THE	1795
86	THE HISTORY OF THE	1796
87	THE HISTORY OF THE	1797
88	THE HISTORY OF THE	1798
89	THE HISTORY OF THE	1799
90	THE HISTORY OF THE	1800
91	THE HISTORY OF THE	1801
92	THE HISTORY OF THE	1802
93	THE HISTORY OF THE	1803
94	THE HISTORY OF THE	1804
95	THE HISTORY OF THE	1805
96	THE HISTORY OF THE	1806
97	THE HISTORY OF THE	1807
98	THE HISTORY OF THE	1808
99	THE HISTORY OF THE	1809
100	THE HISTORY OF THE	1810



## LIST OF FIGURES (continued)

FIGURE		PAGE
5.21	Torque-Rotation and Torque-Steel Stress Curves - Specimens N	82
5.22	Specimens A Through G after Test	84
5.23	Specimens A Through F after Test	84
5.24	Specimens A Through G after Test	85
5.25	Specimens A Through G after Test	85
5.26	Specimens H Through N after Test	86
5.27	Specimens H Through N after Test	86
5.28	Specimens H Through N after Test	87
5.29	Specimens K Through N after Test	87
6.1	Relation Between Compressive and Tensile Strength	93
6.2	Relation Between Modulus of Rupture and Tensile Strength	94
6.3(a)	Actual Cracking Torques of Specimens	97
6.3(b)	Measured Average Cracking Torques of Various Types of Specimens	97
6.4	Cracking and Ultimate Torques	100
6.5	Contribution of Lateral Reinforcement to the Torsional Strength	101
A.1	Stresses on an Infinitesimal Element	A 5
A.2	Stresses on a Tetrahedron	A 5
A.3	Co-ordinate System	A 5
A.4	Boundary Element	A 8
A.5	Membrane Analogy	A 8
A.6	Rectangular Section	A 8



## CHAPTER I

### INTRODUCTION

#### 1-1 Introductory Remarks

One of the topics in the field of concrete in which probably the least has been done is the strength and behaviour in torsion either alone or in conjunction with bending and shear. This is apparent when compared to the volume of work done in the study of flexure, shear and axial stresses. This is partly due to the fact that torsional stresses are not of such common occurrence as shear and flexural stresses. Besides, in many instances the torsional stresses are only of secondary nature and are generally either totally ignored or vaguely allowed for by reducing the permissible shear stresses. This lack of knowledge of the torsional stresses in concrete section is reflected by the fact that most building codes make no specific provisions for designing concrete section submitted to torsion.

With the development of the concrete industry more and more structures sustaining torsional loads are being evolved. Elaborate methods of analysis are now available to determine the stresses and deformations in monolithic structures particularly the edge members of slabs and shells. The need for proper understanding of torsional stresses is now more keenly felt than ever before.

The experimental work done in the field of torsional stresses in prismatic members has left many issues in dispute. The investigators

127

127

127

127

127

disagree on many vital points. Besides some of the many variables involved have never been investigated. Whereas the plastic theory is now generally recognised for predicting the ultimate flexural strength of concrete members, its status with regard to torsional stresses is still in dispute. Both Nylander (23)\* and Gardner (16) prefer the plastic theory. Cowan (11) and Zia (32) on the other hand, prefer the elastic theory on the ground that the strain capacity is not enough to effect a significant stress redistribution.

There is no rational or accepted procedure for design of concrete sections in torsion with or without shear and bending. The contribution of steel, both longitudinal and transverse, in increasing the torsional strength of reinforced concrete sections has been estimated differently by the investigators. Whereas some investigators feel that the gain over the torsional strength of plain concrete sections is not significant, others, notably Ernst (15), report that the torsional strength may be more than doubled by provision of suitable reinforcement.

The effects, if any, of the disposition and bar size of longitudinal reinforcement, the bar size of transverse steel and the strength properties of reinforcing steel, have yet to be investigated in some detail.

The tests reported herein, together with the related analyses, are an attempt to understand more fully the behaviour of torsional stresses in concrete sections.

---

\* The numbers in parentheses refer to the references in the BIBLIOGRAPHY.



## 1-2 Object

In the first series, reported herein, the following variables were studied:

- (1) Percentage of longitudinal steel.
- (2) Percentage of transverse steel.
- (3) Position and size of longitudinal bars.
- (4) Effect of bar size of ties.
- (5) Effectiveness of ties for two different overlaps; Types P & Q.
- (6) Strength of reinforcing steel.

The concrete strength was not intended as a variable. It, however, varied slightly for the different specimens. Compression and split tests on control cylinders and flexure tests on companion specimens were conducted to study the inadvertent variation in the concrete strength. Due to the importance of the tensile strength in assessing the torsional strength, the relationship between the compressive strength, the tensile strength and the Modulus of rupture was examined.

The object of the investigation was to study more closely the nature of torsional stresses, the suitability or otherwise of elastic and plastic theories and the part played by steel of varying amount and disposition in modifying the behaviour of concrete sections in torsion.

## 1-3 Scope

Thirty beams were tested. All specimens were square - 4" x 4" in cross-section. Three beams, Type A, were of plain concrete and the rest were reinforced in such a way as to cover the variables under study. There were two specimens of each type, except types A and N, each of which





had three specimens.

The concrete cylinder strength varied from 3335 to 4190 psi, the tensile strength from 325 to 368 psi and the Modulus of rupture from 577 to 670 psi.

Three different grades of steel were used. The yield point stress varied from 24,110 to 58,860 psi. The ultimate strength varied from 42,330 to 83,460 psi. The size of steel varied from 0.144" (No. 7 SWG) to 3/8" diameter. Both deformed and plain rods were used.

The amount of longitudinal steel varied from nothing to 2.75 percent and that of transverse steel from nothing to 2.72 percent. Also for the same percentage of longitudinal or transverse steel, the rods were selected in different sizes and relative positions in the specimens to study their effect upon the behaviour of the specimen.

#### 1-4 Notations

All the notations are explained when they are first introduced. They are collected here for ready reference.

$x, y, z$	Rectangular co-ordinates
$N$	Outward normal to the surface of a body.
$l, m, n$	Direction cosines of outward normal.
$A$	Cross-sectional area.
$q$	Intensity of continuously distributed load
$X, Y, Z$	Components of body force per unit volume.
$\bar{X}, \bar{Y}, \bar{Z}$	Components of distributed surface force per unit area.
$T$	Twisting moment.
$T_E$	Elastic resisting torque.



$T_p$	Plastic resisting torque.
$T_{EP}$	Elasto-plastic resisting torque.
$T_u$	Ultimate torque.
$T_{cr}$	Cracking torque.
$T_s$	Contribution of steel to the ultimate torque.
$\sigma_x, \sigma_y, \sigma_z$	Normal components of stress parallel to x, y and z axes.
$\tau$	Shearing stress.
$\tau_{xy}, \tau_{xz}, \tau_{yz}$	Shearing stress components in the rectangular co-ordinates.
$\tau_{max}$	Maximum shearing stress.
$S$	Force per unit length; slope or length of a curve.
$u, v, w$	Components of displacements.
$\epsilon$	Unit elongation; plasticity ratio.
$\epsilon_x, \epsilon_y, \epsilon_z$	Unit elongations in x, y and z directions.
$\gamma$	Unit shear strain.
$\gamma_{xy}, \gamma_{xz}, \gamma_{yz}$	Shear strain components in rectangular co-ordinates.
$E$	Modulus of elasticity in tension or compression.
$G$	Modulus of elasticity in shear. Modulus of rigidity.
$\mu$	Poisson's ratio.
$\phi$	Stress function (elastic).
$\phi_p$	Plastic stress function.
$J$	The polar moment of inertia.
$K$	Torsion constant.
$r$	Variable distance from axis.
$R$	Radius of circular section. Stress factor.
$\theta$	The angle of twist per unit length.
$\xi$	A function equal to $\phi/G\theta$ .



$\psi$	A function defining longitudinal warping. (Eq. A.6)
$f'_c$	Cylinder strength of concrete.
$f'_t$	Tensile strength of concrete.
$f_r$	Modulus of Rupture of concrete.
$b, d$	The shorter and longer side of a rectangular section.

THE UNIVERSITY OF CHICAGO PRESS

CHICAGO, ILLINOIS 60607

TEL: 773-936-5000

FAX: 773-936-5001

INTERNET: <http://www.uchicago.edu>

## CHAPTER II

### REVIEW OF PREVIOUS WORK

#### 2-1 Introduction

Coulomb (5) first developed in 1784 the theory of torsion for circular prismatic bars assuming that the cross-sections of the bar remain plane and rotate without distortion during twist. This theory was later (1864) applied by Navier (29) to prismatical bars of non-circular sections. Making the above assumption, he arrived at the erroneous conclusions that for a given torque, the angle of twist of bars is inversely proportional to the centroidal polar moment of inertia of the cross-section and that the maximum shearing stress occurs at the points most remote from the centroid of the cross-section.

The correct solution of the problem of torsion of prismatical bars was first given by Saint Venant (25) by using the so-called semi-inverse method. He assumed that the deformation of a twisted shaft consists of (a) rotations of the cross-section as in the case of circular shaft and (b) warping of the cross-section which is the same for all cross-sections.

A significant development in the theory of torsion was the introduction of the stress function by L. Prandtl (29) who also proposed the membrane analogy for the torsion problem. Nadai (22) has suggested the corresponding analogy called sand heap analogy based on full plasticity. More recently, the membrane analogy has been extended to cover partial





plasticity by assuming a roof of constant slope erected over the membrane. Thus a problem, for which no analytical solution exists, has been tackled by a physical analogy.

## 2-2 Tests on Plain Concrete

Tests conducted by Morsch (21) at Stuttgart in 1903-4 indicated that the plain concrete sections fractured as soon as the first  $45^{\circ}$  helical crack was formed. Miyamoto (20) also reported similar results for 16 plain concrete specimens tested by him. Turner and Davies (30) reported that at ultimate torque, the stress across the section was nearly uniform, specially for 'T' sections. The specimens exhibited partial plasticity. He also found that in the elastic range, the torque-deformation curve was nearly straight. This portion of the curve did not change due to addition of reinforcement. It was implied that the reinforcement did not increase the stiffness of the specimen. Andersen (1) tested 6 circular plain concrete specimens. He reported that the specimens showed no ductility and collapsed at the formation of first  $45^{\circ}$  crack.

On the basis of tests on circular and rectangular sections, Marshall and Tembe (19) reported that the maximum shear stress in a rectangular section was a function of the ratio of sides, increasing for higher values of this ratio.

Nylander (23) preferred plastic theory for assessing the ultimate torsional strength. Cowan (7), however, found the plastic detrusion too small to effect any significant stress redistribution. Cowan and Armstrong (13) reported sudden fracture of plain concrete specimens at the cracking torque.



## 2-3 Tests on Reinforced Concrete

### (a) Uni-directional Reinforcement

Bach and Graf (4) reported that the increase in the ultimate torsional strength with addition of longitudinal reinforcement only was small being of the order of 10 percent. Sloping longitudinal bars were, however, reported to be more effective. Graf and Morsch (18) found that the increase in ultimate torsional strength was insignificant with addition of either longitudinal or transverse steel only. Young, Sagar and Hughes (31) reported that the ultimate strength did not increase by provision of longitudinal steel only. Tests by Turner and Davies (30) indicated that the longitudinal reinforcement alone did not impart any ductility to the specimen. The failure for such specimen was sudden and destructive as for plain concrete specimen. The gain in strength was little. Andersen (2) also reported brittle failure for specimens with longitudinal steel only. Marshall and Tembe (19) agreed with Graf and Morsch (18) and concluded that uni-directional reinforcement either longitudinal or transverse did not increase the ultimate strength. Nylander (23), who tested plain and longitudinally reinforced sections in various combinations of torsion, bending and shear, found the plastic theory to yield better results. Cowan's (7) tests indicated no ductility and insignificant plastic detrusion for longitudinally reinforced specimens. Ernst (15) reported that the ultimate torsional strength is increased when either the longitudinal or the transverse steel is increased.

### (b) Two-directional Reinforcement

Most of the investigators conducted tests on specimens having both longitudinal and transverse steel. Graf and Morsch (18) reported



significant increase in torsional strength. Miyamoto (20) reported that the reinforced specimens had a greater cracking torque and significantly greater ultimate capacity as compared to corresponding plain specimens. The cracks were at  $45^{\circ}$  as for plain specimens. Miyamoto reported that the behaviour was neither completely elastic nor completely plastic. Turner and Davies (30) found the stress distribution to be practically uniform over the entire section. They reported the torque-rotation curve to be almost straight in the elastic range. The reinforcement had no effect on this portion of the curve. Andersen (1) reported considerable ductility after first cracking. The torque-deformation curve in the elastic range was dependent on the geometry of the cross-section and the concrete strength. Beyond the elastic range, reinforcement had a dominating effect on the shape of the torque-deformation curve. Marshall and Tembe (19) tested specimens with longitudinal bars and transverse ties. They reported that the same stress was induced in both sets of reinforcement if their percentages were equal. Cowan (7) reported that the initial stiffness did not depend on the type or amount of reinforcement. The reinforced specimens were reported to have considerable ductility. There was little stress in steel up to cracking. The stress rose quickly to yield stress at the ultimate torque. The shape of the torque-rotation curve beyond the cracking torque was dominated by the percentage and disposition of reinforcement. Ernst (15) reported that the cracking torque did not depend on the reinforcement. There was a marked reduction in stiffness after cracking. The ultimate torque was reported to have increased considerably by provision of adequate reinforcement.





### (c) Helical Reinforcement

Morsch (21) reported considerable increase in shear stress and cracking torque by provision of  $45^{\circ}$  helical reinforcement. Bach and Graf (4) reported considerable increase in ultimate capacity. Graf and Morsch (18) reported that whereas the cracking torque was unaffected, the ultimate torque was more than doubled by provision of helical reinforcement. Young, Sagar and Hughes (31) reported that the ultimate torsional strength increased in proportion to the percentage of helical reinforcement. A significant increase in ductility was reported. Andersen (1) also reported considerable ductility for specimens with spiral steel. He found the helical reinforcement to be the most efficient form of reinforcement for pure torsion.

### 2-4 Tests on Prestressed Concrete

Tests on prestressed concrete sections in torsion were carried out by Cowan and Armstrong (13), Humphreys (17), Gardner (16) and Zia (32).

Cowan and Armstrong tested their specimens in combined bending and torsion. They reported certain interaction between bending and torsion. A small bending moment increased the torsional strength. The inclination of the cracks to the axis depended upon the ratio of bending and twisting moments. The prestressing increased both the bending and torsional strengths considerably.

Humphreys tested 94 axially and eccentrically prestressed sections in pure torsion. He found the elastic theory to yield satisfactory results. The specimens failed due to diagonal tension distress unless such failure was inhibited by high prestress. The crack inclinations were in conformity with the elastic theory. The criterion of maximum principal





stress was found to be satisfactory for predicting the ultimate strength for specimens failing in tension.

Gardner reported considerable ductility after first cracking for 'I' section prestressed beams without web reinforcement. The cracks first formed in the web but the specimen did not fail until the cracks propagated through the flanges. Plastic theory was preferred for predicting the ultimate torsional strength.

Zia, on the basis of his extensive tests, reported abrupt failure for rectangular and 'T' sections. The 'I' sections, however, showed considerable ductility. They did not fail till the whole section, including the flanges, attained ultimate tensile strength. This was in agreement with the findings of Gardner. The specimens with web reinforcement also showed considerable ductility. Zia agreed with Cowan and preferred elastic theory for predicting the strength of the specimens.

## 2-5 Combined Stresses

Very few tests have been carried out on concrete specimens subjected to torsion and bending with or without shear. Nylander (23), Cowan and Armstrong (13) and Gardner (16) have reported tests involving combined stresses.

Nylander tested 60 specimens in various combinations of bending moment, torque and shear. The specimens were plain and longitudinally reinforced. He preferred plastic theory for predicting the ultimate capacity.

Cowan and Armstrong tested plain, reinforced and prestressed sections in combined bending and torsion. Plain and prestressed specimens had a brittle failure. The crack pattern depended on the ratio of bending and twisting moments.



Gardner reported tests on 'I' section prestressed beams in combined bending and torsion. The specimens showed considerable ductility. Plastic theory was preferred.

While interaction diagrams have been suggested to deal with the case of combined bending and torsion, no such interaction has been established in the case of combined torsion and shear. It has been reported that a small bending (or twisting), less than what is required for first cracking, increases the ultimate torsional (or bending) capacity of a specimen. The tests are, however, considered too few to be conclusive.



## CHAPTER III

### DESCRIPTION OF TESTING EQUIPMENT

#### 3-1 Torsion Testing Rig

A simple set-up for testing the specimens in pure torsion was designed and fabricated. The general layout of the testing rig is shown in FIGURES 3.1, (a) through (d). The details of the various parts are laid out in FIGURES 3.2, 3.3 and 3.4. One end of the specimen was restrained from rotation by securing it on to the fixed grip by wooden wedges. The other end, which was held securely by the movable grip, was twisted by the movable cross-arm. The torsional moment was applied by suspending slotted weights to one end of the movable cross-arm. The force required to overcome the frictional resistance in the pivot was only one pound. This frictional resistance was allowed for in calculating the effective twisting moment. The twist was measured by two "twistmeters" placed 30 inches apart at the two ends of the gage length. The principal components of the torsion testing rig are briefly described below.

##### (a) Fixed Cross-Arm

This consisted of a W<sup>F</sup> section (designation 8B15) restrained against any movement by eight 3/8 inch diameter bolts embedded in concrete pedestals A. The overall length of the cross-arm was 104 inches and the ends were flush with the outer edges of the pedestals. The cross-arm supported the fixed grip at the centre of its length.



### (b) Fixed Grip

The fixed grip was a box-like construction with the front and top open. The inner dimensions of the grip were 9" long, 9" wide and 12" deep. The full details of the grip are shown in FIGURE 3.2. Two angles 1-1/2" x 1-1/2" x 1/4" x 12-1/4" were welded along the front vertical edges of the grip. Each of these angles had eight holes of 11/16 inch diameter, so that another angle 2" x 2" x 3/8" x 15" could be bolted horizontally at any position across the two vertical angles. The fixed grip was supported by the fixed cross-arm to which it was permanently fixed by welded connecting wings. Wooden blocks were sandwiched between the specimen and the grip at the bottom and the two sides. Wooden wedges were driven between the specimen and the horizontal angle to secure the specimen to the fixed grip.

### (c) Pedestals-A

There were two concrete pedestals of overall size 18" x 24" x 36" high. They supported the cross-arm and restrained it from any movement by eight embedded bolts. The twisting moment on the specimen tended to lift up one of the pedestals. The dead weight of the pedestal was enough to counteract this lifting effect. The pedestals rested on the floor and had no special foundation.

### (d) Movable Cross-Arm

The details of the movable cross-arm are shown in FIGURE 3.3. The cross-arm, which was a rolled steel I-section, rocked on a 1" diameter pin at the centre of its length. The overall size of the cross-arm was 8" x 4" x 104". The cross-arm was supported by the support S. Two longitudinal slots were provided in the lower flange of the cross-arm





through which the vertical plates of the support S passed. Holes were provided in the web and the flange of the cross-arm at 50 inches from the pivot. These holes were used to fix the pointer and the suspension rod for the slotted weights.

(e) Movable Grip

This grip was identical in construction to the fixed grip. It was attached permanently to the movable cross-arm by welded wing plates. The end of the specimen was secured to the movable grip by wooden blocks and wedges.

(f) Pedestal-B

This plain concrete pedestal had overall dimensions of 9" x 55-1/2" at the top and 24" x 55-1/2" at the bottom. The height of the pedestal was 30". The details of the pedestal are shown in FIGURE 3.4. This pedestal carried 30 embedded bolts of 3/8" diameter in five groups of six bolts each. The six bolts in a group were adequate to fix the support S in position. These groups of embedded bolts were at 12" distance so that the support S could be shifted by 12" by moving to the next group of bolts. Thus any specimen whose length was between about 3 feet and 7 feet could be tested. The height of the pedestal was kept 30" so that the two grips were at the same level.

(g) Support-S

The support S, whose details are seen in FIGURES 3.2 and 3.4, could be fixed in any desired position along the length of the pedestal B. It supported the movable cross-arm by means of a pin which acted as a pivot for the cross-arm. The upright plates of the cross-arm passed through



the two longitudinal slots in the flange. These slots had adequate length to permit a substantial rotation of the cross-arm. The upright plates of the support S did not touch the ends of the slots till the end of the cross-arm hit the floor.

#### (h) Loading Arrangement

The details of the loading arrangement are shown in FIGURE 3.3. Cast iron slotted weights, weighing nominally 10 and 20 lbs., were applied to one end of the cross-arm by means of a suspension rod.

A pointer was provided at the centre of the web of the movable cross-arm, 50 inches from the pivot. This pointer gave the height on an upright staff graduated in feet. The staff readings were co-related to the lever arm by direct measurement. A graph co-relating the staff reading and lever arm was drawn up.

### 3.2 Twistmeter

Two twistmeters were designed and fabricated. The details of the twistmeter are shown in FIGURES 3.5, (a) through (c). A bubble was supported on a channel 1-1/2" x 1/2" x 16". This channel was pinned at one end and was supported by the needle of a micrometer screw at the other end.

Two slotted angles 2-1/2" x 1-1/2" and two 1/4" bolts formed a closed frame which could be clamped in any desired position on the specimen. Bolts of suitable length could be used to accommodate specimens of any size. The micrometer screw was fixed to one end of the top slotted angle. By working on the micrometer, the bubble could be brought to the centre. The least-count of the micrometer was 0.001 inch. The distance between the



pin-end of the channel and the axis of the micrometer was adjusted to be exactly 15 inches. Thus if the micrometer screw had to be worked through  $x$  inches to bring the bubble back to the centre, the angle of rotation was  $\arctan (x/15)$ . Since for small angles, the tangent is equal to the angle itself in circular measure, the angle of rotation was also  $x/15$  radians. The gage length used in testing was 30 inches, the two twistmeters being fixed at the ends of the gage length. If the movable end micrometer had to be worked through  $d_1$  inches and the fixed end micrometer through  $d_2$  inches for bringing the bubbles back to the centre for any load increment, the net rotation for the whole gage length was  $(d_1 - d_2)/15$  radians. Hence the detrusion per inch length of the specimen was  $(d_1 - d_2)/450$  radians.

Since two twistmeters were used and the difference of the two micrometer readings taken, the net rotation between the two ends of the gage length was obtained. Any yielding of the wedges in the grips did not enter the calculations.

The twistmeters were sensitive to even very small angle changes. Even one pound weight added to the movable cross-arm could displace the bubble. The sensitivity of the twistmeter could be further increased by increasing the length of the supporting channel, using a more sensitive bubble or a micrometer screw of smaller least count.

The channel which supports the bubble had a small longitudinal V groove on the underside of the channel. The needle of the micrometer screw was thus constrained to move along this groove in a straight line.

The micrometer screw had two extra needles which were exactly 1 inch and 2 inches longer than the third one. Thus the run of the micrometer could be extended from 1 inch to 3 inches.





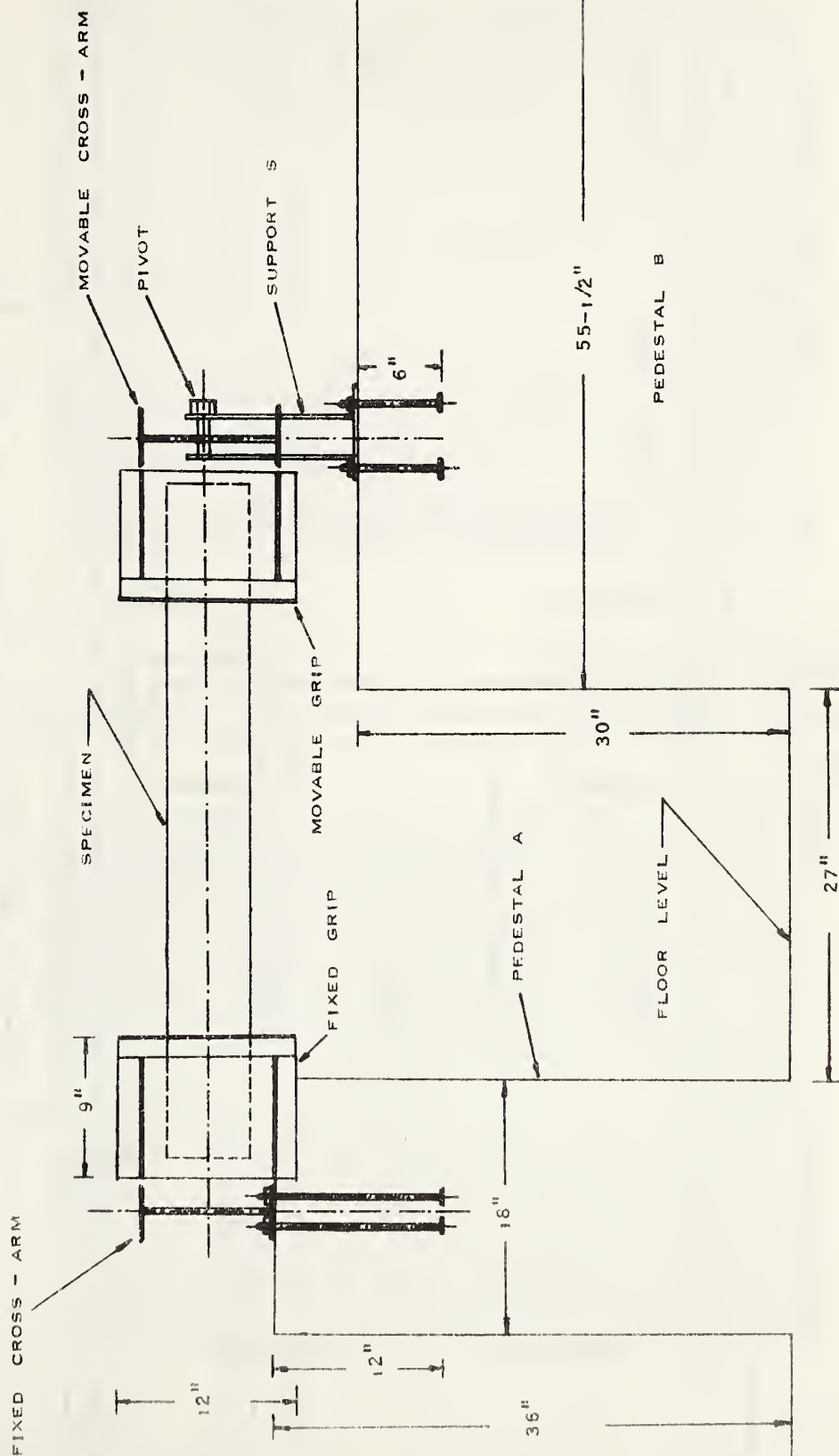
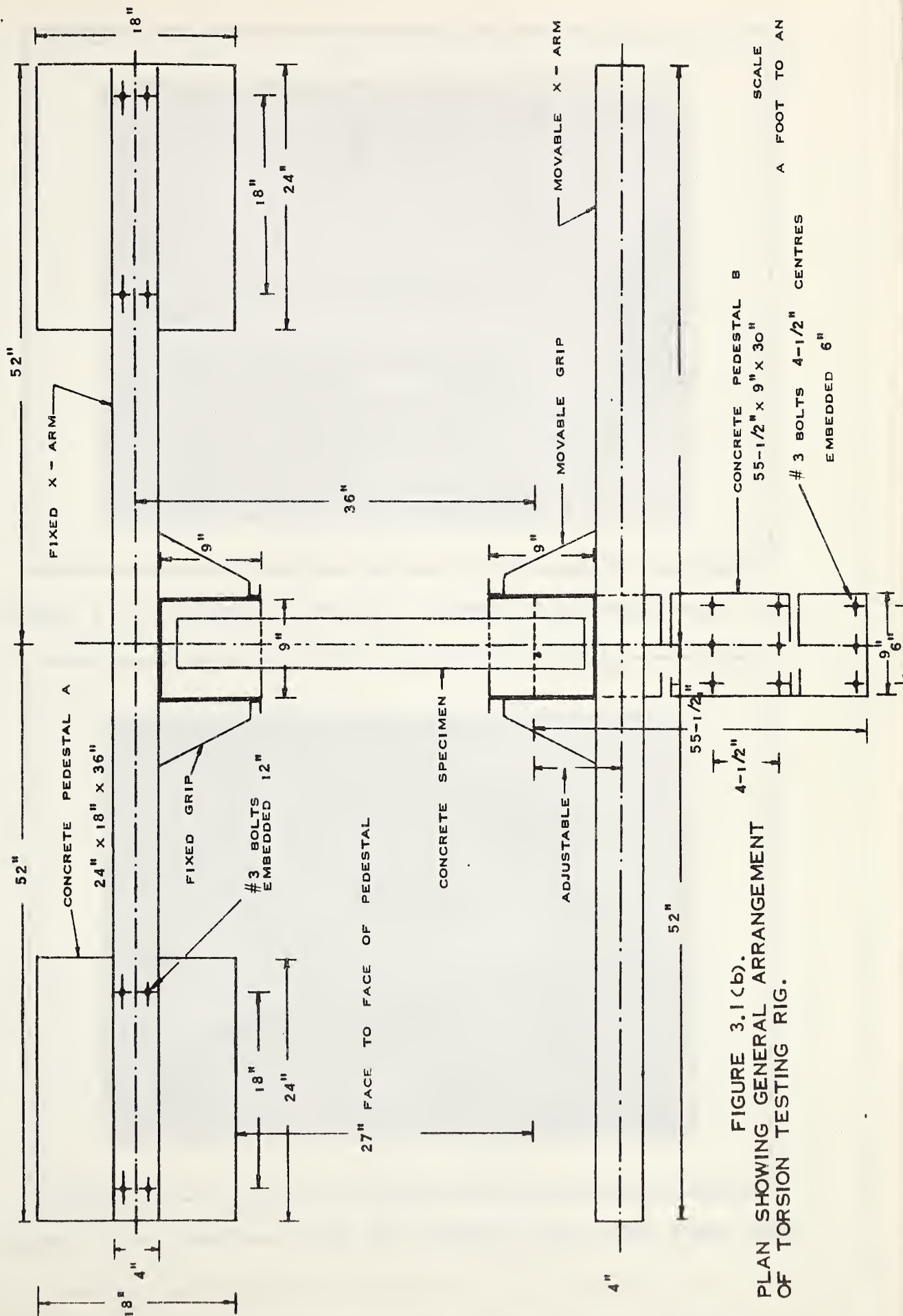


FIGURE 3.1(a) TORSION TESTING RIG. ELEVATION SHOWING GENERAL ARRANGEMENT.

SCALE  
A FOOT TO AN INCH









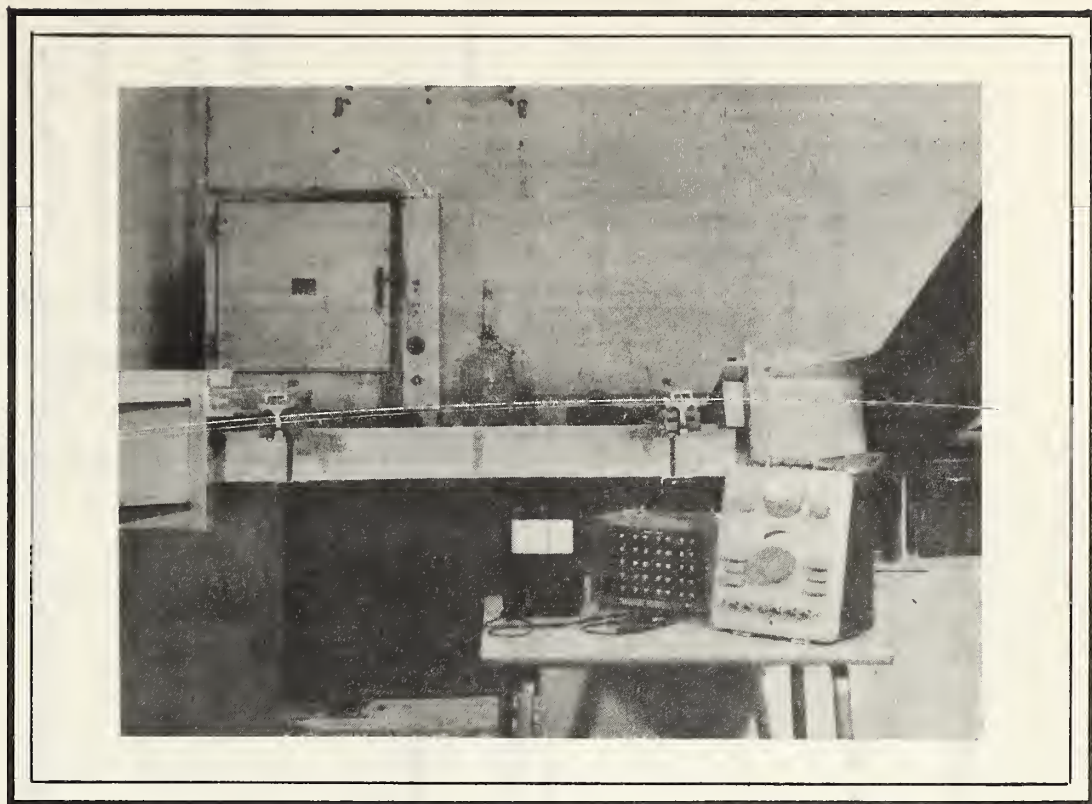


FIGURE 3.1(c) GENERAL VIEW OF TESTING RIG FROM WEST SIDE

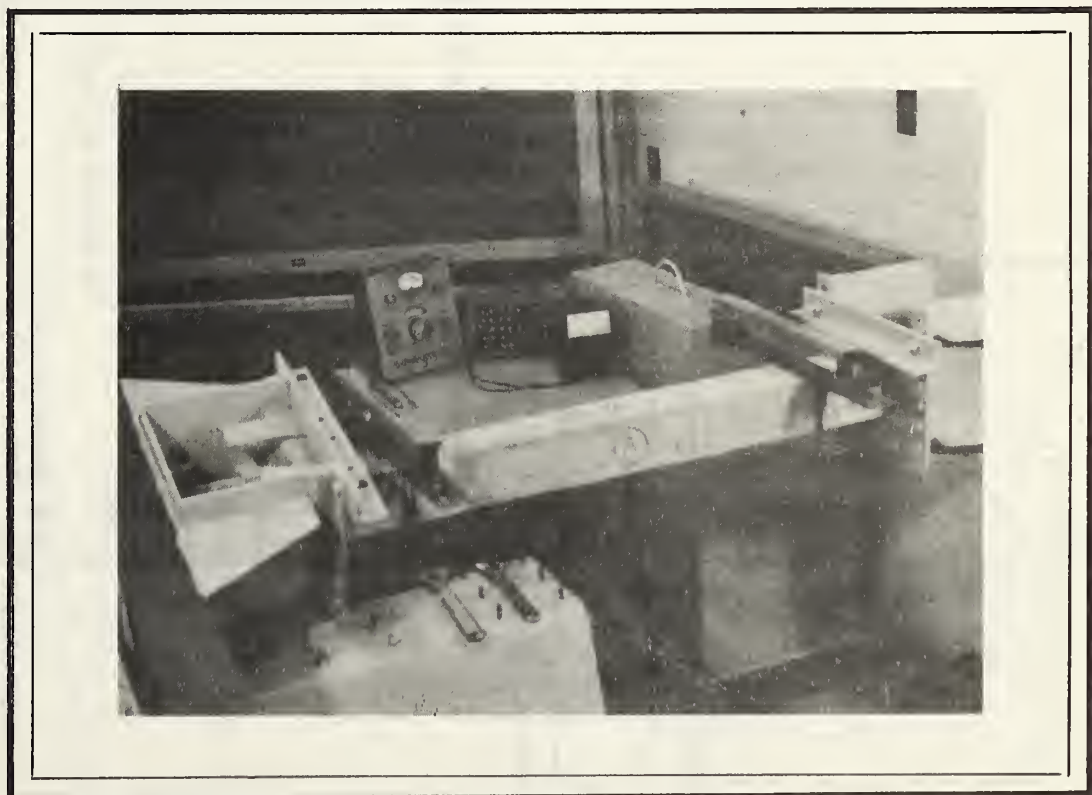


FIGURE 3.1(d) GENERAL VIEW OF TESTING RIG FROM EAST SIDE





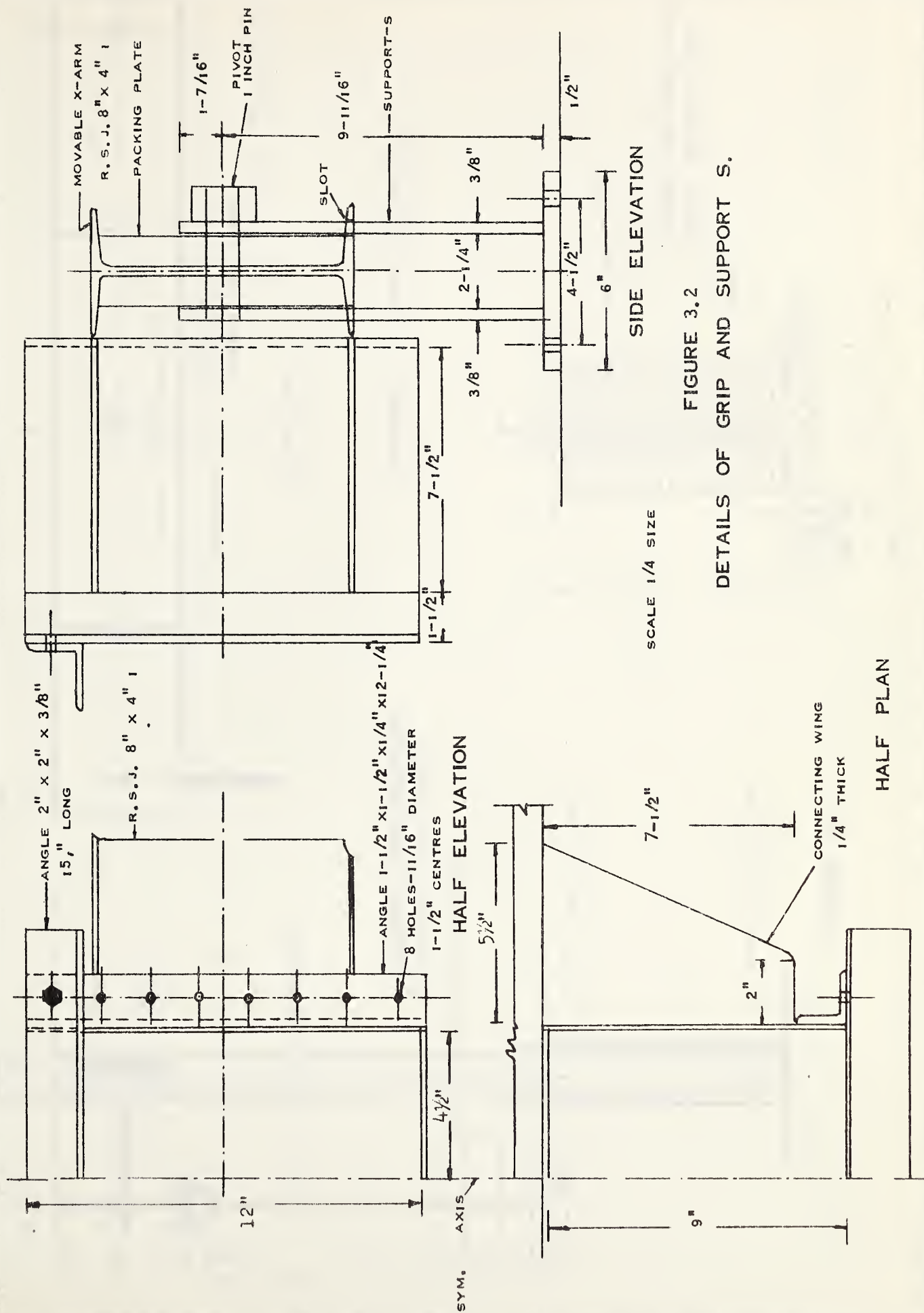


FIGURE 3.2  
DETAILS OF GRIP AND SUPPORT S.



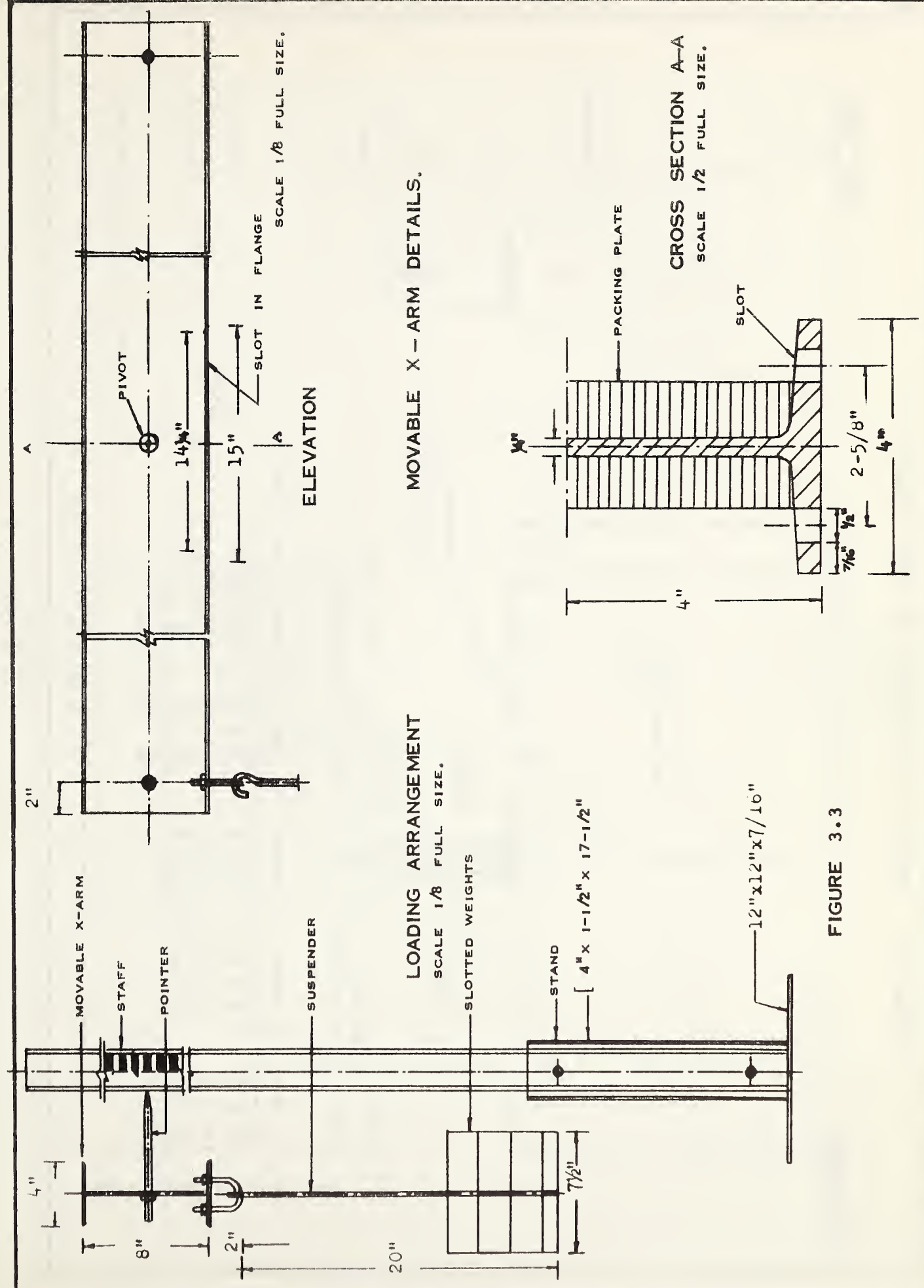


FIGURE 3.3





SCALE - A FOOT TO AN INCH

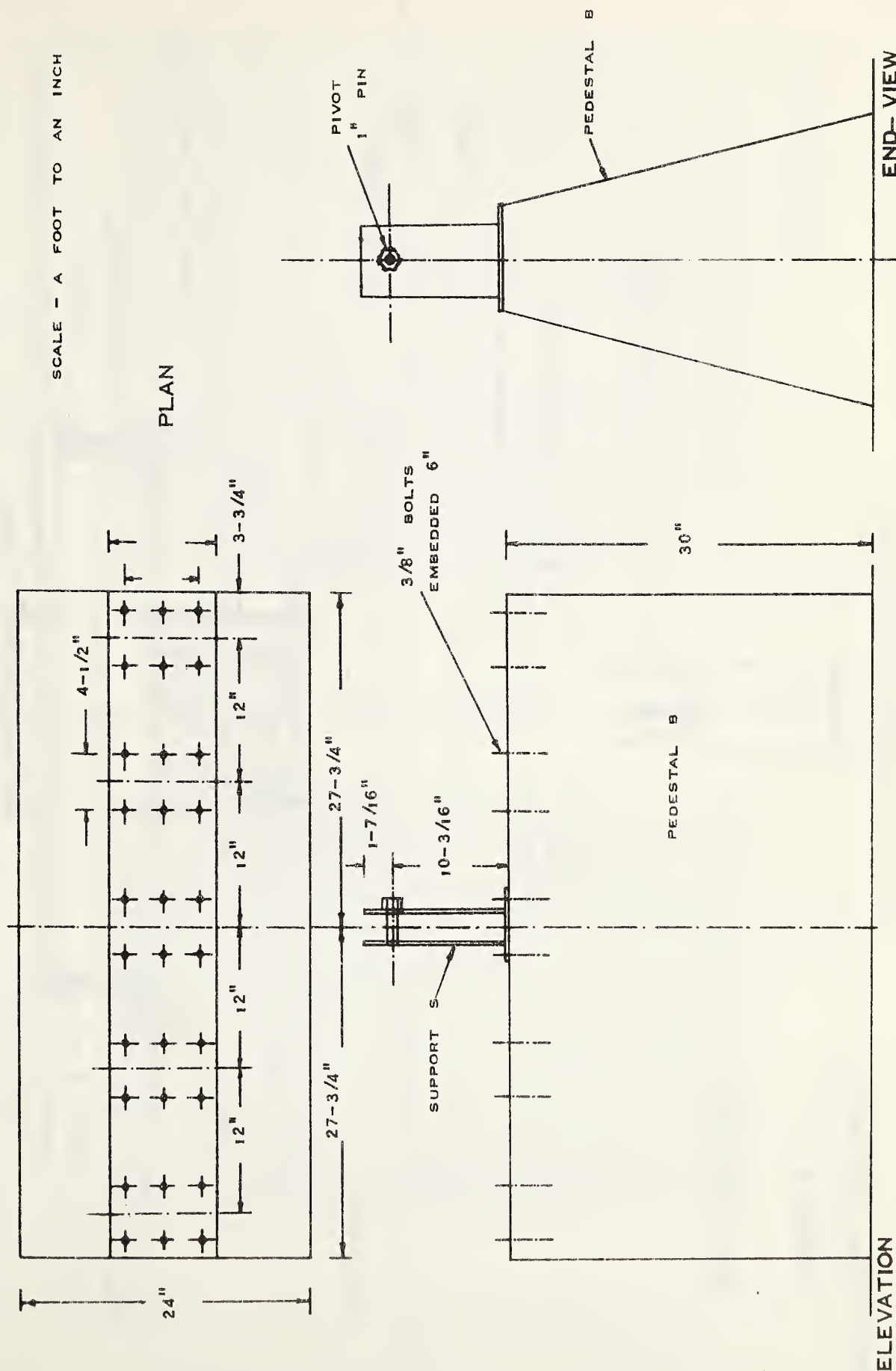
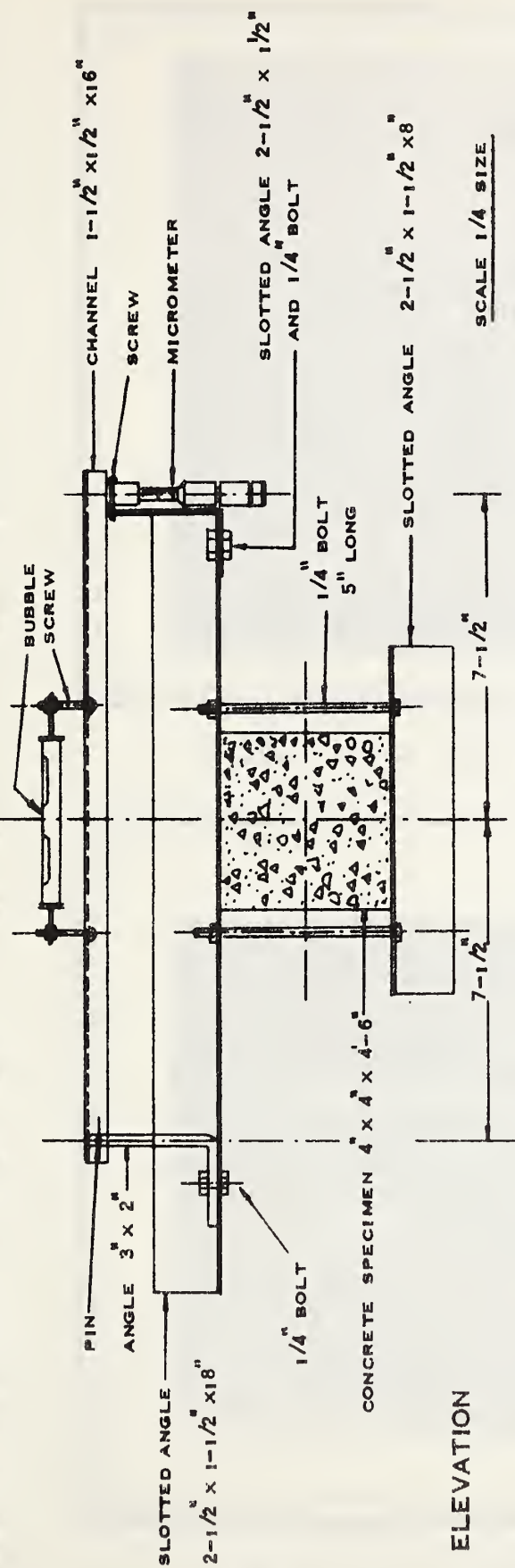
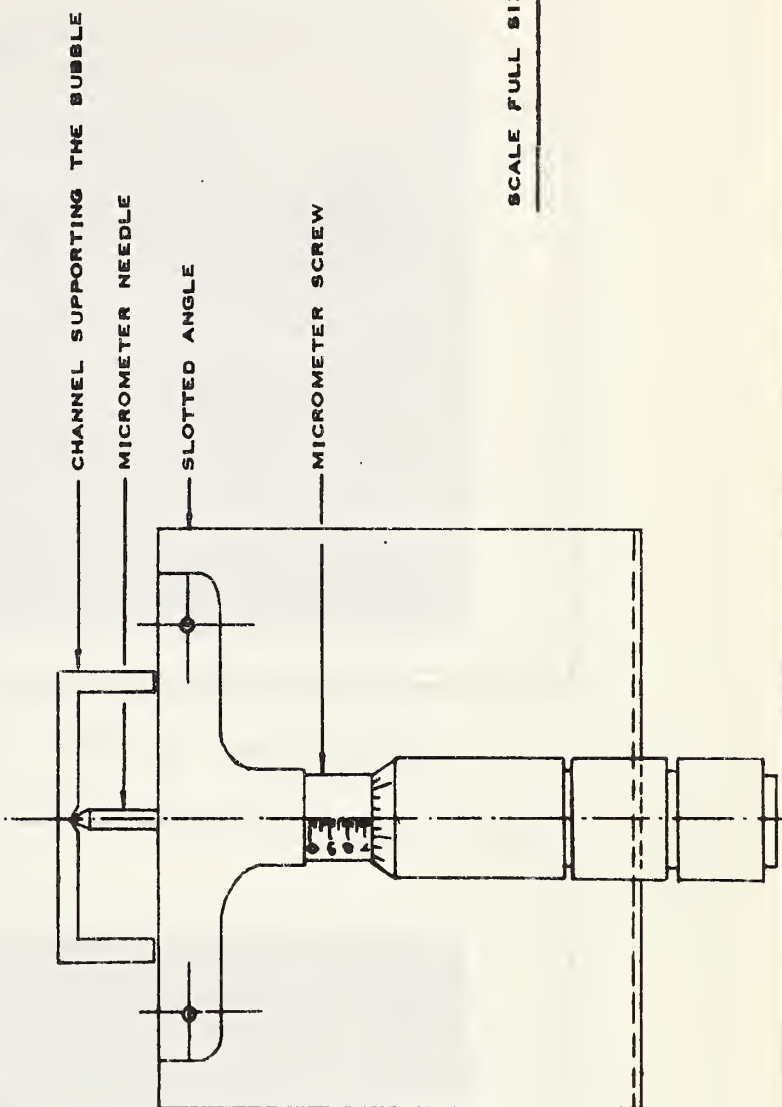


FIGURE 3.4 DETAIL OF PEDESTAL B AND SUPPORT S





ELEVATION



END ELEVATION

FIGURE 3.5 [ a ]

DETAILS OF TWISTMETER

SCALE FULL SIZE



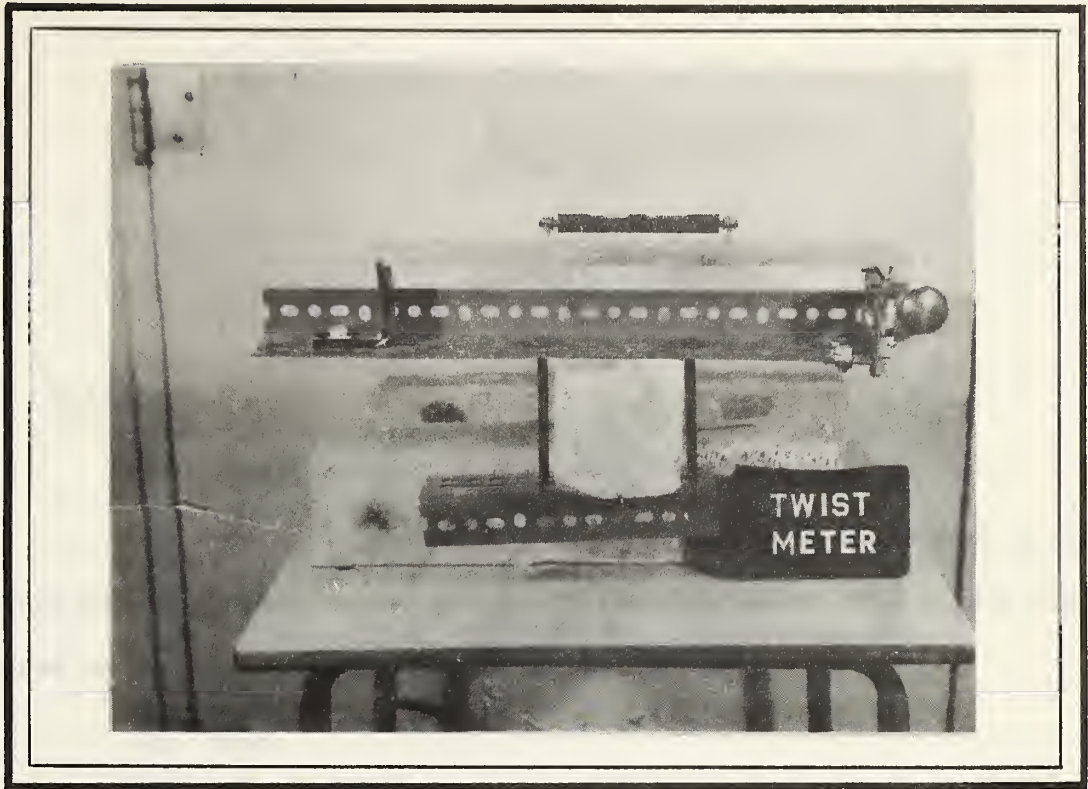


FIGURE 3.5(b) FRONT VIEW OF TWISTMETER

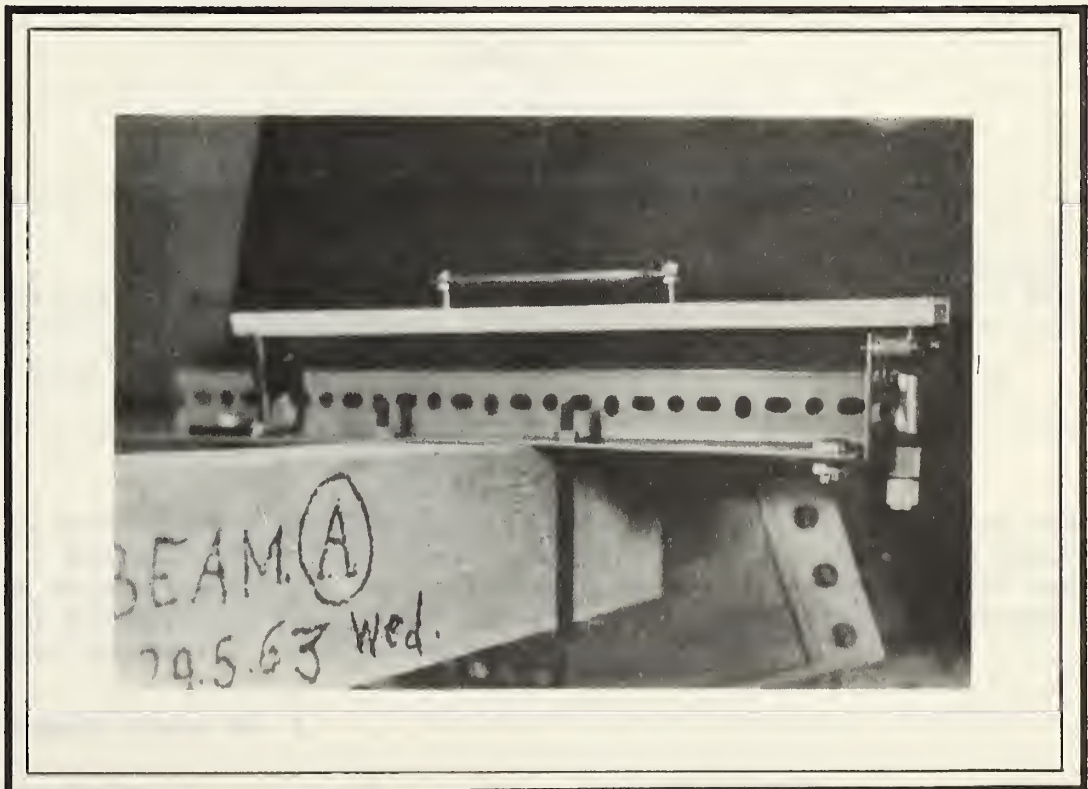


FIGURE 3.5(c) CLOSE - UP OF TWISTMETER





## CHAPTER IV

### DESCRIPTION OF MATERIAL, FABRICATION AND TEST SPECIMENS

#### 4-1 Materials

##### (a) Cement

The high early strength cement\* supplied in paper bags by the Inland Cement Company was used for all the specimens. The cement was stored under proper conditions until it was used.

##### (b) Sand

The properties of the sand are given in TABLES IV-1 and IV-2. The tests were conducted according to A.S.T.M. Standards, 1961, Part 4.

TABLE IV-1

#### PHYSICAL PROPERTIES OF SAND

Material	Absorption	Color Test	Specific Gravity		
			Bulk	Apparent	Saturated Surface Dry
Sand	1.28%	No. 1**	2.53	2.62	2.57

\*The earlier tests on this type of cement gave an initial setting time of 4 hours 25 minutes and final setting time of 5 hours and 25 minutes. The water required for normal consistency was 34.4 percent. The tensile strengths at one, three and seven days, taken from the average of three briquettes, were respectively 411, 655 and 749 psi.

\*\*Organic plate No. 1.





TABLE IV-2  
SIEVE ANALYSIS OF SAND

Sieve Size	Weight retained (gms)	% retained	Cumulative % retained	A.S.T.M. Standard
No. 4	9.8	2.0	2.0	0-5
No. 8	61.3	12.2	14.2	
No. 16	66.3	13.2	27.4	20-55
No. 30	46.0	9.2	36.6	
No. 50	179.0	35.8	72.4	70-90
No. 100	101.9	20.4	92.8	90-98
Pan	27.5	5.5	-	
Silt	8.9	1.8	-	
Total	500.7	100.1	245.4	
Fineness Modulus 2.45				

Material passing No. 200 sieve = 1.8 percent.

The average moisture content of sand was found to be 4.9 percent.

(c) Coarse Aggregate

The coarse aggregate used was crushed rock, 3/4 inch maximum size. The physical properties of coarse aggregate are given in TABLES IV-3 and IV-4. The tests were performed according to the A.S.T.M. Standards, 1961, Part 4.

TABLE IV-3  
PHYSICAL PROPERTIES OF COARSE AGGREGATE

Material	Absorption %	Dry Rodded Unit Weight lbs/cft	Specific Gravity		
			Bulk	Apparent	Saturated Surface Dry
Crushed rock	1.48	96	2.54	2.64	2.58



TABLE IV-4

## SIEVE ANALYSIS OF COARSE AGGREGATE

Sieve Size	Weight Retained (lbs)	% Retained	Cumulative % Retained
3/4"	0.2	1.7	1.7
3/8"	8.8	75.2	76.9
No. 4	2.6	22.2	99.1
Pan	0.1	0.9	100.0
Total	11.7	100.0	277.7

## (d) Concrete Mix

The concrete mix was the same for all specimens. The materials used for a 3 cu.ft. concrete mix were:

- (i) water 42.4 lbs.
- (ii) cement 62.7 lbs.
- (iii) sand 167.0 lbs.
- (iv) coarse aggregate 245 lbs.

The water cement ratio was fairly high (0.68) so that a good workability was obtained. Good workability was necessary because the reinforcement was fairly congested in some of the specimens. All materials were proportioned by weight to ensure greater uniformity.

## (e) Reinforcement

The load deformation characteristics of the reinforcement were determined by obtaining coupon tests on 2 specimens of standard No. 3 deformed bar and 3 specimens each of No. 2 plain rods and No. 7 SWG (0.144" diameter) wire. The load-deformation curves for the reinforcing



steel are shown in FIGURES 4.1, 4.2 and 4.3. The average yield point stress for No. 3 rods was fairly high (58,860 psi) and fairly low for the 0.144" diameter wire (24,110 psi). The corresponding ultimate stresses were 83,460 and 42,330 psi respectively. The 1/4" bars had intermediate values; the yield point stress and ultimate stress were 47,490 and 56,330 psi respectively. The observations and the calculations are given in TABLE IV-5.

TABLE IV-5  
STRENGTH PROPERTIES OF REINFORCEMENT

Bar Size (in)	Spec. No.	Cross-Sect. Area (sq.in)	Y.P. Load (lbs)	Ave. Y.P. Load (lbs)	Y.P. Stress (psi)	Ult. Load (lbs)	Ave. U.L. (lbs)	Ult. Stress (psi)	Remarks
3/8	1 2	0.110	6570 6380	6475	58,860	9280 9080	9180	83,460	standard deformed reinforcing bar
1/4	1 2 3	0.049	2340 2250 2390	2327	47,490	2750 2650 2880	2760	56,330	plain reinforcing bar
0.144 No. 7 SWG	1 2 3	0.0163	380 400 400	393	24,110	670 700 700	690	42,330	low strength black wire supplied in coils

#### 4-2 Electrical Strain Gages

SR-4 electrical strain gages were mounted on the reinforcement, both longitudinal and transverse. A-18, A-7, and A-5.S6 gages were used. The particulars of these gages are given below:



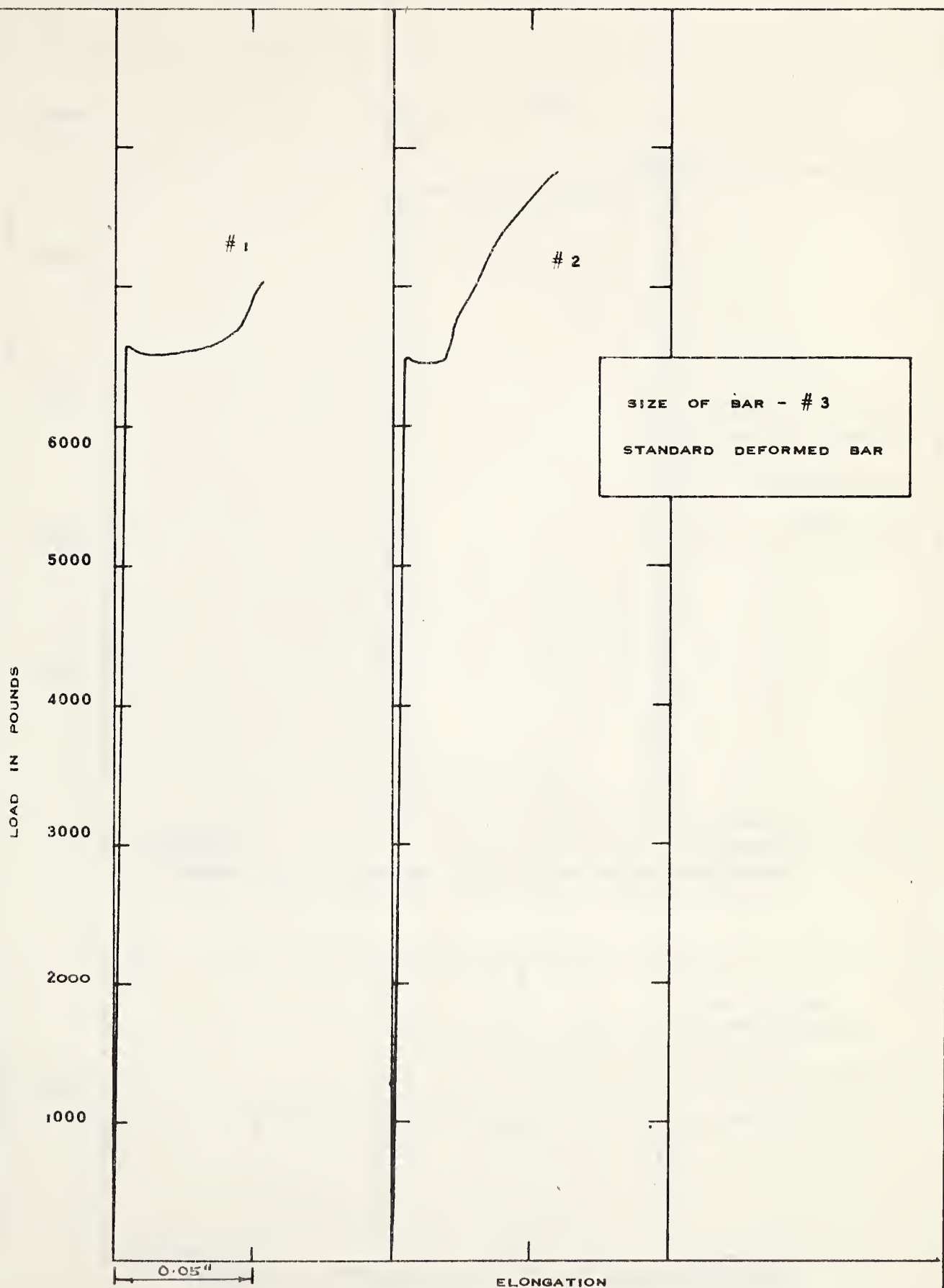


FIGURE 4.1 TENSION TESTS ON REINFORCEMENT





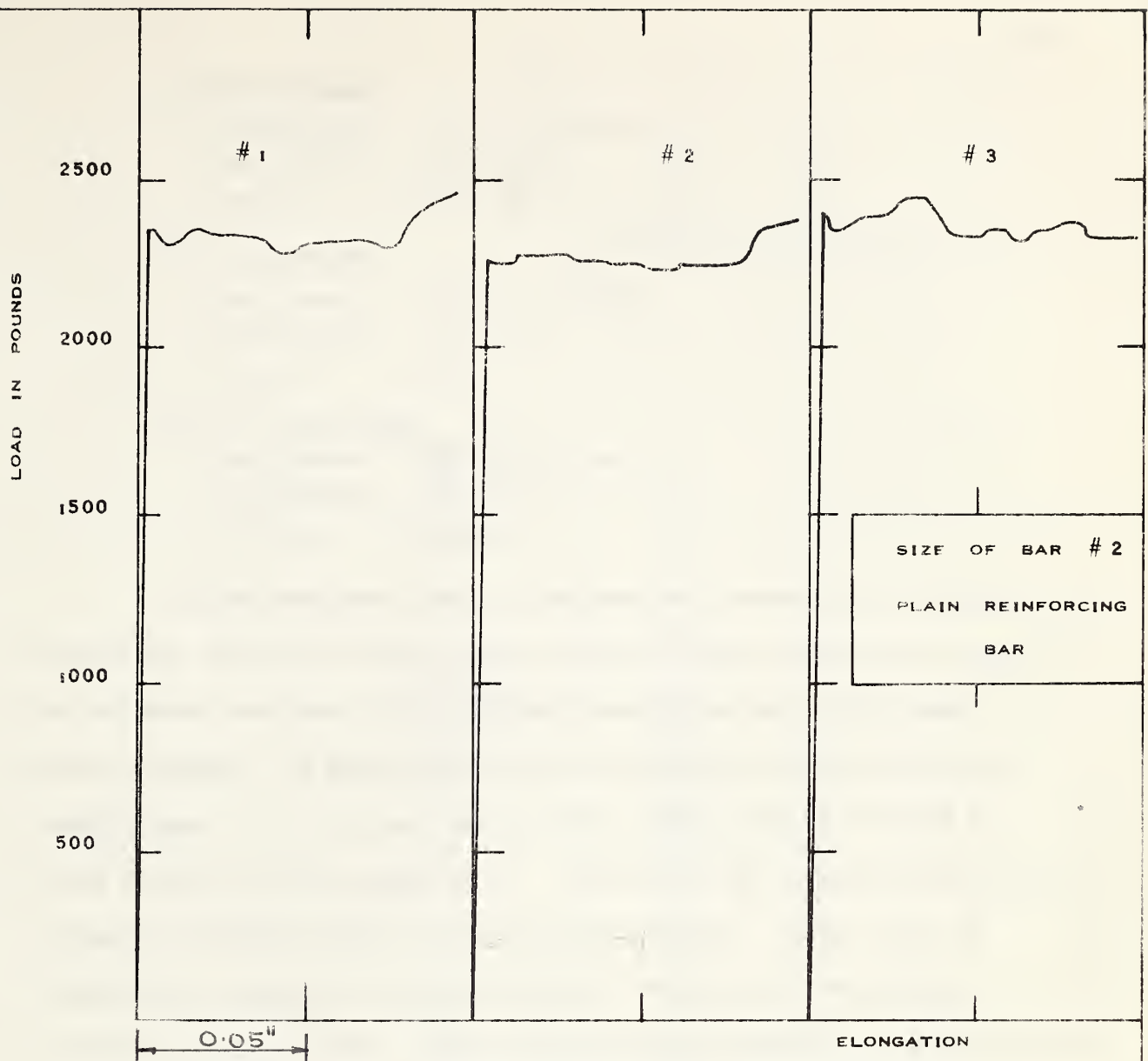


FIGURE 4.2 TENSION TESTS ON REINFORCEMENT

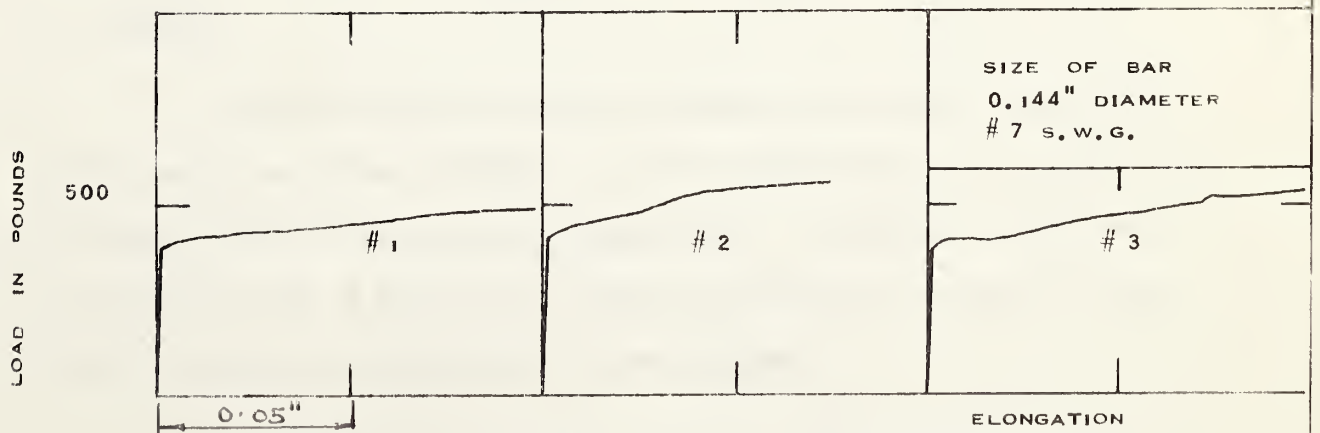


FIGURE 4.3 TENSION TESTS ON REINFORCEMENT



#### A-18 Type Gages

Resistance:  $119.5 \pm 0.3$  ohms

Gage Factor:  $1.81 \pm 2\%$

Lot No: B-31

#### A-7 Type Gages

Resistance:  $120.0 \pm 0.3$  ohms

Gage Factor:  $1.97 \pm 2\%$

Lot No: B-31

#### A-5-S.6 Type Gages

Resistance:  $120.4 \pm 0.2$  ohms

Gage Factor:  $2.00 \pm 1\%$

Lot No: B-29-02

On the specimens type N, the gages were mounted after casting and curing. Small ducts were left to obtain access to the reinforcement. For all other specimens, the gages were mounted on the reinforcement before casting. The gages were mounted according to the manufacturer's instructions. All scale was removed and a smooth surface obtained by using a fine file and emery paper. The surface was thoroughly cleaned by acetone. Household cement was used as the adhesive. Three coats of neoprene were applied for water-proofing. As a further protection, insulation tape was used. The leads were kept as short as possible and the connections were soldered.

#### 4-3 Moulds

3/4 inch plywood was used for making the moulds. The details of the mould are shown in FIGURE 4.4. Four such moulds were made so that four beams could be cast from a single batch. In addition to the two bolts at the ends of the mould, clamps were fixed at the centre of the mould to ensure exact dimensions of the specimen.



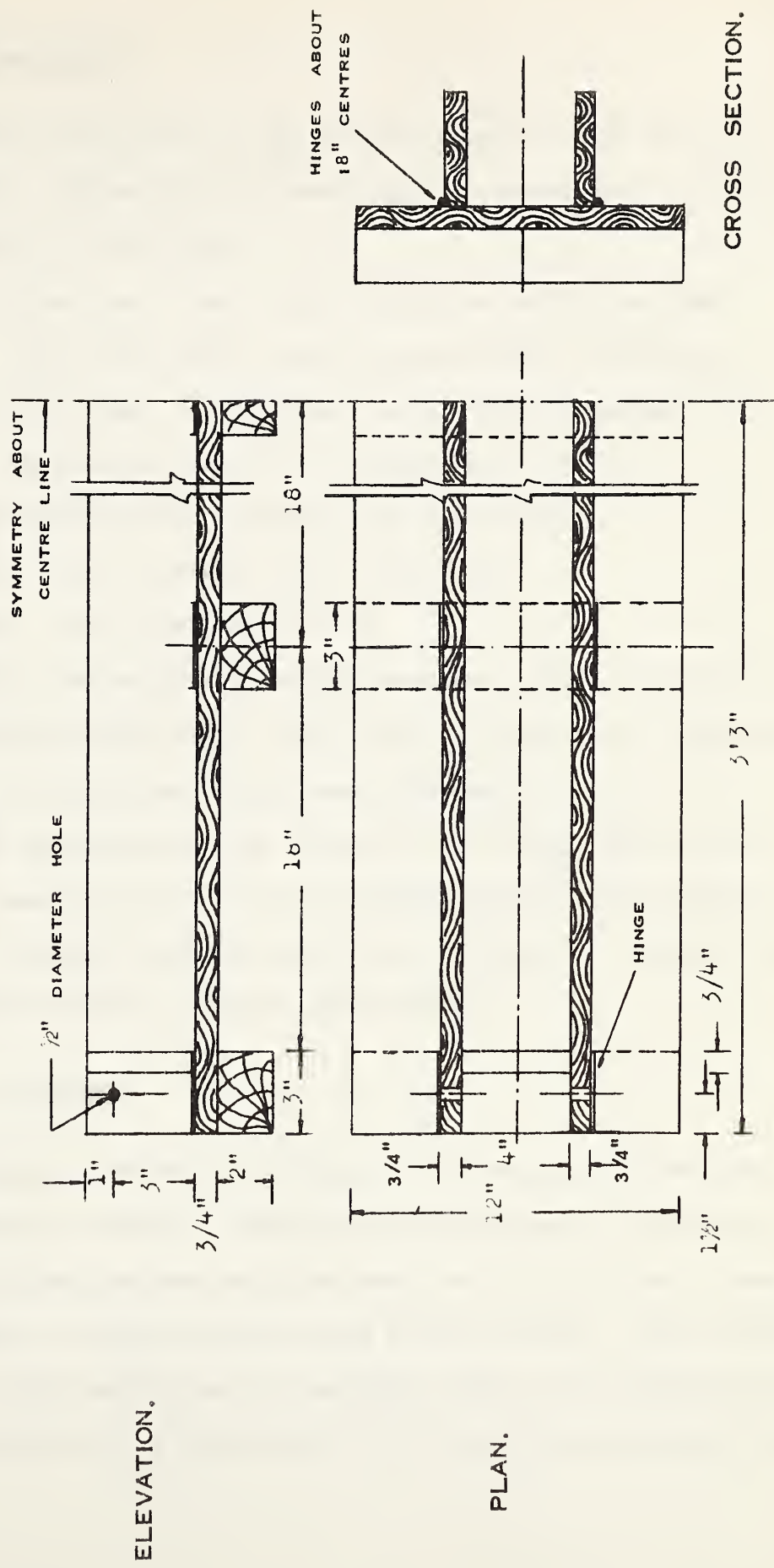


FIGURE 4.4 DETAILS OF MOULD



#### 4-4 Casting and Curing

About 3 cubic feet of concrete was mixed for each batch in a concrete mixer. The materials of exact weight, as mentioned in section 4-1, were taken for each batch.

The forms were oiled before placing the reinforcing cages in position. After the concrete was thoroughly mixed in the mixer, it was placed in the forms. An immersion type of vibrator was used for compaction. Concrete was placed in two layers and vibrated.

The following were cast from each batch mixed:

- (i) Four specimens, two of each type
- (ii) Five cylinders, 6" x 12"
- (iii) Two modulus of rupture specimens 4-1/2" x 3-1/2" x 16"

From the first batch, however, three A-type beams, eight control cylinders 6" x 12" and two control beams were cast.

The specimens were kept covered by wet burlap bags until the moulds were removed on the third day following casting. The specimens, the control cylinders and beams were marked and stored in the moist room until the date of testing, 28 days after casting.

#### 4-5 Control Specimens

Control cylinders and modulus of rupture specimens were cast from each batch of concrete. Generally five cylinders 6" x 12" and two modulus of rupture specimens were cast each time. Of the five cylinders two were tested in compression and three in split testing. The cylinders were capped before performing the compression tests. The tests were performed on the 28th day of casting when the corresponding beams were also







tested in torsion.

Of the eight cylinders cast with A-type specimens, two were tested on the 7th day one each in compression and split test, likewise two on the 14th day and remaining four on the 28th day, two in compression and two in splitting. FIGURES 4.5 and 4.6 show the variation of compressive and tensile strength with time.

The 28th day test results for all specimens are given in TABLE IV-6. In this table, the average values of compressive strength, tensile strength as determined by split test, and the modulus of rupture have been calculated.

The flexure specimens were tested for third-point loading over a span of 12". The broader 4-1/2" face was horizontal and narrower 3-1/2" face vertical during testing.

The following formulas were used:

$$\begin{aligned} \text{(i) Compressive strength} &= \frac{\text{Maximum load in lbs}}{\text{c.s. area of cylinder}} \\ &= \frac{\text{Maximum load in lbs}}{28.26} \text{ psi} \end{aligned}$$

$$\begin{aligned} \text{(ii) Tensile strength} &= \frac{\text{Maximum load in lbs}}{\pi DL/2} \\ &= \frac{\text{Maximum load in lbs}}{113} \text{ psi} \end{aligned}$$

Since D the diameter and L the length of cylinder were 6" and 12" respectively.

$$\text{(iii) Modulus of rupture} = \frac{M \cdot Y}{I}$$

$$M = \frac{P}{2} \times 4 = 2P \text{ lb ins.}, \text{ where } P \text{ was the total load in lbs. on the specimen.}$$



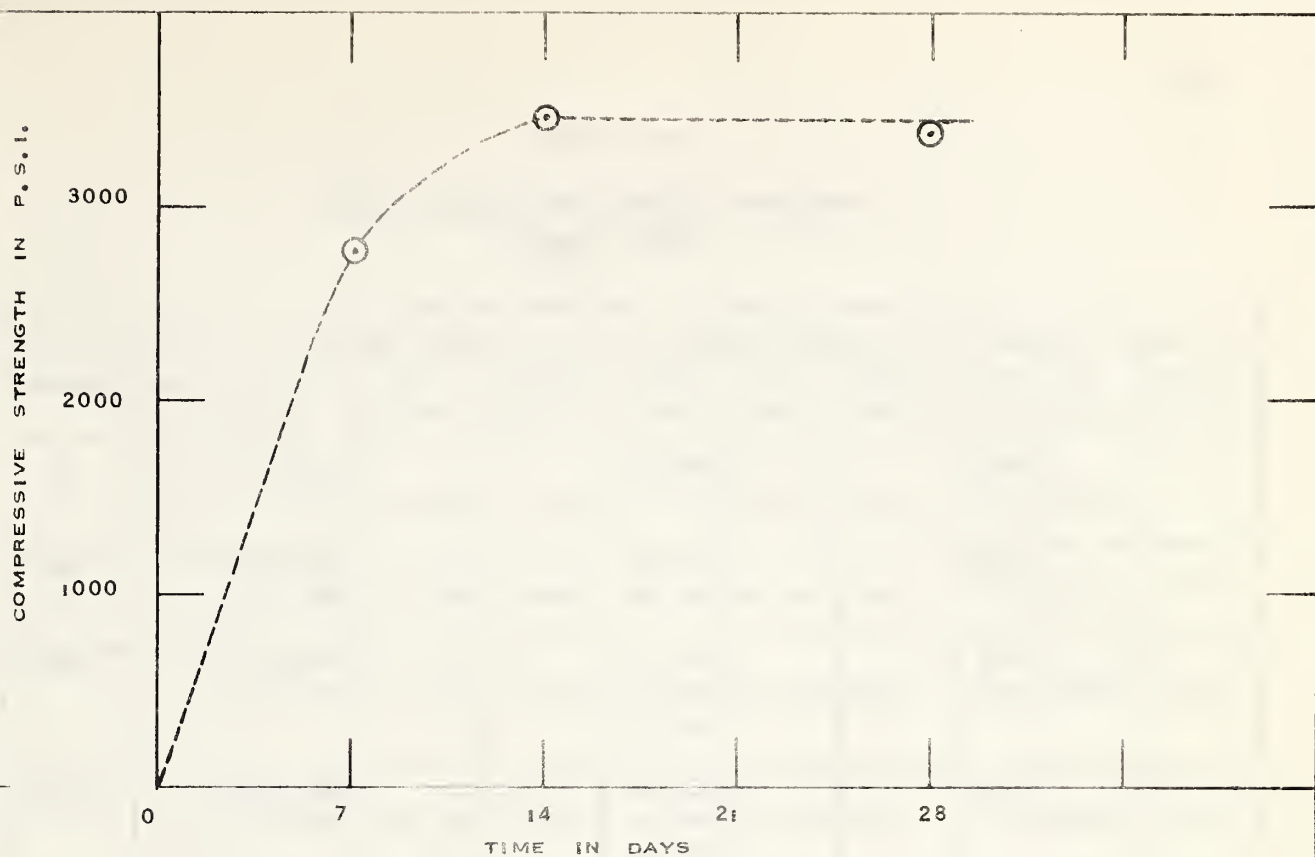


FIGURE 4.5 VARIATION OF CONCRETE COMPRESSIVE STRENGTH WITH TIME

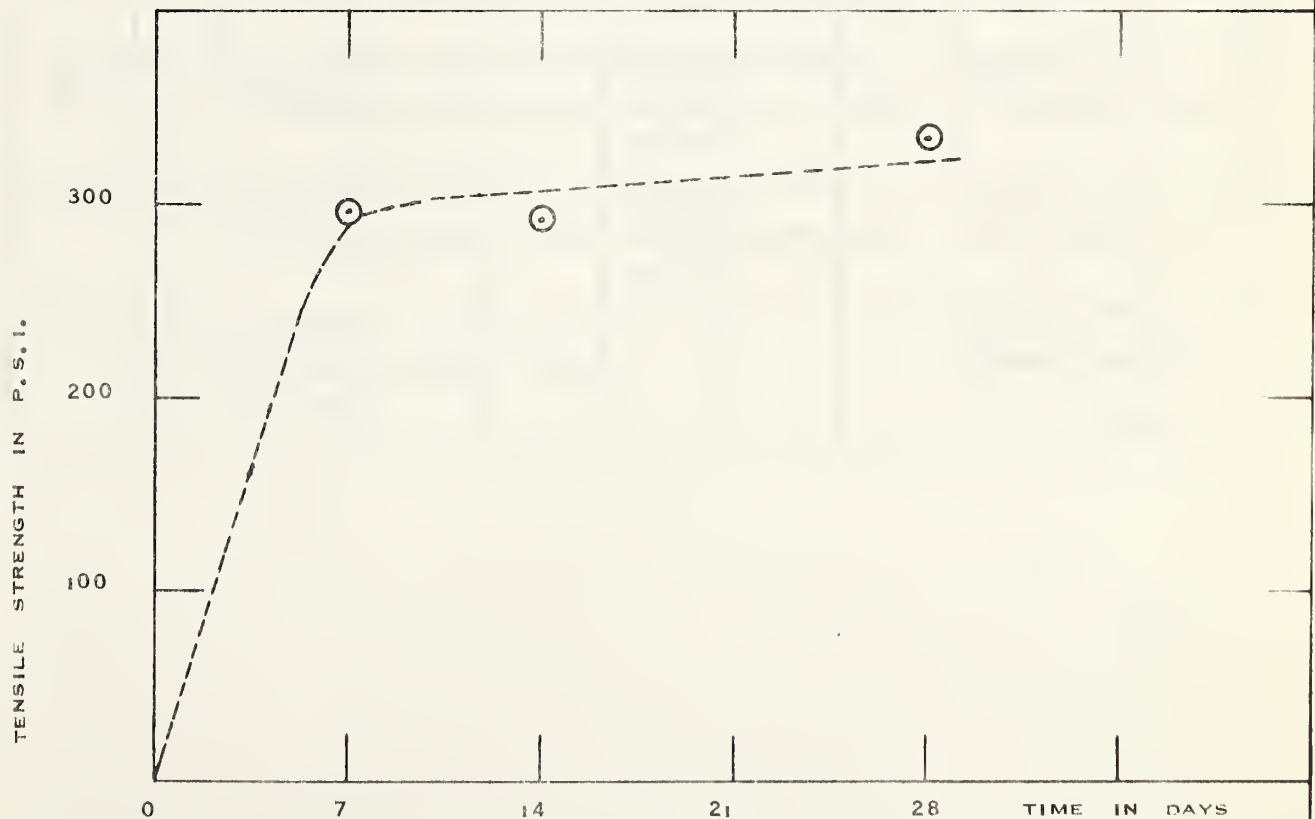


FIGURE 4.6 VARIATION OF CONCRETE TENSILE STRENGTH WITH TIME



TABLE IV-6

TEST RESULTS OF CONTROL SPECIMENS  
(28-DAY TESTS)

Designation	Sp. No.	Comp. Test			Split Test			Mod. of Rup.		
		Load (lbs)	Av. (lbs)	Stress (psi)	Load (lbs)	Av. (lbs)	Stress (psi)	Load (lb)	Av. (lb)	Stress (psi)
A	1	92,000			39,100			2500		
	2	98,500	92,250	3370	36,200	37,650	333	2800	2650	577
B&C	1	86,500			42,400			2800		
	2	114,500	100,500	3560	39,200	40,800	361	2700	2750	599
D&E	1	113,000			41,600			3000		
	2	116,500	114,750	4060	38,300	39,633	350	2800	2900	632
	3				39,000					
F&G	1	106,500			41,000			3000		
	2	103,000	104,750	3710	43,000	41,467	367	3100	3050	664
	3				40,400					
H&I	1	91,500			37,100			3100		
	2	97,000	94,250	3335	36,000	36,700	325	2500	2800	610
	3				37,000					
J&K	1	120,000			42,150			2950		
	2	117,000	118,500	4190	43,900	41,617	368	3000	2975	648
	3				38,800					
L&M	1	116,000			39,800			3100		
	2	116,000	116,000	4105	41,450	40,800	361	3050	3075	670
	3				41,150					
N	1	112,000						2900		
	2	110,000	110,500	3910	-	-	-	2800	2850	621
	3	109,500								



$$Y = \frac{1}{2} \times 3.5 = 1.75 \text{ inches}$$

$$I = \frac{1}{12} bh^3 = \frac{1}{12} \times 4.5 \times 3.5^3$$

$$\begin{aligned} \text{Modulus of rupture} &= \frac{2P \times 1.75}{\frac{1}{12} \times 4.5 \times 3.5^3} \text{ psi} \\ &= \frac{P}{4.59} \text{ psi} \end{aligned}$$

#### 4-6 Description of Test Specimens

A total of 30 specimens were tested in pure torsion. All specimens were square in cross-section. The overall size was 4" x 4" x 4' 6". Of these, three specimens, type A, were of plain concrete. Four specimens had only longitudinal steel: the percentage of longitudinal steel in two beams, type B was 1.23 and in another two beams, type H, was 2.75. The B type beams had 4 and H type beams 9 plain bars of diameter 1/4". All other beams had both longitudinal steel and transverse ties. The percentage of transverse steel varied from nothing to 2.72.

There were three identical beams of type A and three of type N. There were two identical beams of all other types from B through M. At least two beams of each type were made so that an average could be taken. It also helped to make an estimate of the possible variation in strength and behaviour even when the specimens appeared to be identical.

The concrete strength was not intended to be a variable. However, it still varied somewhat with each batch. The companion cylinders and modulus of rupture specimens made with every batch were, however, expected to give the strength properties of the concrete. The cylinder strength varied from 3335 psi to 4190 psi. The tensile strength, as





determined by split tests, varied from 325 to 368 psi. The modulus of rupture ranged from 577 to 670 psi. The details of tests on control specimens are given in TABLE IV-6.

The details of the reinforcement provided in various types are given in TABLE IV-7 and FIGURE 4.7. The strength properties of the concrete in the various types of specimens are also given in TABLE IV-7. The specimens were designed so that the following variables could be studied:

- (i) Longitudinal steel ratio.
- (ii) Transverse steel ratio.
- (iii) Position and size of longitudinal steel.
- (iv) Bar size of ties.
- (v) Effectiveness of ties for two different overlaps, types P&Q.
- (vi) Strength of reinforcing steel.

Specimen types A, B and H were designed to study the first variable viz. longitudinal steel percentage. The percentages of steel in A, B and H types were respectively 0, 1.23 and 2.75. These specimens had no transverse steel in the gage length.

The second variable, the transverse steel ratio, could be studied from series:

(i) specimen types B, C, D, F and G in which the percentages of transverse steel were 0, 0.17, 0.34, 0.51 and 1.02 respectively. The longitudinal steel percentage was constant at 1.23. The size of ties for this series was 0.144" diameter (No. 7 SWG). It was a low strength (Y.P. 24,110 psi, ultimate 42,330 psi) black wire supplied in coils.



(ii) specimen types L, M and N in which the percentages of transverse steel were 0.51, 2.72 and 0.77 respectively. The longitudinal steel percentage was constant at 2.75. No. 2 plain reinforcing bar was used for the ties (Y.P. 47,490 psi, ultimate 56,330 psi).

Specimen types I, J and K were designed to study the third variable, viz. position and size of longitudinal steel. In these specimens, the transverse reinforcement was identical (0.144" dia. ties at 2" spacing). The percentage of longitudinal steel was also constant at 2.75. However, in types I & J the nine No. 2 bars were arranged in two different ways, types S and T (see FIGURE 4.7). In type T, some of the bars had been placed closer to the axis of twist. Specimens K had four bars No. 3 one in each corner.

The behaviour of specimens K and L could be compared to study the fourth variable, the bar size of ties. These specimens had the same longitudinal steel viz. four bars of No. 3. The percentage of transverse steel was also constant at 0.51. However, the size and consequently the spacing was different. Type K had 0.144" wire ties at 2" spacing whereas type L had No. 2 ties at 6" spacing.

The fifth variable, the effectiveness of ties for two different overlaps, could be studied by comparing the behaviour of specimen types D and E. Specimens D and E had all other things same except the overlap used for making the ties. Specimens D had ties with greater overlap as shown in type P and specimens E had ties with lesser overlap as shown in type Q. See FIGURE 4.7.

The last variable, the strength of reinforcing steel could be studied by comparing the performance of two grades of steel used in the ties.



The 0.144" wire had a yield stress of 24,110 psi and ultimate stress of 42,330 psi. The 1/4" bar had a yield stress of 47,490 psi. and ultimate stress of 56,330 psi. Specimens K and L had same longitudinal steel viz. four bars of No. 3. The percentage of transverse steel was also constant at 0.51. However, the properties of the steel used for the ties were different as given above.

The overall length of the specimens was 4' 6". However, 6" at each end was treated as gripping length. The gage length was taken as 30 inches, 15 inches each side of the centre. Thus there was a gap of 6" between the gripping length and gage length. This gap was considered adequate to ensure that the stresses in the gage length were not affected by the distribution of stresses in the gripping length. According to St. Venant's principle, if the forces acting on a small portion of an elastic body are replaced by another statically equivalent system of forces acting on the same portion of the surface, this redistribution of loading produces substantial changes in stresses locally but has negligible effect on the stresses at distances which are large in comparison with the linear dimensions of the surface on which the forces are changed.



TABLE IV-7

## DETAILS OF SPECIMENS

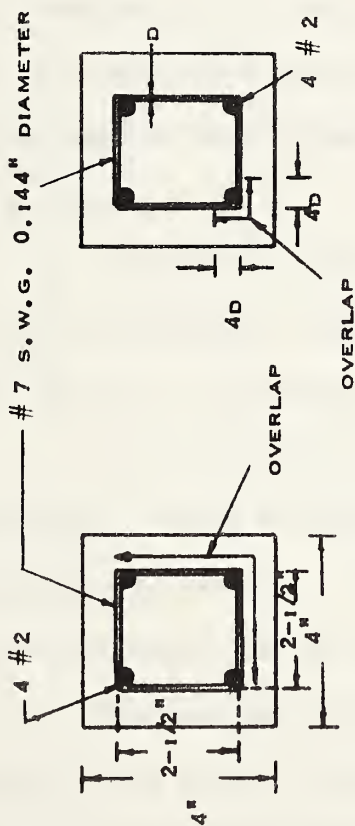
Type	No. of Specimen	Longitudinal Reinforcement		Transverse Reinforcement						P %	P %	28 Day Tests					
		Bars No. & Size	Type*	In Gage Length		Outside Gage Length		Type*	Size (in)			Spacing (in)	Spacing (in)	Type*	Comp (psi)	Split (psi)	Mod. of rupture (psi)
				Size (in)	Spacing (in)	Size (in)	Spacing (in)										
A	3	None	R	None	-	-	1/8	3	P	0	0	3370	333	577			
B	2	4 No. 2 outside gage length	"	"	-	-	"	"	"	1.23	0	3560	361	599			
C	2	"	"	0.144	6	P	0.144	"	"	"	0.17	"	"	"			
D	2	"	"	"	3	"	"	2	"	"	0.34	4060	350	632			
E	2	"	"	"	3	Q	"	"	Q	"	"	"	"	"			
F	2	"	"	"	2	P	"	1-1/2	P	"	0.51	3710	367	664			
G	2	"	"	"	Double at 2"	"	"	Double	"	"	1.02	"	"	"			
H	2	9 No. 2	S	None	-	-	"	3	"	2.75	0	3335	325	610			
I	2	"	"	0.144	2	P	"	1-1/2	"	"	0.51	"	"	"			
J	2	"	T	"	"	"	"	"	"	"	"	4190	368	648			
K	2	4 No. 3	U	"	"	"	"	"	"	"	"	"	"	"			
L	2	"	"	1/4	6	"	1/4	3	"	"	"	4105	361	670			
M	2	"	"	"	Double at 2-1/4	"	"	Double	"	"	2.72	"	"	"			
N	3	"	"	"	4	"	"	3	"	"	0.77	3910	-	621			

\* See FIGURE 4.7





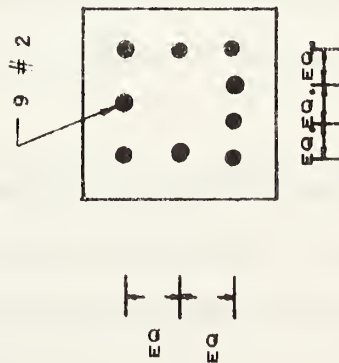
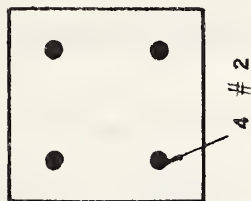




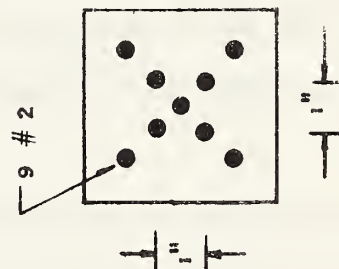
TYPE P

TYPE Q

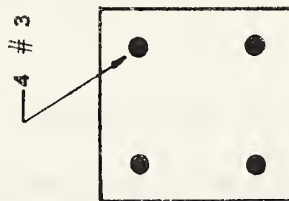
TYPE R



TYPE S



TYPE T



TYPE U

ALL TIES 2-1/2" x 2-1/2"  
ON CENTRE LINES

FIGURE 4.7 REINFORCEMENT DETAILS.

SCALE 1/4 FULL SIZE.



## CHAPTER V

### PRESENTATION OF TEST RESULTS

#### 5-1 The Testing Procedure

The specimens and the control cylinders were cured in the moist room till they were tested on the 28th day of their casting. For testing a specimen, it was fixed in the two grips of the testing rig by wooden blocks and wedges. The twistmeters were placed symmetrically at the two ends of the gage length of 30". The electrical strain gages were connected to the strain indicator through a twenty-point switching unit in cases where there were two or more gages on the same specimen. All connections were soldered and the length of the leads was kept to the minimum.

The rate of loading for all specimens was maintained constant at 2 lbs. per minute. Hence the twisting moment increased at the rate of about 100 lb.in. per minute.

The staff reading and the lever arm were co-related by direct measurement. TABLE V-1 shows the measured lengths of lever arm for the observed staff readings. FIGURE 5.1 shows a graph of co-relation between the staff reading and the lever arm.

The readings of the two twistmeters, the staff reading and the reading on the strain indicator were recorded immediately after each load increment. The bubbles on the twistmeters were brought to centre simultaneously before reading the micrometers.



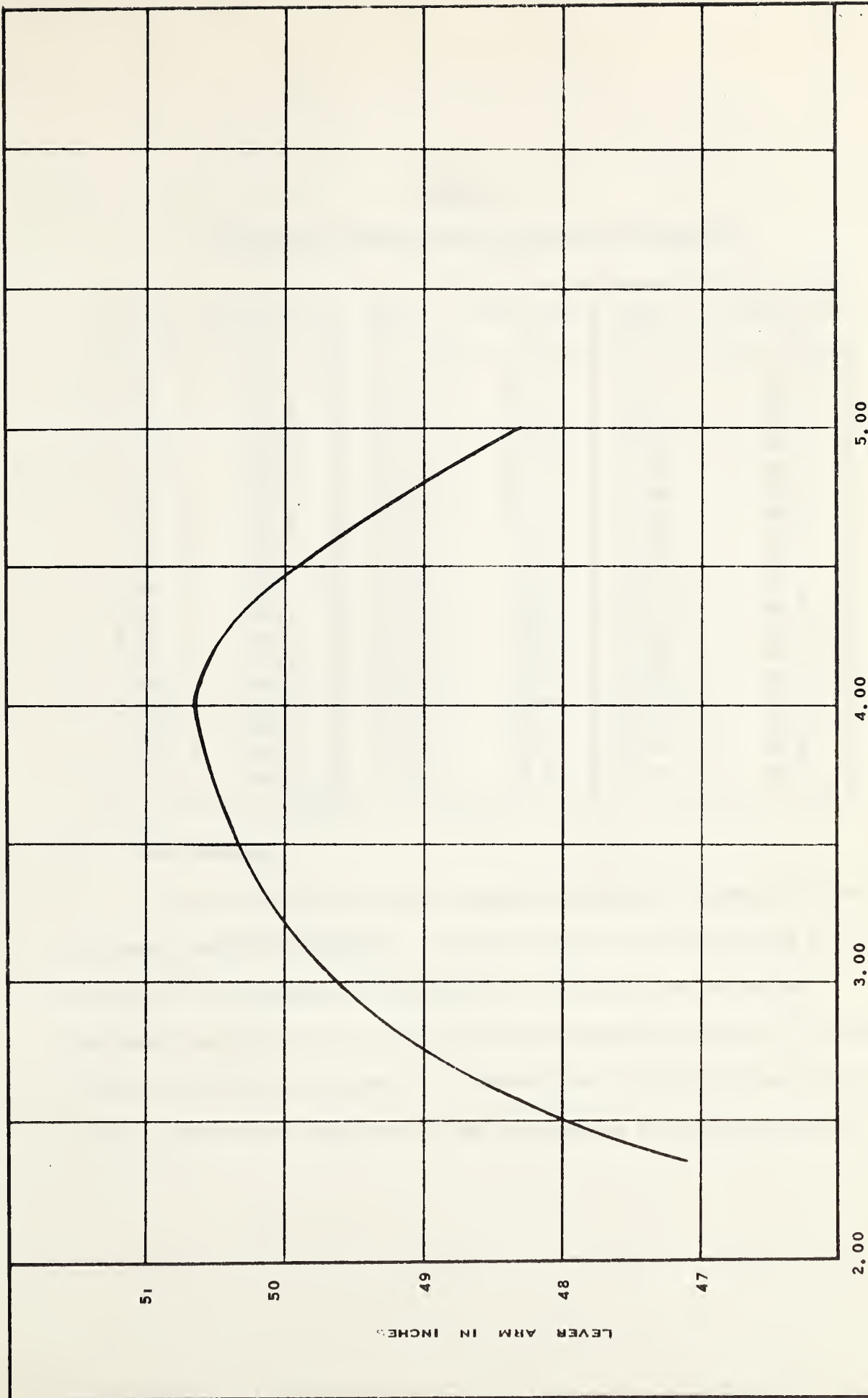


FIGURE 5.1 CO-RELATION BETWEEN STAFF READING AND LEVER ARM



TABLE V-1  
CO-RELATION BETWEEN STAFF READING AND LEVER-ARM

Staff (ft)	Lever Arm (in)	Staff (ft)	Lever Arm (in)	Staff (ft)	Lever Arm (in)
2.35	47.1	3.25	50.0	4.15	50.6
2.40	47.4	3.30	50.1	4.20	50.5
2.45	47.7	3.35	50.2	4.25	50.5
2.50	48.0	3.40	50.2	4.30	50.4
2.55	48.2	3.45	50.3	4.35	50.3
2.60	48.5	3.50	50.3	4.40	50.2
2.65	48.6	3.55	50.4	4.45	50.0
2.70	48.8	3.60	50.4	4.50	49.9
2.75	49.0	3.65	50.5	4.55	49.8
2.80	49.1	3.70	50.5	4.60	49.7
2.85	49.2	3.75	50.5	4.65	49.5
2.90	49.4	3.80	50.6	4.70	49.4
2.95	49.5	3.85	50.6	4.75	49.2
3.00	49.6	3.90	50.6	4.80	49.1
3.05	49.7	3.95	50.6	4.85	48.9
3.10	49.8	4.00	50.6	4.90	48.7
3.15	49.9	4.05	50.6	4.95	48.6
3.20	49.9	4.10	50.6	5.00	48.4

## 5-2 Test Results

The observed and the calculated values are presented in the following TABLES AND FIGURES. The full details of calculations are shown only for specimen A.1 (TABLE V-2). Calculations for other specimens were similar and have not been presented in detail. The calculated values are presented in a tabular form. Following each table a brief note on the behaviour of the specimen up to failure is given.





TABLE V-2

## SPECIMEN A.1

Weight added (lbs)	Total Weight (lbs)	Effective Weight (lbs)	Staff Reading (ft)	Lever Arm (in)	Effective Twisting Moment (lb.in)	Movable End Bubble (in)	Different d <sub>1</sub> (in)	Fixed End Bubble (in)	Difference d <sub>2</sub> (in)	d <sub>1</sub> -d <sub>2</sub> (in)	Rotation per inch x 10 <sup>-6</sup> (Radians)
0	0	0	4.68	49.4	0	0.686	-	0.752	-	-	-
19.5	19.5	18.5	4.66	49.5	920	0.718	0.032	0.780	0.028	0.004	8.9
20.2	39.7	38.7	4.61	49.7	1920	0.871	0.185	0.924	0.172	0.013	28.9
20.6	60.3	59.3	4.53	49.8.	2950	1.117	0.431	1.157	0.405	0.026	57.8
20.4	80.7	79.7	4.46	50.0	4040	1.318	0.632	1.345	0.593	0.039	86.7
20.5	101.2	100.2	-	50.0	5010	-	-	-	-	-	-

The specimen A.1 collapsed due to diagonal tension at the formation of first 45° crack a few seconds after the application of the last load increment. The failure was sudden, brittle and without warning. The fracture occurred at about 15" from the fixed grip well within the gage length.



TABLE V-3

## SPECIMEN A.2

Effective Dead Weight (lbs)	Effective Twisting Moment (lb.in)	Rotation per inch $\times 10^{-6}$ (Radians)	Remarks
0	0	0	cracking and collapse
18.5	920	11.1	
38.7	1920	28.9	
59.7	2970	51.1	
79.7	3980	71.1	
100.2	5010	111	
117.3	5870	-	

The failure was brittle and sudden. The failure occurred as soon as the  $45^{\circ}$  diagonal tension crack developed.

TABLE V-4

## SPECIMEN A.3

Effective Dead Weight (lbs)	Effective Twisting Moment (lb.in)	Rotation per inch $\times 10^{-6}$ (Radians)	Remarks
0	0	0	cracking and collapse
18.5	910	8.9	
38.7	1910	26.7	
59.3	2940	42.2	
79.7	3980	62.2	
100.2	5010	104	
120.5	6050	138	
131.1	6580	-	

Failure was brittle and sudden. Breakdown occurred immediately on the development of  $45^{\circ}$  diagonal tension crack.



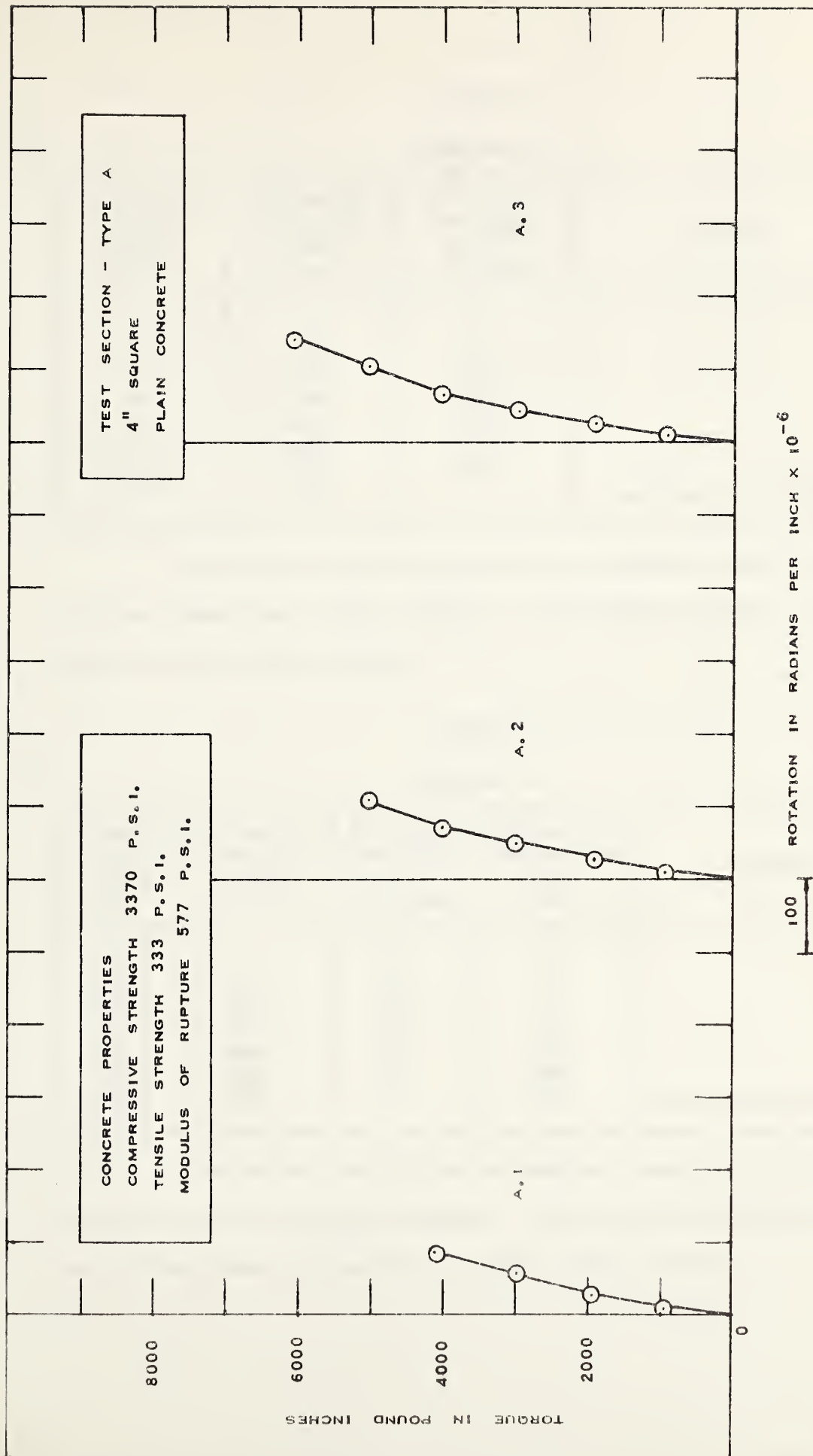


FIGURE 5.2 TORQUE ROTATION CURVES - SPECIMENS A



TABLE V-5

## SPECIMEN B.1

Effective Dead Weight (lbs)	Effective Twisting Moment (lb.in)	Rotation per inch $\times 10^{-6}$ (Radians)	Remarks
0	0	0	cracking and collapse
18.5	910	13.3	
38.7	1910	28.9	
59.3	2930	48.9	
79.7	3950	68.9	
100.2	4980	97.8	
120.5	6000	136	
140.9	7020	-	

The failure, which occurred due to diagonal tension, was brittle, sudden and without warning. The breakdown occurred a few seconds after the last load increment.

TABLE V-6

## SPECIMEN B.2

Effective Dead Weight (lbs)	Effective Twisting Moment (lb.in)	Rotation per inch $\times 10^{-6}$ (Radians)	Stress in Longitudinal Steel (psi)	Remarks
0	0	0	0	cracking and collapse
18.5	910	11.1	0	
38.7	1910	31.1	0	
59.3	2930	62.2	150	
79.7	3950	147	450	
100.2	4990	300	1800	
110.4	5500	-	5700	

The failure was brittle and sudden. There was no sign of distress up to the last load increment. The breakdown followed immediately on the development of the first diagonal tension crack.





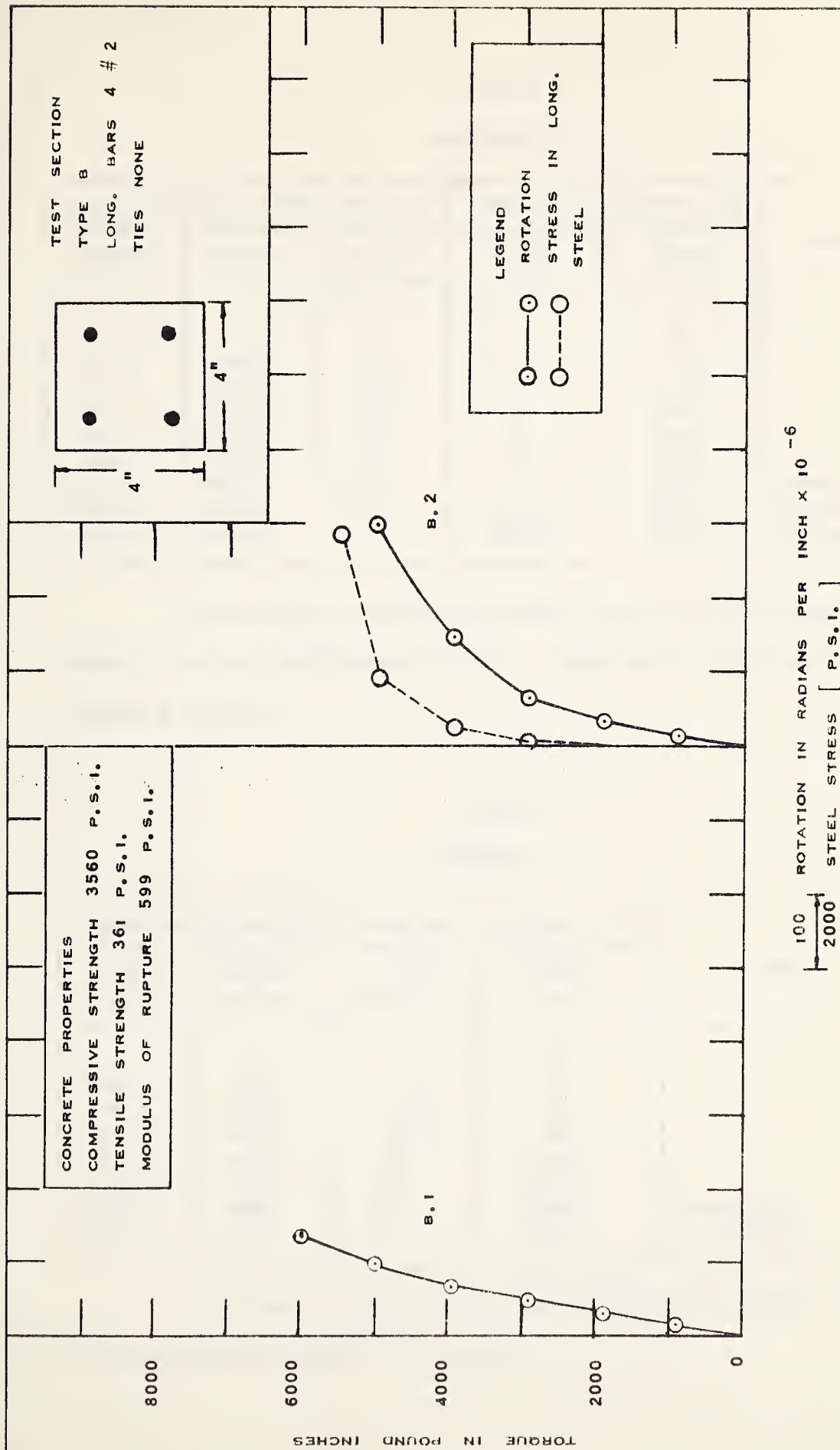


FIGURE 5.3 TORQUE-ROTATION AND TORQUE-STEEL STRESS CURVES  
SPECIMENS B



TABLE V-7  
SPECIMEN C.1

Effective Dead Weight (lbs)	Effective Twisting Moment (lb.in)	Rotation per inch $\times 10^{-6}$ (Radians)	Stress in Longitudinal Steel (psi)	Stress in Transverse Steel (psi)	Remarks
0	0	0	0	0	
18.5	920	13.3	0	750	
38.7	1920	28.9	0	1350	
59.3	2950	46.7	0	1800	
79.7	3960	73.3	0	2850	
100.2	5000	113	0	3450	
120.5	6030	231	0	4650	cracking
130.3	6540	522	5100	6450	cracks widened
135.3	6790	-	6300	7950	collapse

The failure occurred soon after the last load increment. The cause of failure was diagonal tension. There was a little warning of the impending distress.

TABLE V-8  
SPECIMEN C.2

Effective Dead Weight (lbs)	Effective Twisting Moment (lb.in)	Rotation per inch $\times 10^{-6}$ (Radians)	Stress in Longitudinal Steel (psi)	Remarks
0	0	0	0	
18.5	920	13.3	0	
38.7	1920	35.6	600	
59.3	2950	62.2	900	
79.7	3980	88.9	1050	
100.2	5010	116	1200	
120.5	6050	149	1800	cracking
124.5	6250	-	12600	collapse

The cause of failure was diagonal tension distress. The breakdown occurred with very little warning.



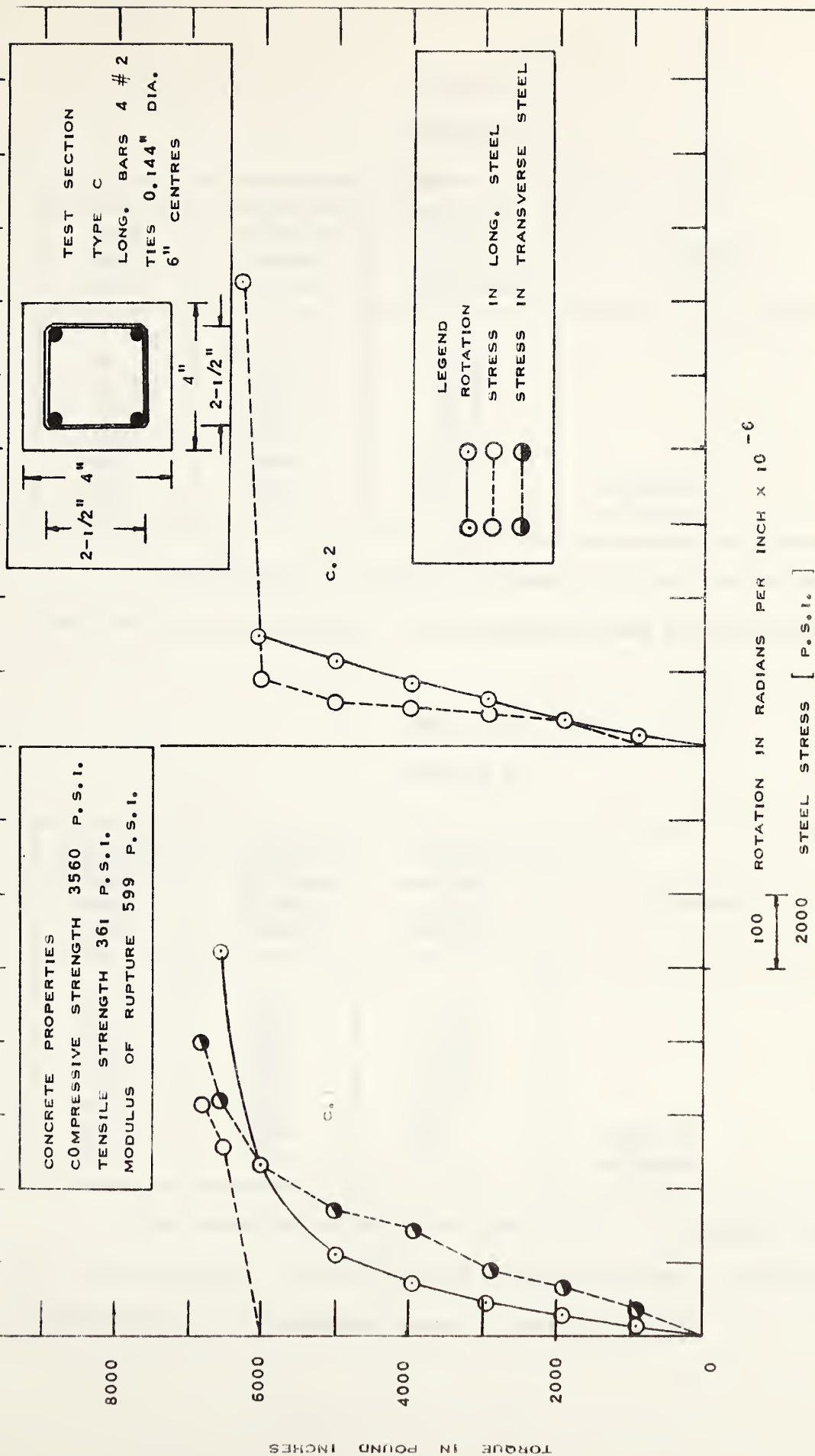


FIGURE 5.4 TORQUE - ROTATION AND TORQUE -STEEL STRESS CURVES  
 SPECIMENS C



TABLE V-9  
SPECIMEN D.1

Effective Dead Weight (lbs)	Effective Twisting Moment (lb.in)	Rotation per inch $\times 10^{-6}$ (Radians)	Remarks
0	0	0	
18.5	910	15.6	
38.7	1910	33.3	
59.3	2940	55.6	
79.7	3950	77.8	
100.2	4980	116	
120.5	6000	164	cracking
140.9	7020	-	collapse

The breakdown occurred at the centre of the specimen soon after the last load increment. The specimen showed a little ductility.

TABLE V-10  
SPECIMEN D.2

Effective Dead Weight (lbs)	Effective Twisting Moment (lb.in)	Rotation per inch $\times 10^{-6}$ (Radians)	Remarks
0	0	0	
18.5	920	15.6	
38.7	1920	35.6	
59.3	2940	60.0	
79.7	3950	88.9	
100.2	4980	124	
120.5	6000	931	cracking
130.3	6540	-	collapse

The breakdown occurred near the centre a few seconds after last load increment. The  $45^{\circ}$  helical cracks developed at other sections before failure. The specimen showed a little ductility.





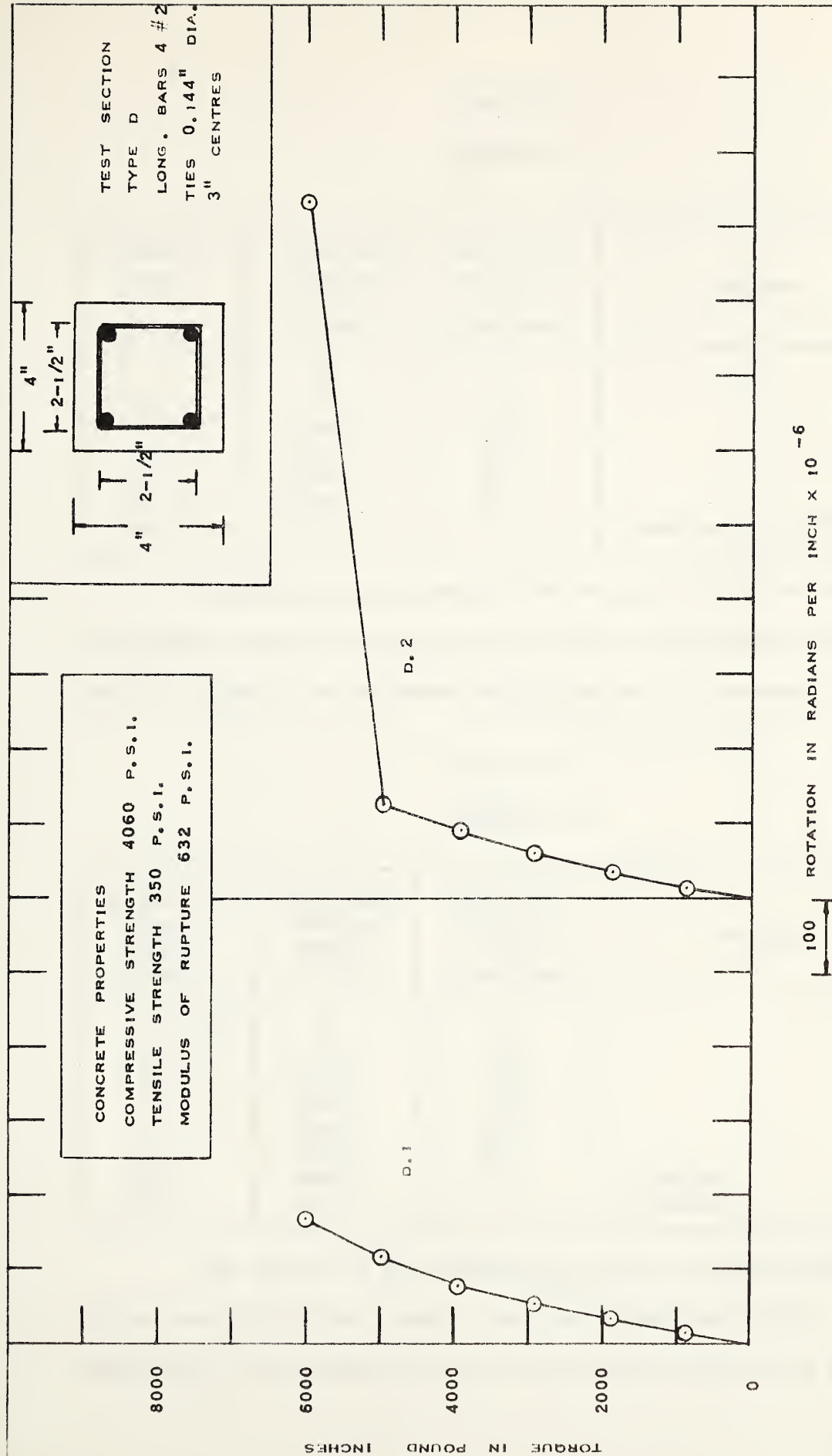


FIGURE 5.5 TORQUE-ROTATION CURVES - SPECIMENS D



TABLE V-11

## SPECIMEN E.1

Effective Dead Weight (lbs)	Effective Twisting Moment (lb.in)	Rotation per inch $\times 10^{-6}$ (Radians)	Remarks
0	0	0	cracking and collapse
18.5	910	15.6	
38.7	1900	33.3	
59.3	2920	60.0	
79.7	3940	91.1	
100.2	4960	122	
120.5	5970	-	

The breakdown occurred at the centre. The failure was due to diagonal tension. The failure was brittle and without warning. The ties had opened up and appeared ineffective due to inadequate overlap.

TABLE V-12

## SPECIMEN E.2

Effective Dead Weight (lbs)	Effective Twisting Moment (lb.in)	Rotation per inch $\times 10^{-6}$ (Radians)	Remarks
0	0	0	cracking collapse
18.5	920	13.3	
38.7	1920	33.3	
59.3	2940	57.8	
79.7	3960	84.4	
100.2	4990	120	
120.5	6000	162	
130.3	6540	-	

The failure of the specimen was due to diagonal tension. The failure was brittle and sudden. The ties seemed ineffective. They had opened up in that portion of the specimen where concrete was destroyed.



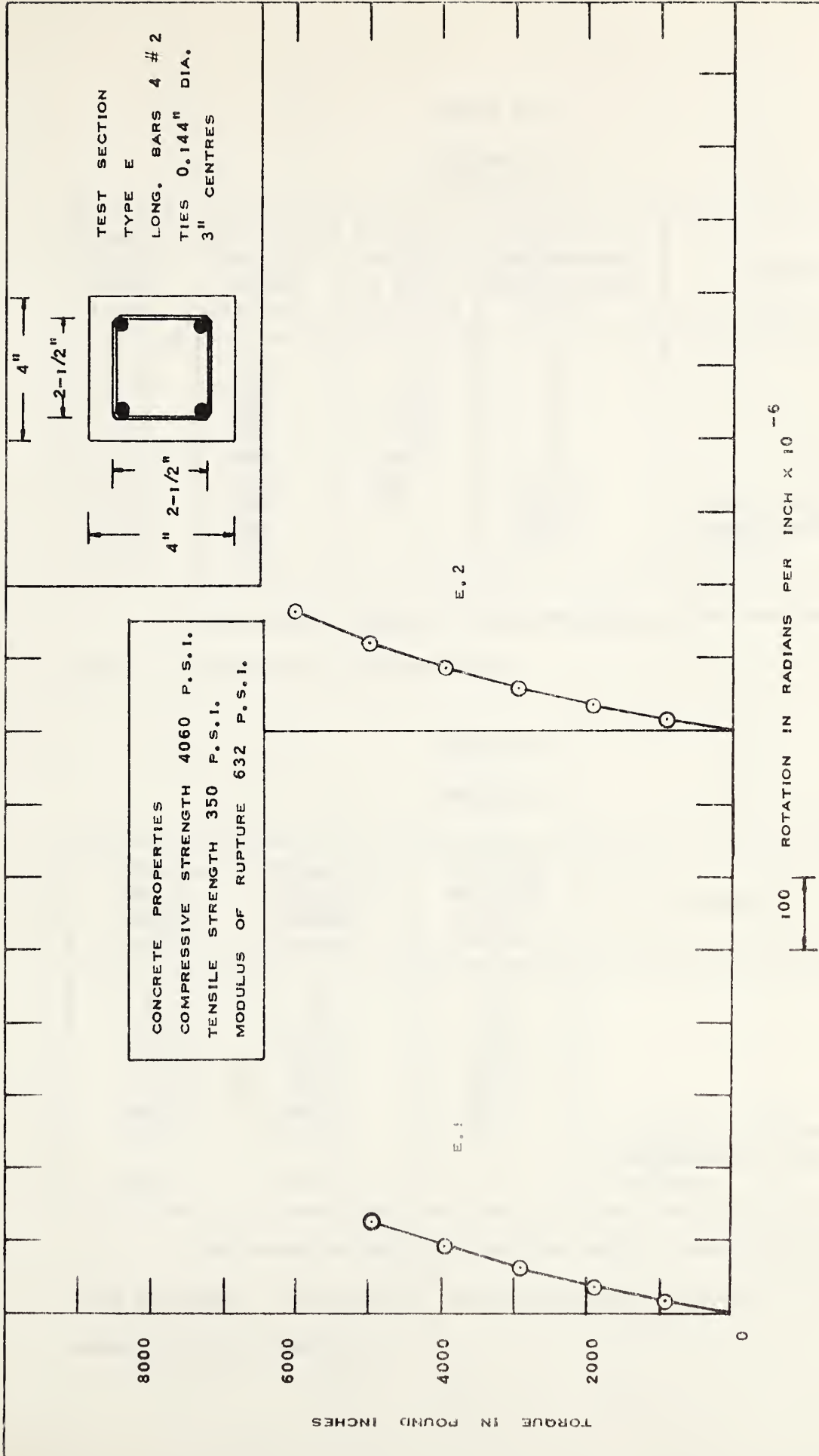


FIGURE 5.6 TORQUE - ROTATION CURVES SPECIMENS E



TABLE V-13

## SPECIMEN F.1

Effective Dead Weight (lbs)	Effective Twisting Moment (lb.in)	Rotation per inch $\times 10^{-6}$ (Radians)	Stress in Longitudinal Reinforcement (psi)	Remarks
0	0	0	0	fine cracks cracks widened collapse
18.5	910	15.6	0	
38.7	1900	28.9	0	
59.3	2920	53.3	0	
79.7	3940	68.9	0	
100.2	4960	109	150	
120.5	5990	296	8100	
130.6	6490	-	16350	
143.9	7190	-	-	

The specimen showed a little ductility. The breakdown occurred almost at the centre of the specimen.

TABLE V-14

## SPECIMEN F.2

Effective Dead Weight (lbs)	Effective Twisting Moment (lb.in)	Rotation per inch $\times 10^{-6}$ (Radians)	Remarks
0	0	0	cracking. 45° crack ran across whole width collapse
18.5	910	11.1	
38.7	1910	31.1	
59.3	2940	53.3	
79.7	3950	80.0	
100.2	4990	113	
120.5	6010	153	
139.6	6970	-	

The breakdown occurred near the centre soon after the last load increment. The cause of failure was diagonal tension. The specimen showed a little ductility.





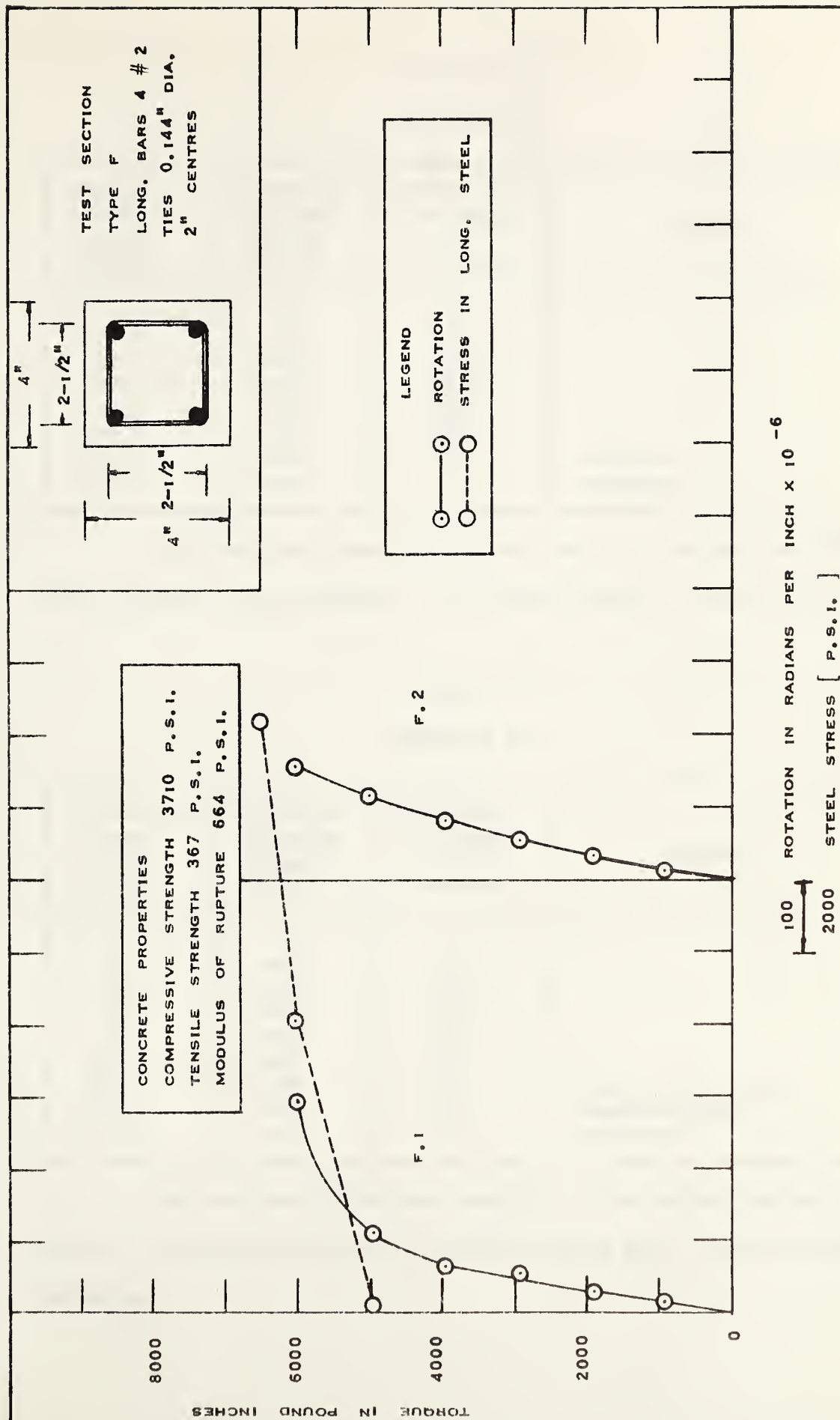


FIGURE 5.7 TORQUE - ROTATION AND TORQUE -STEEL STRESS CURVES  
 SPECIMENS F



TABLE V-15

## SPECIMEN G.1

Effective Dead Weight (lbs)	Effective Twisting Moment (lb.in)	Rotation per inch $\times 10^{-6}$ (Radians)	Remarks
0	0	0	
18.5	910	15.6	
38.7	1900	35.6	
59.3	2910	60.0	
79.7	3920	86.7	
100.2	4940	122	
120.5	5970	160	cracking
140.9	6980	-	collapse

The breakdown occurred near the centre of the specimen soon after the last load increment. The specimen showed a little ductility.

TABLE V-16

## SPECIMEN G.2

Effective Dead Weight (lbs)	Effective Twisting Moment (lb.in)	Rotation per inch $\times 10^{-6}$ (Radians)	Remarks
0	0	0	
18.5	910	15.6	
38.7	1910	37.8	
59.3	2940	62.2	
79.7	3950	91.1	
100.2	4980	133	
120.5	6000	167	fine cracks at 45°
140.9	7030	236	cracks widened
151.0	7540	-	collapse

The specimen showed some ductility. The failure was due to diagonal tension. The breakdown occurred near the centre soon after last load increment.



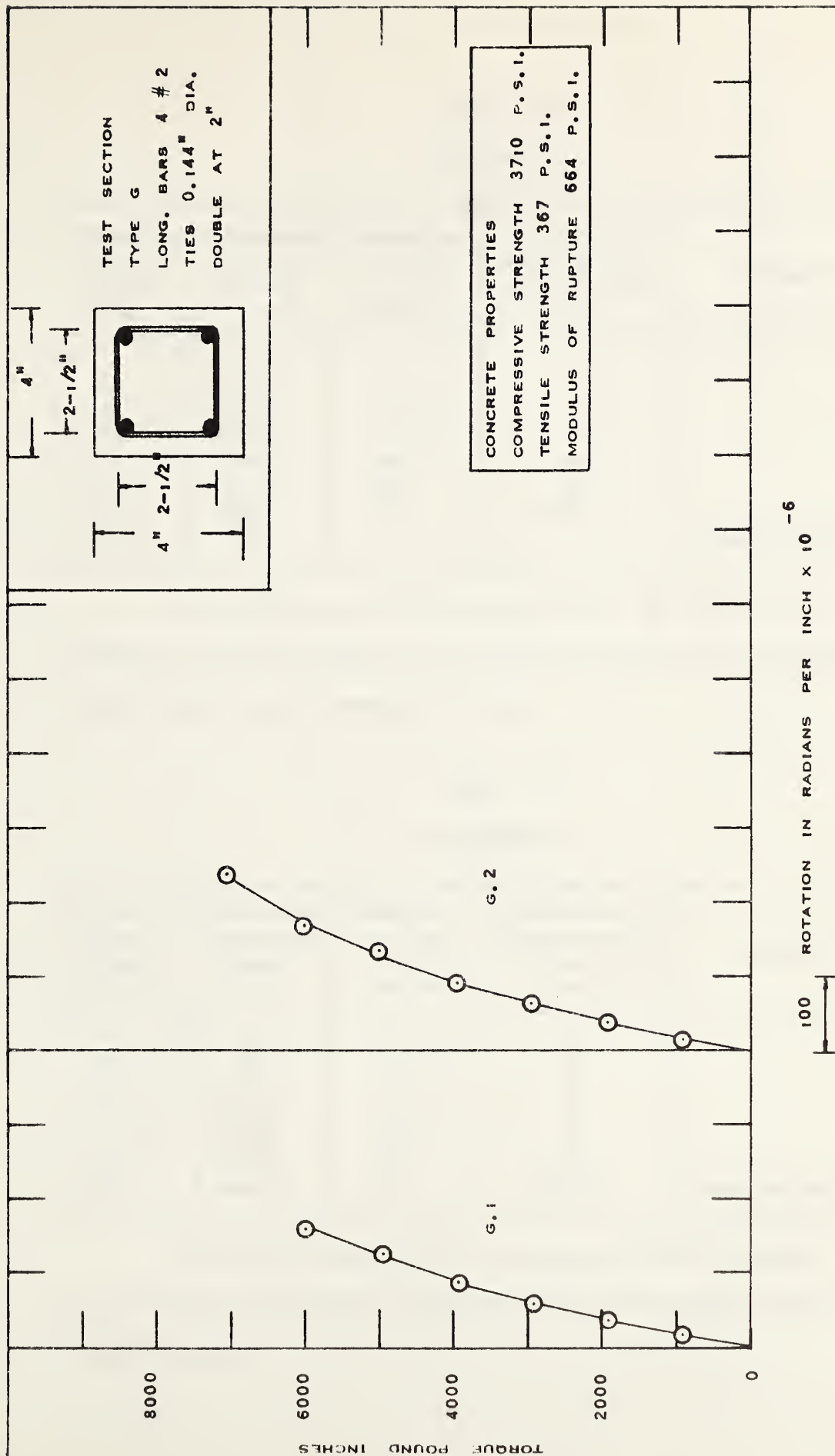


FIGURE 5.8 TORQUE -- ROTATION CURVES SPECIMENS G



TABLE V-17

## SPECIMEN H.1

Effective Dead Weight (lbs)	Effective Twisting Moment (lb.in)	Rotation per inch $\times 10^{-6}$ (Radians)	Stress in Corner Longitudinal bar (psi)	Remarks
0	0	0	0	cracking and collapse
18.5	920	15.6	0	
38.7	1930	35.6	0	
59.3	2950	57.8	0	
79.7	3980	86.7	150	
100.2	5010	120	600	
120.5	6030	171	1950	
140.9	7050	-	-	

The failure was brittle and sudden. No cracks were visible till breakdown occurred suddenly. The failure occurred due to diagonal tension a minute after last increment of load.

TABLE V-18

## SPECIMEN H.2

Effective Dead Weight (lbs)	Effective Twisting Moment (lb.in)	Rotation per inch $\times 10^{-6}$ (Radians)	Stress in Corner Longitudinal bar (psi)	Remarks
0	0	0	0	cracking and collapse
18.5	910	15.6	0	
38.7	1910	33.3	0	
59.3	2930	57.8	0	
79.7	3950	80.0	0	
100.2	4980	111	300	
120.5	6000	213	4200	

The failure was brittle, sudden and without warning. The breakdown occurred five minutes after the last load increment due to diagonal tension distress.





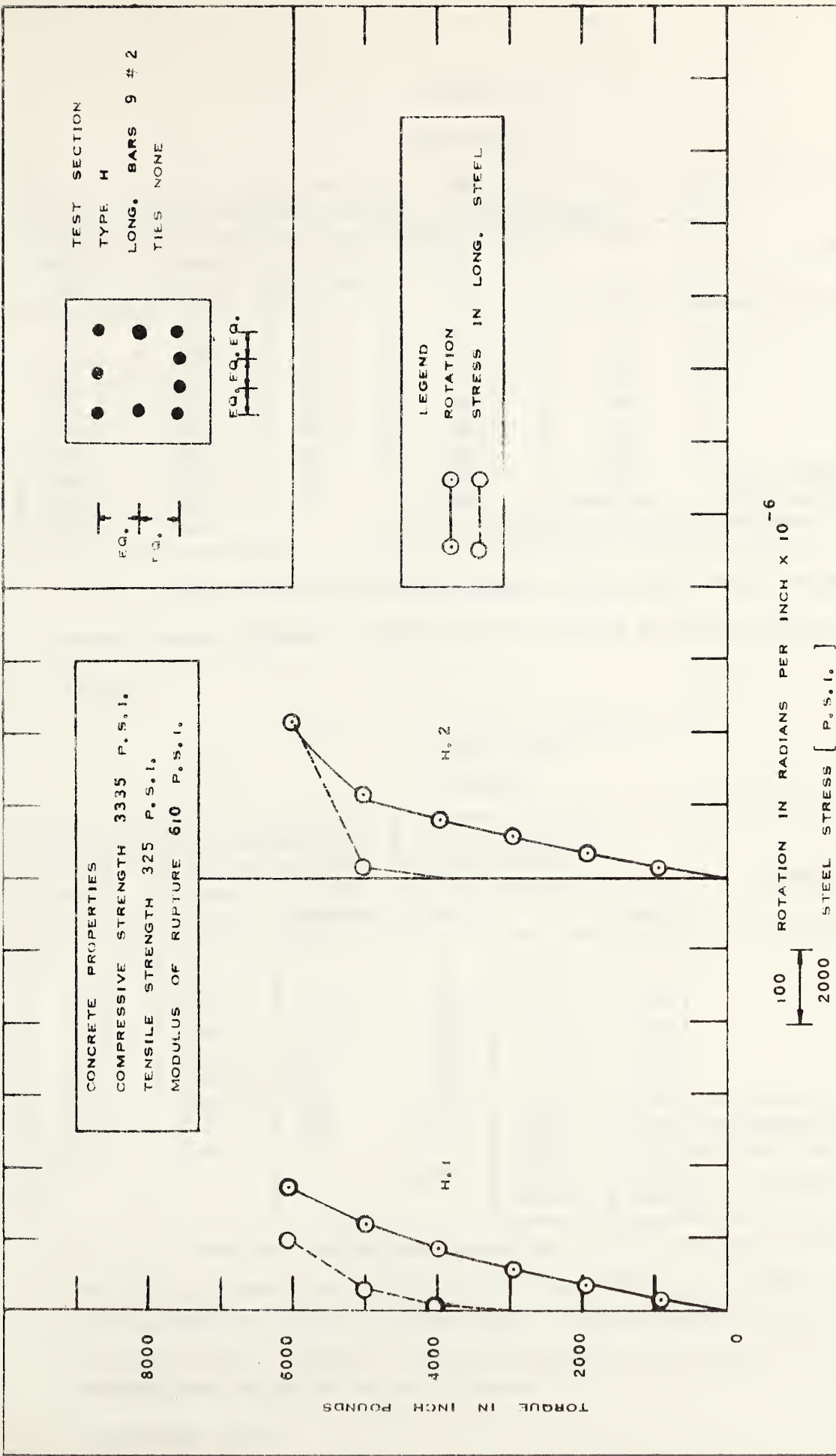


FIGURE 5.9 TORQUE - ROTATION TORQUE - STEEL STRESS CURVES  
SPECIMENS H

11  
 12  
 13  
 14  
 15  
 16  
 17  
 18  
 19  
 20  
 21  
 22  
 23  
 24  
 25  
 26  
 27  
 28  
 29  
 30  
 31  
 32  
 33  
 34  
 35  
 36  
 37  
 38  
 39  
 40  
 41  
 42  
 43  
 44  
 45  
 46  
 47  
 48  
 49  
 50  
 51  
 52  
 53  
 54  
 55  
 56  
 57  
 58  
 59  
 60  
 61  
 62  
 63  
 64  
 65  
 66  
 67  
 68  
 69  
 70  
 71  
 72  
 73  
 74  
 75  
 76  
 77  
 78  
 79  
 80  
 81  
 82  
 83  
 84  
 85  
 86  
 87  
 88  
 89  
 90  
 91  
 92  
 93  
 94  
 95  
 96  
 97  
 98  
 99  
 100

1  
 2  
 3  
 4  
 5  
 6  
 7  
 8  
 9  
 10  
 11  
 12  
 13  
 14  
 15  
 16  
 17  
 18  
 19  
 20  
 21  
 22  
 23  
 24  
 25  
 26  
 27  
 28  
 29  
 30  
 31  
 32  
 33  
 34  
 35  
 36  
 37  
 38  
 39  
 40  
 41  
 42  
 43  
 44  
 45  
 46  
 47  
 48  
 49  
 50  
 51  
 52  
 53  
 54  
 55  
 56  
 57  
 58  
 59  
 60  
 61  
 62  
 63  
 64  
 65  
 66  
 67  
 68  
 69  
 70  
 71  
 72  
 73  
 74  
 75  
 76  
 77  
 78  
 79  
 80  
 81  
 82  
 83  
 84  
 85  
 86  
 87  
 88  
 89  
 90  
 91  
 92  
 93  
 94  
 95  
 96  
 97  
 98  
 99  
 100

1911



TABLE V-19

## SPECIMEN I.1

Effective Dead Weight (lbs)	Effective Twisting Moment (lb.in)	Rotation per inch $\times 10^{-6}$ (Radians)	Steel Stress		Remarks
			Longitudinal Bar No. 1* (psi)	Tie (psi)	
0	0	0	0	0	
18.5	910	13.3	0	150	
38.7	1920	33.3	150	300	
59.3	2940	60.0	300	450	
79.7	3950	88.9	450	600	
100.2	4990	131	900	750	
120.5	6010	222	8100	6750	fine cracks at 45° 45° cracks at 4 places collapse
140.9	7050	733	15300	creeping	
151.1	7560	-	yield stress	yield stress	

The specimen showed appreciable ductility. The cracking was wide-spread before collapse. The breakdown occurred at the centre due to diagonal tension.

TABLE V-20

## SPECIMEN I.2

Effective Dead Weight (lbs)	Effective Twisting Moment (lb.in)	Rotation per inch $\times 10^{-6}$ (Radians)	Steel Stress		Tie (psi)	Remarks
			Longitudinal cor.bar (psi)	Bar No.1* (psi)		
0	0	0	0	0	0	
18.5	910	11.1	0	0	0	
38.7	1910	31.1	150	0	150	
59.3	2940	62.2	300	0	300	
79.7	3970	86.7	450	0	450	
100.2	4990	142	750	0	600	
120.5	6030	224	1350	300	1050	fine cracks at 45° wide-spread 45° cracks at load increment at collapse
140.9	7070	578	9000	6900	3600	
151.1	7600	-	-	12000	6150	
			34200	yield stress	yield stress	

There was appreciable creeping at effective load of 140.9 lbs.

The steel stresses rose from 9000, 6900 and 3600 psi as shown in table to 10,500, 9000 and 4500 psi respectively. The breakdown occurred five minutes after last load increment. The specimen showed appreciable ductility. The cracking was extensive before collapse.

\*See FIGURE 5.10



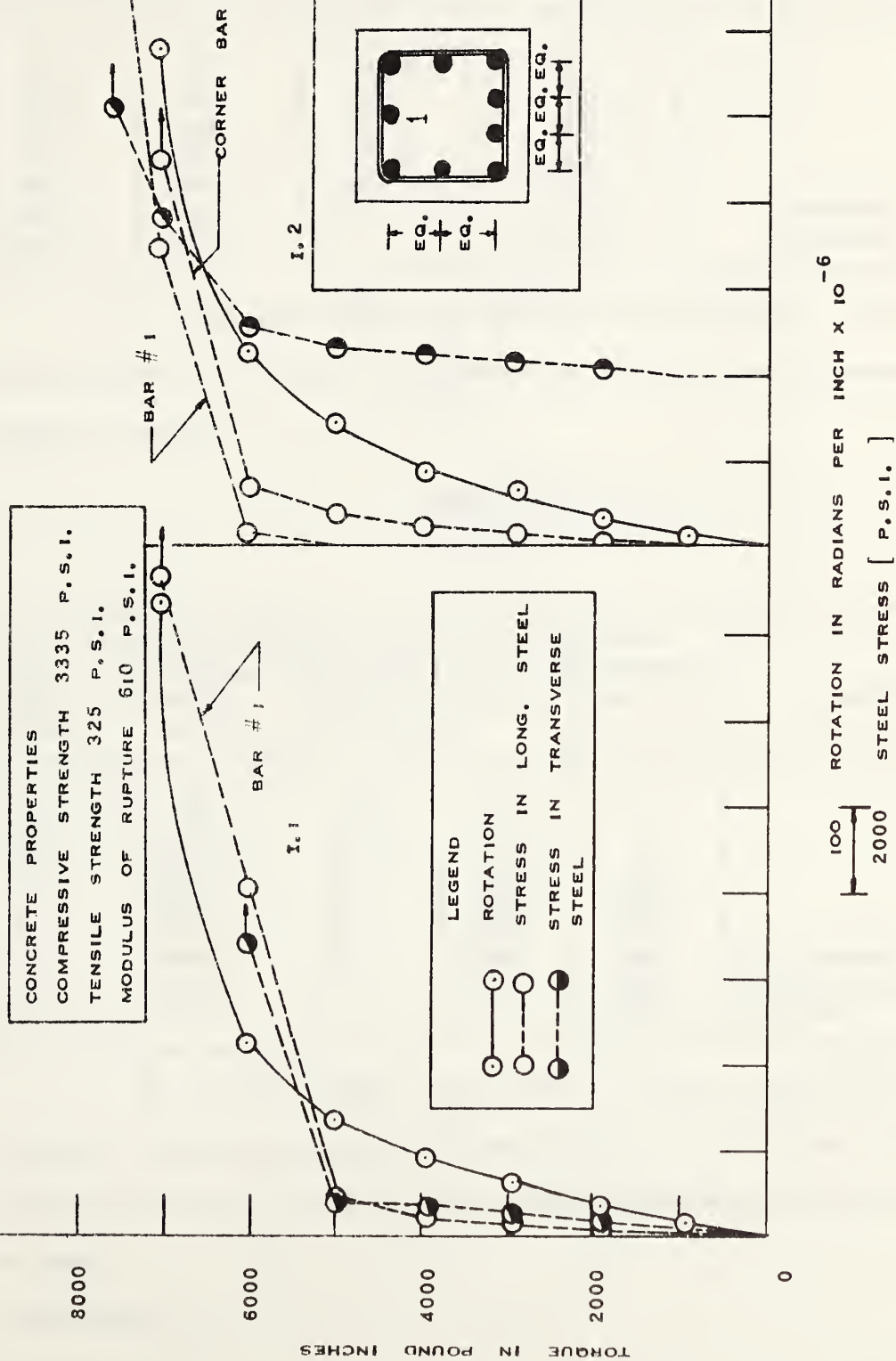


FIGURE 5.10 TORQUE - ROTATION AND TORQUE - STEEL STRESS CURVES  
 SPECIMENS I





TABLE V-21  
SPECIMEN J.1

Effective Dead Weight (lbs)	Effective Twisting Moment (lb.in)	Rotation per inch $\times 10^{-6}$ (Radians)	Stress in Longitudinal Bar No.1* (psi)	Remarks
0	0	0	0	cracking collapse
18.5	910	8.9	0	
38.7	1910	26.7	150	
59.3	2930	55.6	300	
79.7	3950	82.2	300	
100.2	4990	111	450	
120.5	6010	171	1050	
140.9	7030	-	13950	

The specimen showed some ductility before failure. The break-down occurred at the centre a minute after the last load increment due to diagonal tension.

TABLE V-22  
SPECIMEN J.2

Effective Dead Weight (lbs)	Effective Twisting Moment (lb.in)	Rotation per inch $\times 10^{-6}$ (Radians)	Steel Stresses		Remarks
			Bar No.1*	Bar No.2*	
0	0	0	0	0	fine cracks at 45° cracks widened collapse
18.5	920	15.6	0	0	
38.7	1920	37.8	150	0	
59.3	2940	66.7	600	150	
79.7	3960	116	4500	1800	
100.2	4990	300	10350	5700	
120.5	6050	653	14700	9000	
130.7	6570	987	17250	9900	
141.2	7100	-	-	12000	

The specimen showed some ductility before ultimate load was reached. There was extensive diagonal tension splitting over a length of 15" near the centre of the specimen. There were wide-spread 45° cracks before collapse.

\*See FIGURE 5.11





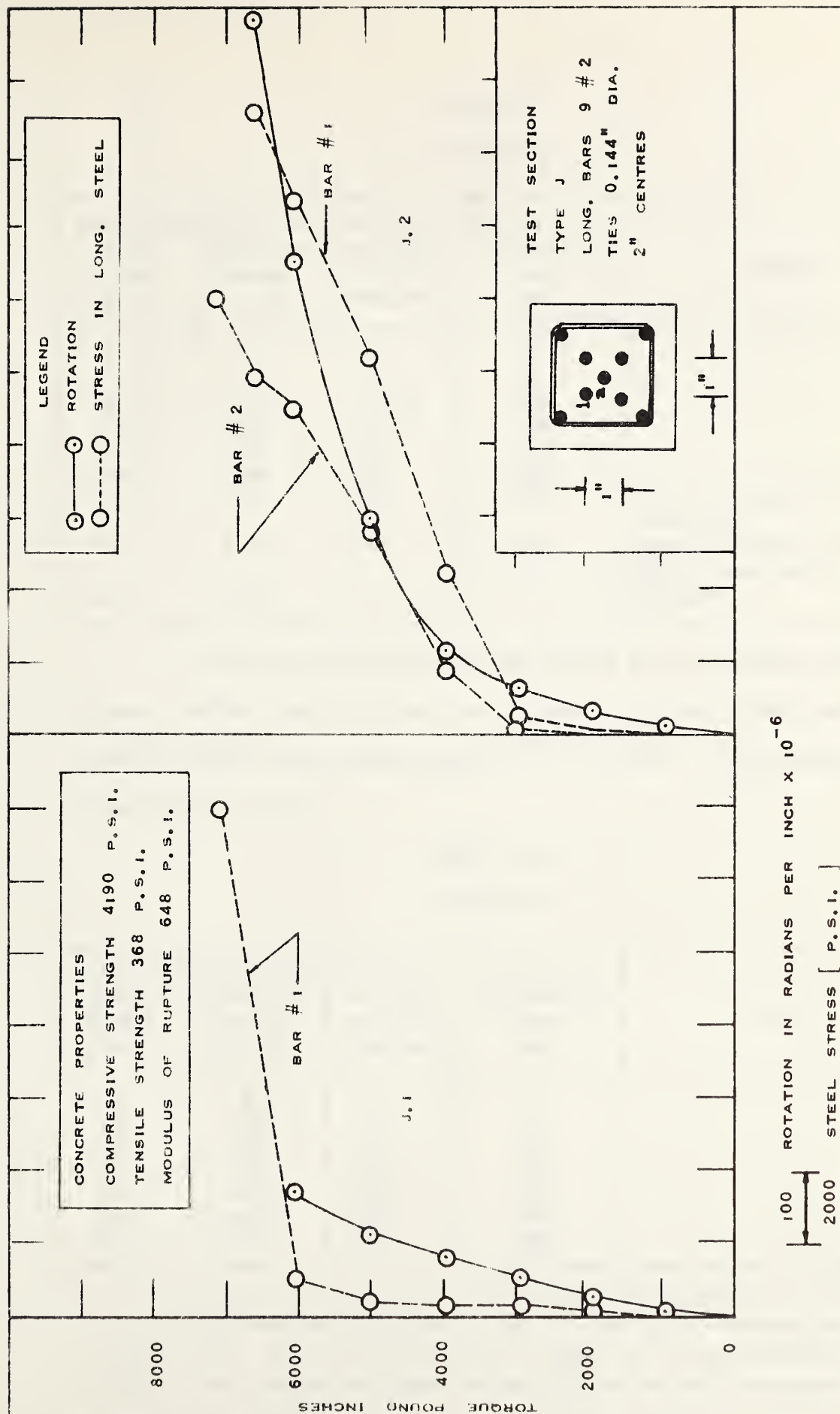


FIGURE 5.11 TORQUE - ROTATION AND TORQUE - STEEL STRESS CURVES  
 SPECIMENS J



TABLE V-23

## SPECIMEN K.1

Effective Dead Weight (lbs)	Effective Twisting Moment (lb.in)	Rotation per inch $\times 10^{-6}$ (Radians)	Stress in Longitudinal Steel (psi)	Remarks
0	0	0	0	
18.5	910	13.3	0	
38.7	1910	35.6	150	
59.3	2940	64.4	300	
79.7	3950	102	750	
100.2	4980	173	2100	
120.5	6000	269	5850	fine 45° cracks at 3 locations
140.9	7060	769	17250	cracks widened, new cracks developed
151.1	7570	-	-	collapse

The failure occurred near the centre of the specimen due to diagonal tension soon after the last increment of load. There was extensive cracking in the entire gage length prior to failure. The specimen exhibited appreciable ductility.

TABLE V-24

## SPECIMEN K.2

Effective Dead Weight (lbs)	Effective Twisting Moment (lb.in)	Rotation per inch $\times 10^{-6}$ (Radians)	Stress in Longitudinal Steel (psi)	Remarks
0	0	0	0	
18.5	910	11.1	0	
38.7	1900	31.1	300	
59.3	2920	55.6	750	
79.7	3920	84.4	1050	
100.2	4950	122	1500	
120.5	5970	200	2250	
140.9	6980	-	yield stress	cracking and collapse

The breakdown occurred at the centre of the specimen and extended over about 18". There were no visible cracks up to the effective load of 120.5 lbs. The cracks developed on application of last increment and quickly widened till failure occurred two minutes later.



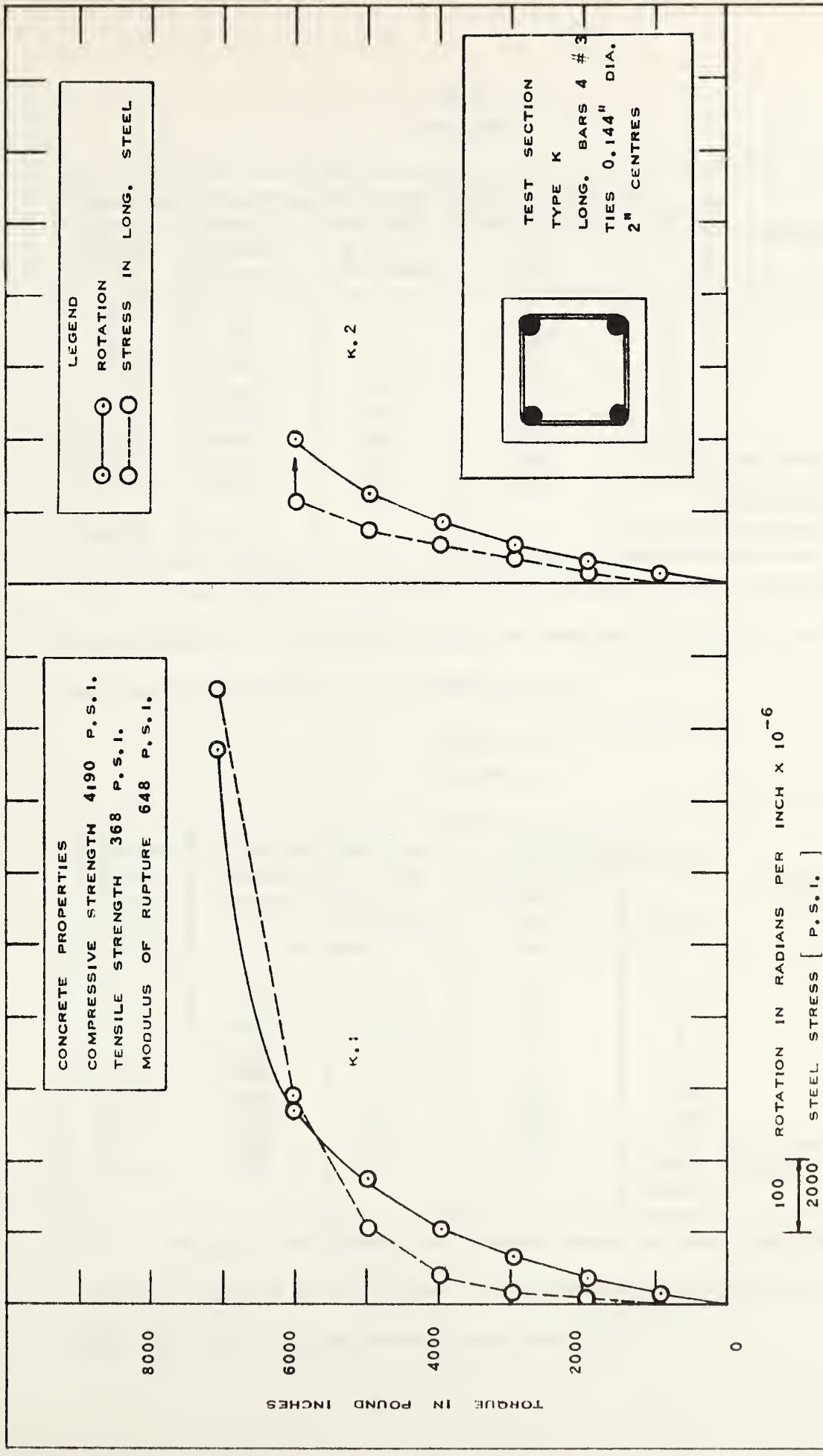


FIGURE 5.12 TORQUE - ROTATION AND TORQUE - STEEL STRESS CURVES  
SPECIMEN K



TABLE V-25  
SPECIMEN L.1

Effective Dead Weight (lbs)	Effective Twisting Moment (lb.in)	Rotation per inch $\times 10^{-6}$ (Radians)	Steel Stress		Remarks
			Longitudinal Steel (psi)	Tie (psi)	
0	0	0	0	0	
18.5	920	11.1	0	0	
38.7	1920	28.9	150	0	
59.3	2940	48.9	300	0	
79.7	3960	68.9	600	0	
100.2	4990	102	1050	300	
120.5	6010	238	7050	2850	cracking
130.7	6590	302	7500	4500	further cracks developed
140.9	7050	-	-	43500	collapse

The breakdown occurred near the centre a minute after the last load increment. The specimen exhibited some ductility prior to failure. Concrete was destroyed over a length of 15".

TABLE V-26  
SPECIMEN L.2

Effective Dead Weight (lbs)	Effective Twisting Moment (lb.in)	Rotation per inch $\times 10^{-6}$ (Radians)	Steel Stress		Remarks
			Longitudinal Steel (psi)	Tie (psi)	
0	0	0	0	0	
18.5	920	13.3	0	0	
38.7	1920	31.1	0	0	
59.3	2950	51.1	0	0	
79.7	3960	77.8	0	0	
100.2	4990	109	300	300	
120.5	6000	158	1350	750	
130.7	6510	218	3600	1200	cracking
140.9	7030	371	-	yield stress	collapse

The beam collapsed five minutes after the last load increment. The breakdown occurred at the centre. Concrete was destroyed over a length of about 15". The specimen showed some ductility.







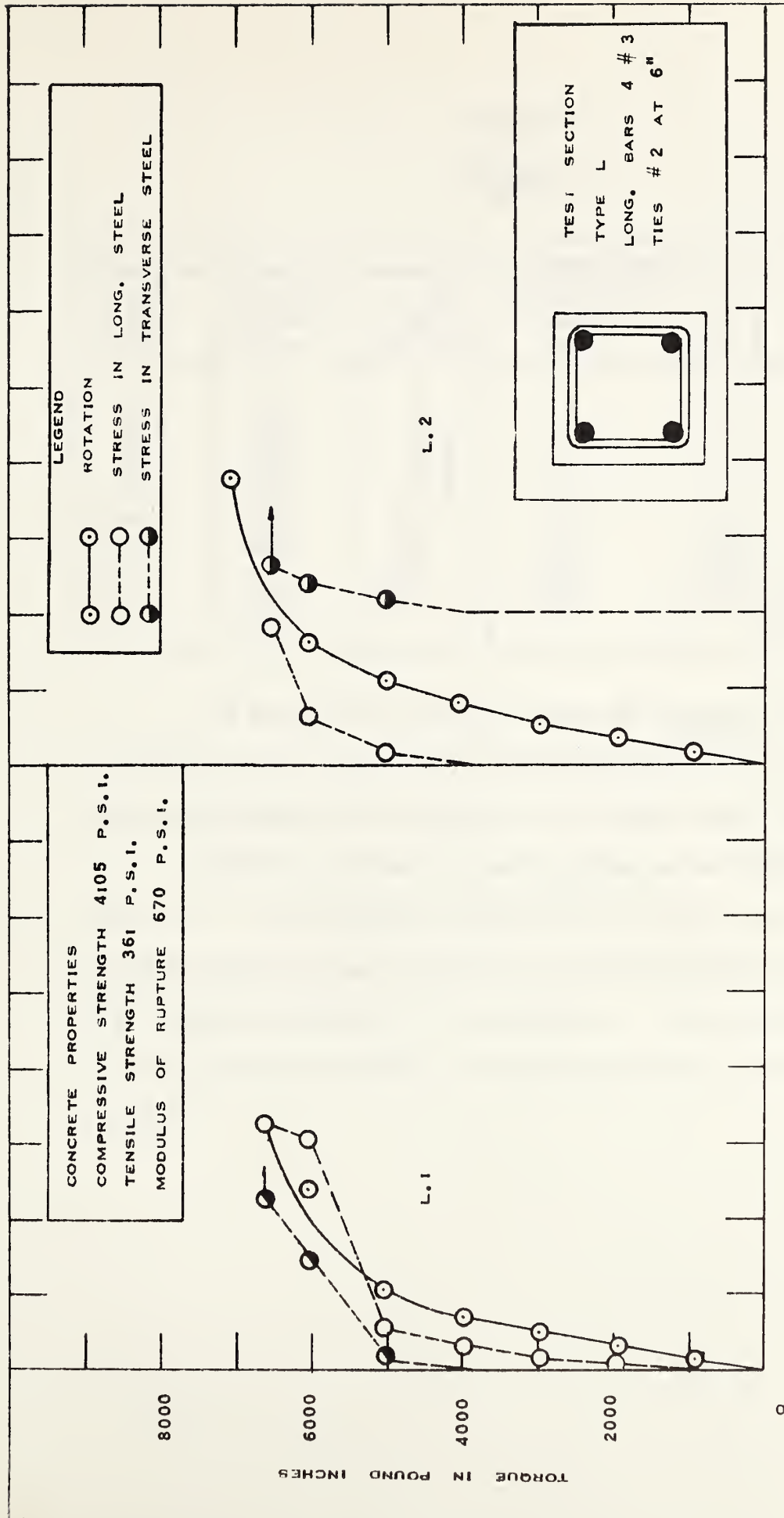


FIGURE 5.13 TORQUE - ROTATION AND TORQUE - STEEL STRESS CURVES  
SPECIMEN L



TABLE V-27  
SPECIMEN M.1

Effective Dead Weight (lbs)	Effective Twisting Moment (lb.in)	Rotation per inch $\times 10^{-6}$ (Radians)	Steel Stress		Remarks
			Longitudinal Steel (psi)	Tie (psi)	
0	0	0	0	0	
18.5	920	11.1	0	0	
38.7	1920	28.9	0	0	
59.3	2940	48.9	0	0	
79.7	3950	77.8	0	0	
100.2	4980	120	0	0	
120.5	6000	176	150	300	
140.9	7030	493	12150	5550	cracking
161.4	8100	1104	23250	7950	cracks widened
182.2	9150	-	-	-	collapse

The failure was ductile. There was extensive cracking prior to collapse. The breakdown occurred almost at the centre soon after the last load increment. The concrete was destroyed over a length of about 18".

FIGURE 5.15 shows the test specimen at an effective torque of 7030 lb. in. The cracks were almost at  $45^{\circ}$  to the axis of the specimen. The cracks developed and widened at the effective torque of 8100 lb. in. This is shown in FIGURE 5.16. In FIGURE 5.17, the specimen is seen from the east side and in FIGURE 5.18 from the west side after the specimen collapsed.



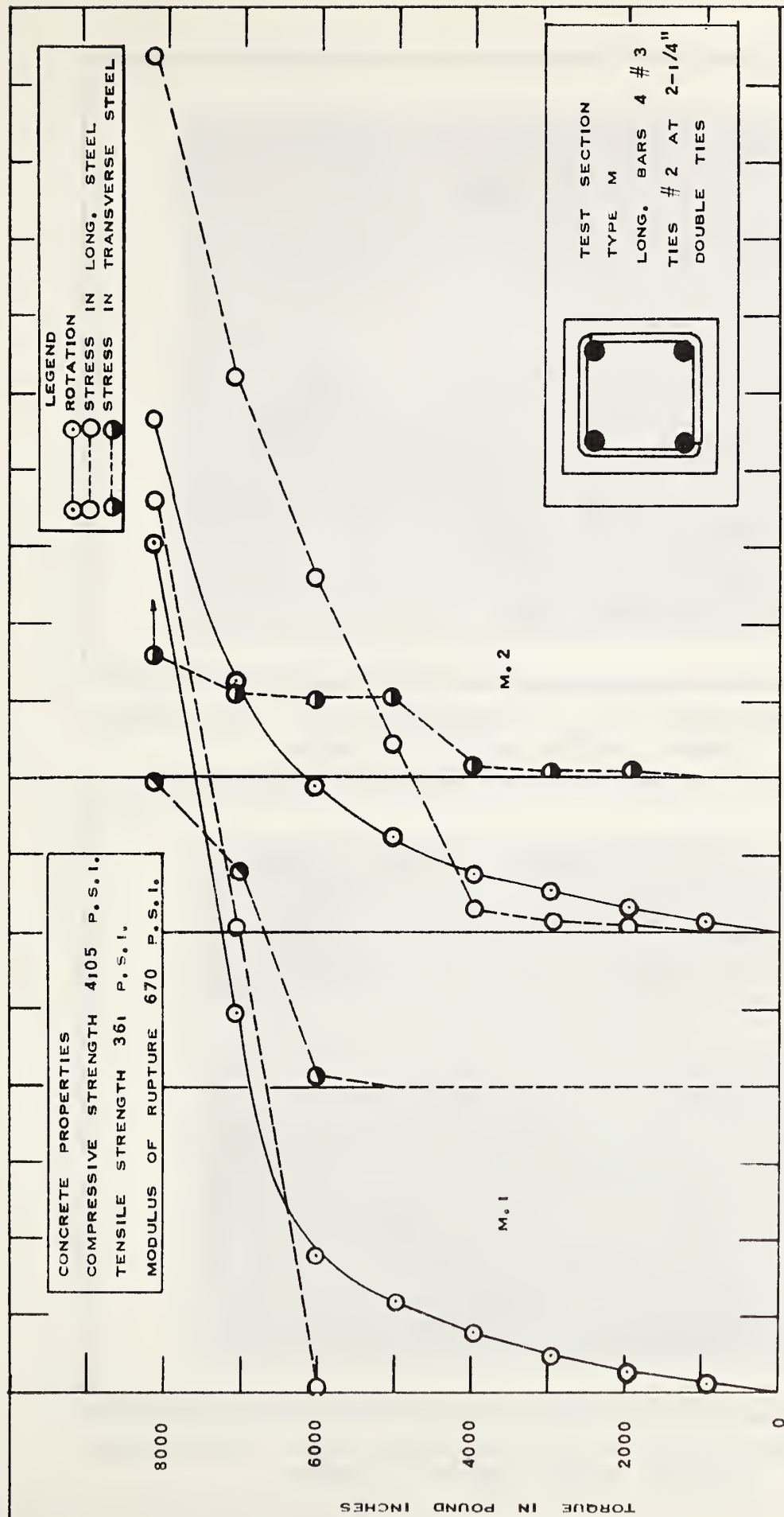
TABLE V-28  
SPECIMEN M.2

Effective Dead Weight (lbs)	Effective Twisting Moment (lb.in)	Rotation per inch $\times 10^{-6}$ (Radians)	Steel Stress		Remarks
			Longitudinal Steel (psi)	Tie (psi)	
0	0	0	0	0	
18.5	920	11.1	0	0	
38.7	1920	31.1	150	150	
59.3	2950	53.3	300	150	
79.7	3960	75.6	600	300	
100.2	4990	124	4950	2100	
120.5	6010	189	9150	2100	fine 45° cracks more cracks developed
140.9	7030	324	14400	2250	
161.4	8100	667	22800	3150	
171.6	8610	-	-	-	extensive cracking
181.4	9110	-	-	yield stress	extensive cracking collapse

The breakdown occurred near the centre of the specimen soon after the last increment of load. The cracking was extensive before collapse. The specimen showed lot of ductility.

FIGURE 5.19 shows the west face and FIGURE 5.20 the east face of the specimen M.2 after collapse.





100 ROTATION IN RADIAN PER INCH X 10<sup>-6</sup>  
 2000 STEEL STRESS [ P.S.I. ]

FIGURE 5.14 TORQUE - ROTATION AND TORQUE - STEEL STRESS CURVES  
 SPECIMENS M





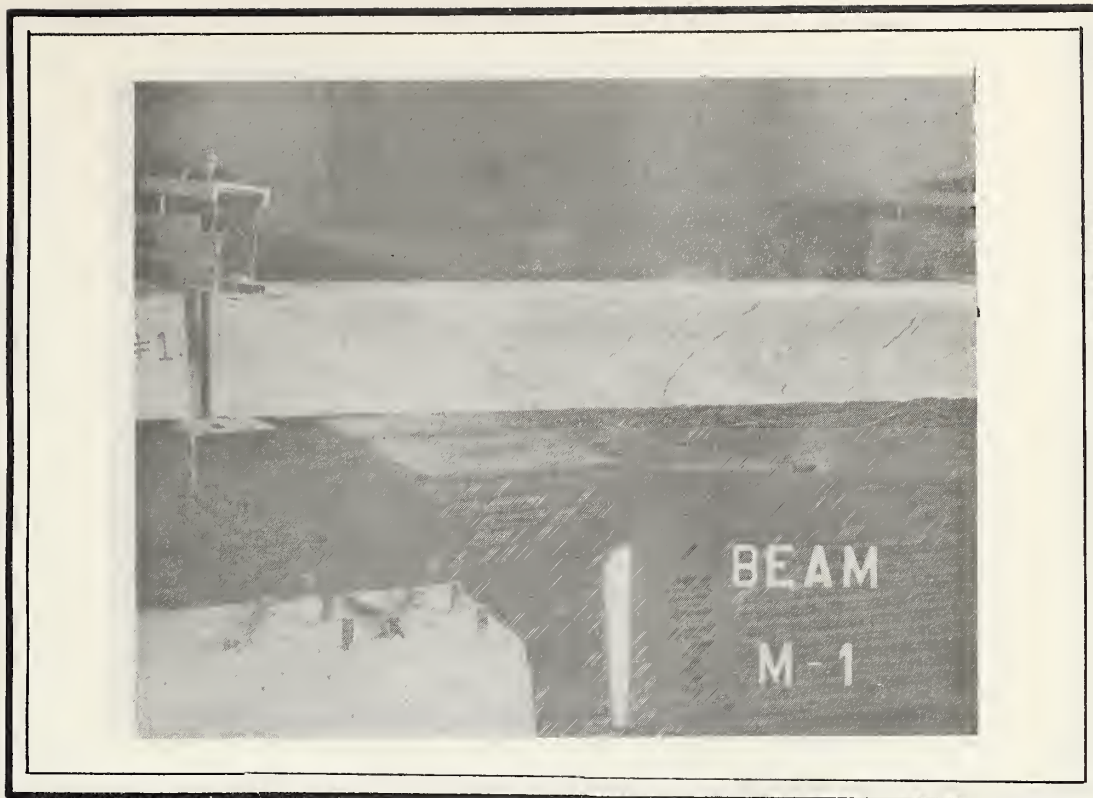


FIGURE 5.15 TEST SPECIMEN M.1 AT EFFECTIVE TWISTING MOMENT OF 7030 POUND INCHES

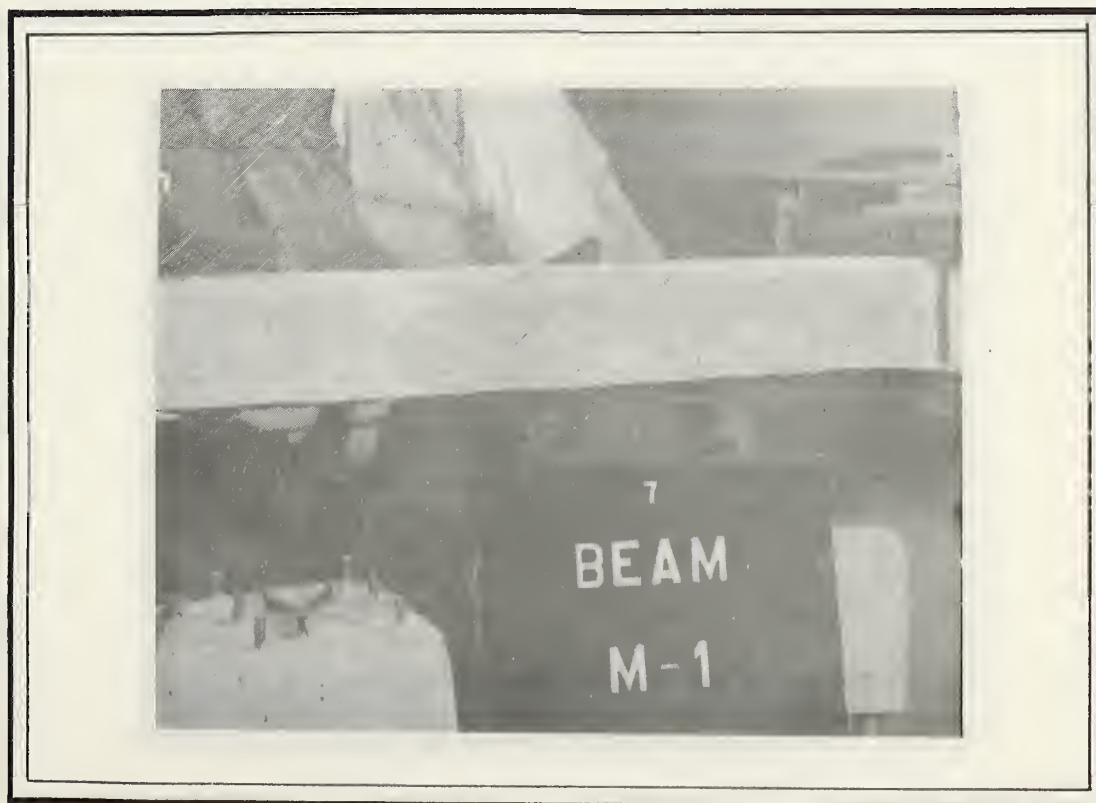


FIGURE 5.16 TEST SPECIMEN M.1 AT EFFECTIVE TWISTING MOMENT OF 8100 POUND INCHES





FIGURE 5.17 TEST SPECIMEN M.1 SEEN FROM EAST SIDE AFTER COLLAPSE



FIGURE 5.18 TEST SPECIMEN M.1 SEEN FROM WEST SIDE AFTER COLLAPSE





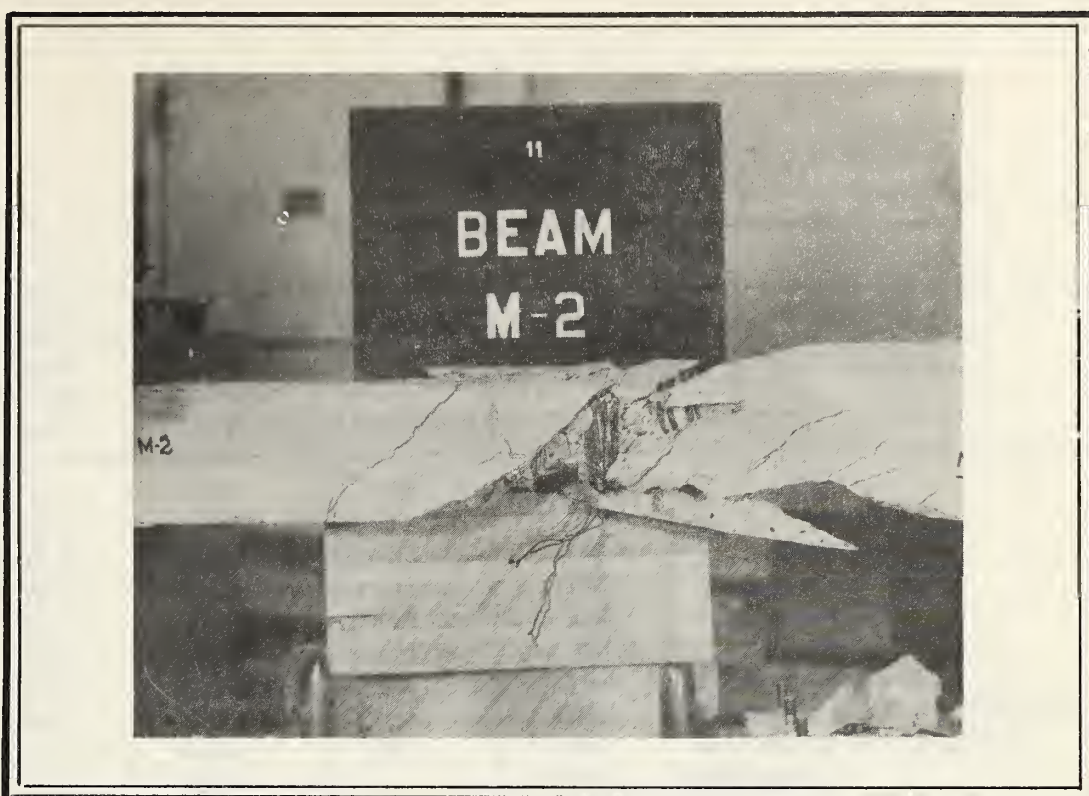


FIGURE 5.19 TEST SPECIMEN M.2 SEEN FROM WEST SIDE AFTER COLLAPSE

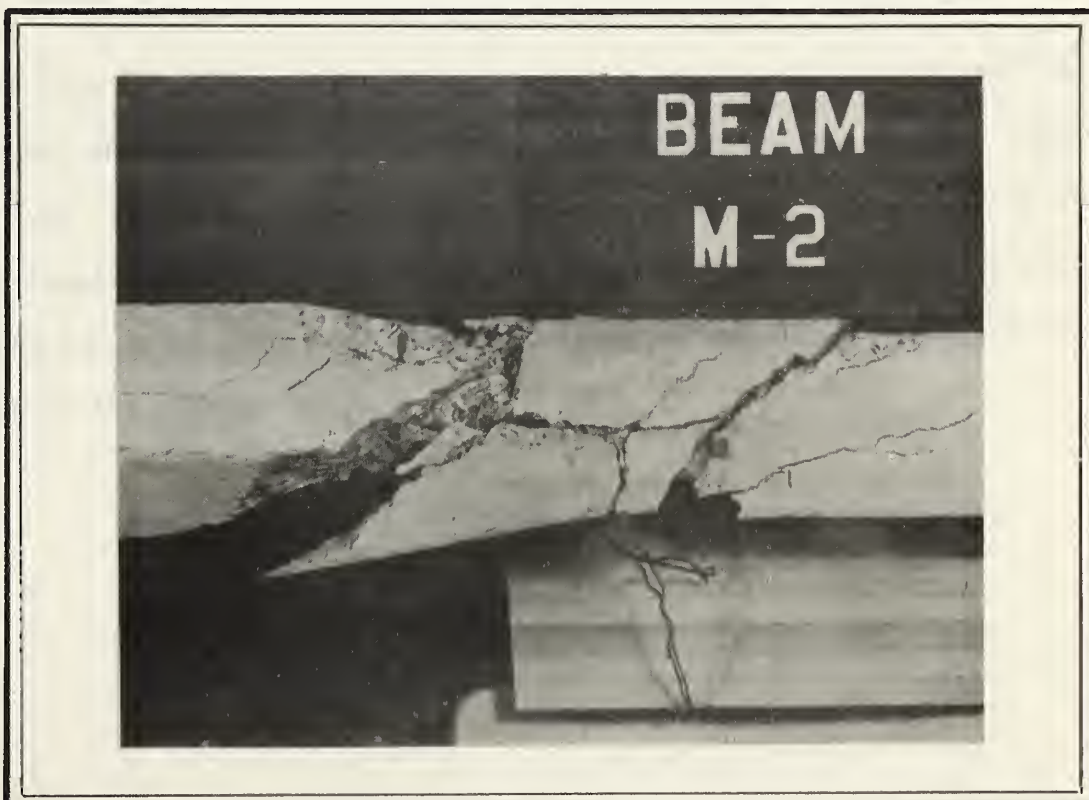


FIGURE 5.20 TEST SPECIMEN M.2 SEEN FROM EAST SIDE AFTER COLLAPSE



TABLE V-29

## SPECIMEN N.1

Effective Dead Weight (lbs)	Effective Twisting Moment (lb.in)	Rotation per inch $\times 10^{-6}$ (Radians)	Stress in Tie (psi)	Remarks
0	0	0	0	
18.5	920	11.1	60	
38.7	1920	33.3	150	
59.3	2940	55.6	180	
79.7	3960	75.6	300	
100.2	4990	97.8	360	
120.5	6000	120	750	fine cracks
140.9	7050	184	2850	cracks developed further
161.4	8100	513	14700	appreciable creeping
171.6	8600	-	yield stress	collapse

The specimen showed appreciable ductility. At 161.4 lb. effective load, there were two distinct helical cracks and the specimen crept appreciably. The breakdown occurred soon after the last increment of load. The concrete was completely destroyed over a length of about 6". The longitudinal bars and two of the ties were exposed. The ties were effective up to failure and made the longitudinal bars distort locally between the consecutive ties.





TABLE V-30

SPECIMEN N.2

Effective Dead Weight (lbs)	Effective Twisting Moment (lb.in)	Rotation per inch x 10 <sup>-6</sup> (Radians)	Stress in Longitudinal Bar (psi)	Remarks
0	0	0	0	
18.5	920	20.0	0	
38.7	1920	35.6	0	
59.3	2940	60.0	0	
79.7	3960	127	0	
100.2	4990	156	0	
120.5	6000	231	0	
140.9	7050	420	0	fine cracks at 45°
151.1	7600	613	6390	cracks widened, more cracks
154.1	7740	729	14100	cracks widened, more cracks
160.9	8100	873	18600	at load increment
			yield stress	at collapse

There was appreciable ductility prior to failure. Concrete was completely destroyed over a length of about 6" near the centre of the specimen. Here all four bars and the ties were exposed. The ties were effective up to failure. The bars distorted locally between the ties.



TABLE V-31  
SPECIMEN N.3

Effective Dead Weight (lbs)	Effective Twisting Moment (lb.in)	Rotation per inch $\times 10^{-6}$ (Radians)	Stress in Tie (psi)	Remarks
0	0	0	0	
18.5	920	13.3	0	
38.7	1920	31.1	0	
59.3	2940	57.8	240	
79.7	3960	82.2	540	
100.2	5000	136	900	
120.5	6000	167	2100	
140.9	7050	233	4500	
161.4	8070	429	15000	cracking
171.6	8580	587	20400	more cracks
181.4	9070	713	24000	cracks developed
192.4	9620	1851	yield stress	cracks widened
196.4	9820	-	-	collapse

The specimen showed appreciable ductility. The breakdown occurred near the centre of the specimen. Concrete was destroyed over a length of about a foot. The longitudinal bars were distorted locally between the ties. There was appreciable creeping at and above the effective load of 161.4 lbs. Cracks formed at an angle of about  $45^{\circ}$  to the axis.



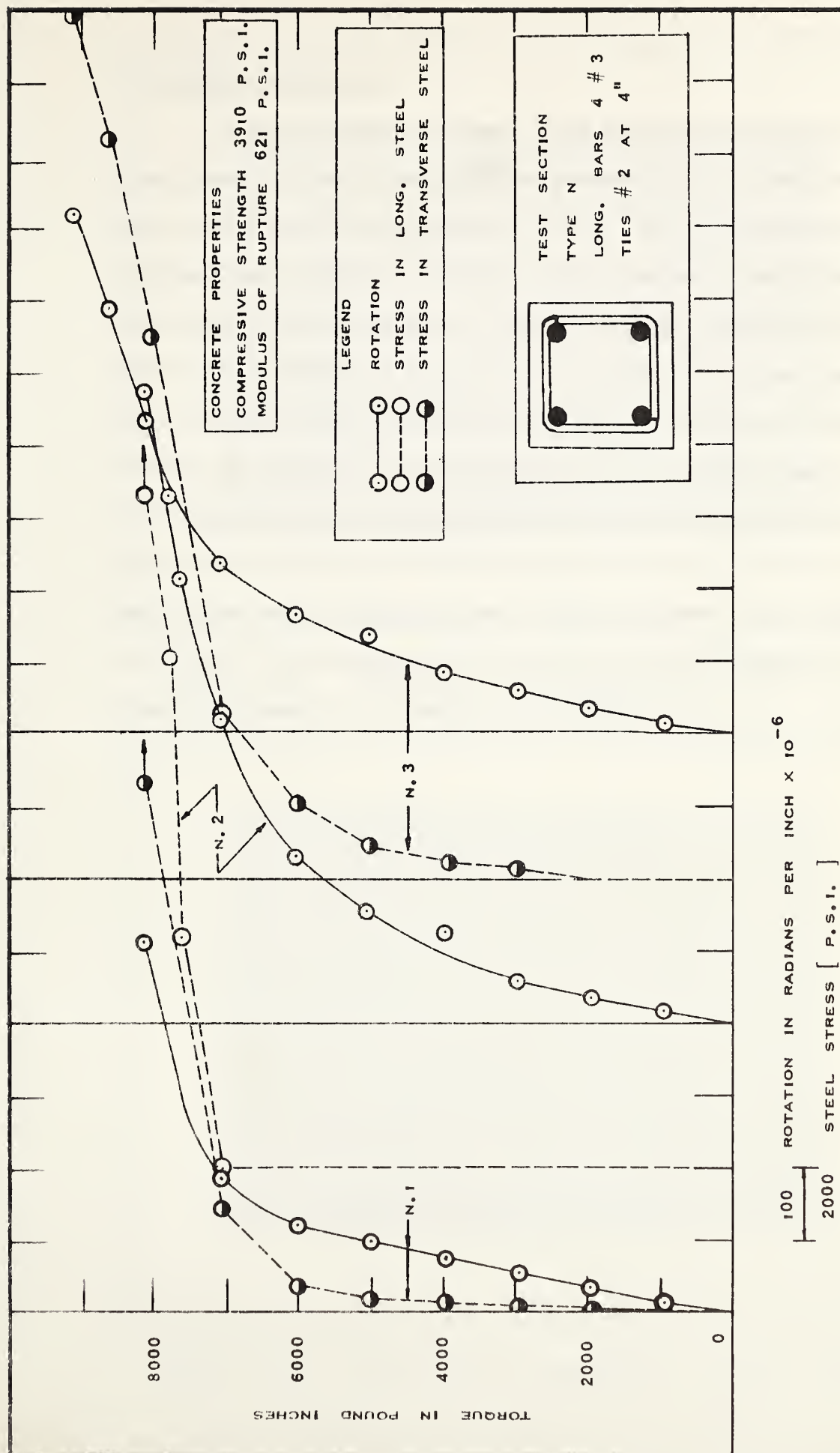


FIGURE 5.21 TORQUE - ROTATION AND TORQUE - STEEL STRESS CURVES  
 SPECIMENS N



### 5-3 General Behaviour

Plain concrete specimens (Type A) and those having only longitudinal reinforcement (Types B and H) failed suddenly at the formation of the first crack; the ultimate torque was the same as the cracking torque. These specimens had no ductility whatever. The specimens showed increasing ductility for higher ratios of longitudinal and transverse steels. The cracks formed helices at about  $45^{\circ}$  in all cases. All specimens broke within and at a fair distance from the ends of the gage length. The cracking was extensive and spread over the entire gage length in specimens with higher ratios of longitudinal and transverse reinforcements. FIGURES 5.22 through 5.29 show all the specimens after they had been tested. Each figure shows a different face of the specimens. The typical  $45^{\circ}$  fractures are evident in many specimens, especially the plain concrete beams; (See broken specimens A.1, A.2 and A.3 in FIGURE A.25).





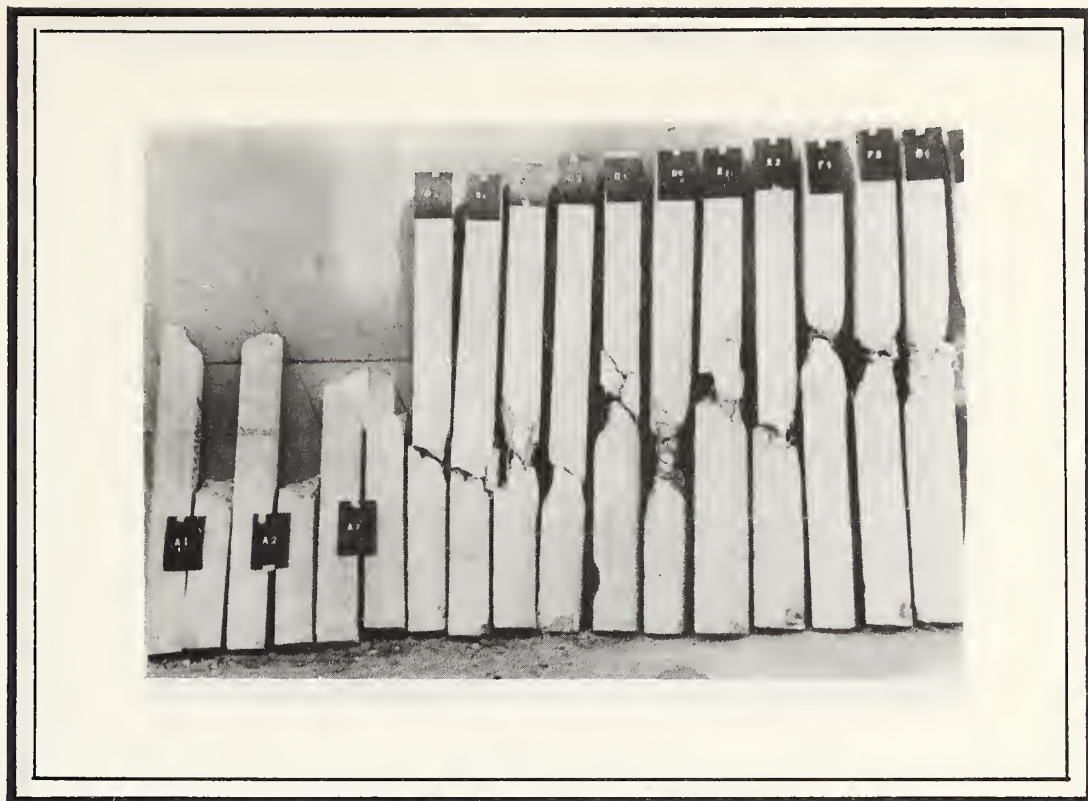


FIGURE 5.22 SPECIMENS A THROUGH G AFTER TEST



FIGURE 5.23 SPECIMENS A THROUGH F AFTER TEST





FIGURE 5.24 SPECIMENS A THROUGH G AFTER TEST



FIGURE 5.25 SPECIMENS A THROUGH G AFTER TEST







FIGURE 5.26 SPECIMENS H THROUGH N AFTER TEST



FIGURE 5.27 SPECIMENS H THROUGH N AFTER TEST



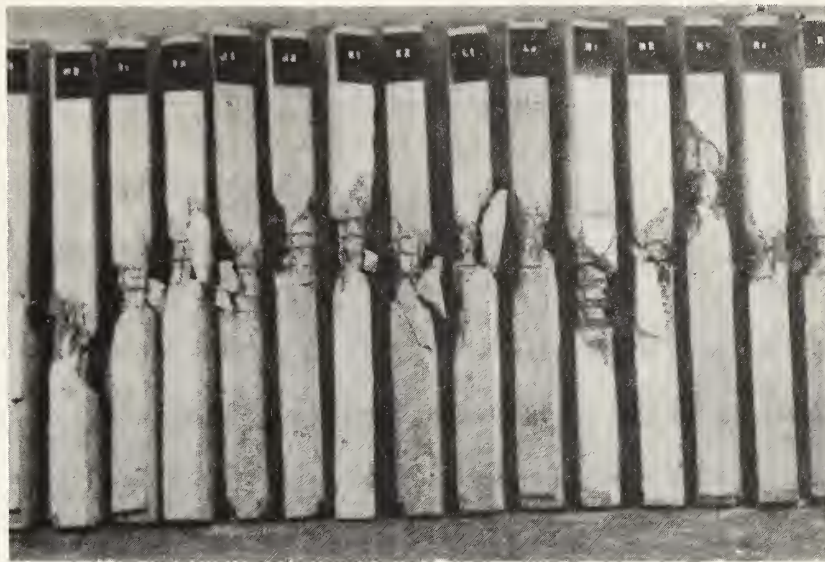


FIGURE 5.28 SPECIMENS H THROUGH N AFTER TEST

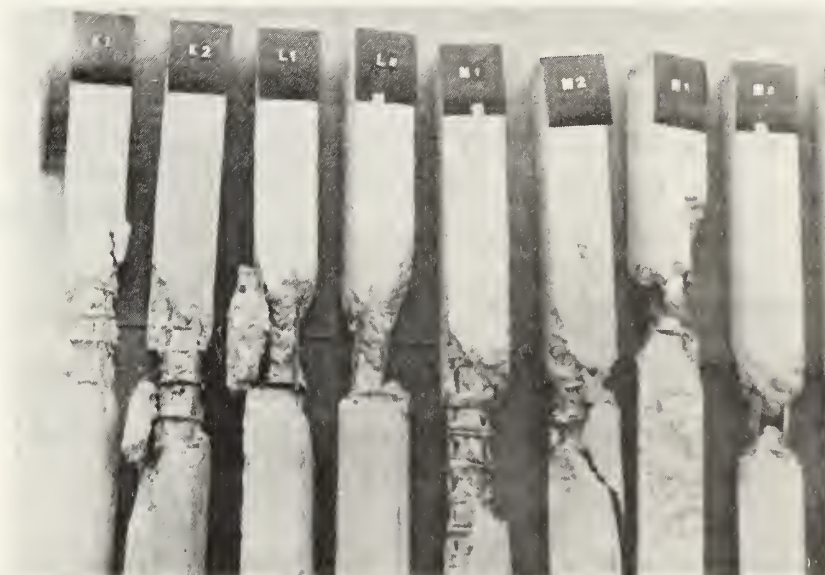


FIGURE 5.29 SPECIMENS K THROUGH N AFTER TEST







## CHAPTER VI

### DISCUSSION OF TEST RESULTS

#### 6-1 Tensile Strength of Concrete

The tensile strength of concrete is probably the most important variable in predicting the ultimate strength of plain or reinforced concrete sections. Unless the tensile strength is determined with fair accuracy, it is difficult to decide whether the elastic or the plastic theory is more suitable or to determine the extent of redistribution of stresses due to inelastic deformation of concrete. Ironically, the tensile strength of concrete is one of the most elusive properties of concrete. Several investigators have attempted to relate the tensile strength to the compressive strength of concrete by a widely varying set of empirical relations. This is probably the main cause of obscurity in the problem of torsion in concrete sections.

In the present program, the following tests were performed on control specimens:

- (i) Compression tests on 6" x 12" control cylinders.
- (ii) Split tests on 6" x 12" control cylinders.
- (iii) Modulus of rupture tests on 3-1/2" x 4-1/2" x 16" control specimens.

The tensile strength of concrete  $f'_t$  may be related to the compressive strength  $f'_c$  by the Equation of the form:



$$f'_t = c(f'_c)^k \quad (6.1)$$

where  $c$  and  $k$  are constants. Gonnerman and Shuman (32), on the basis of their extensive tests found  $c = 0.68$  and  $k = 0.75$ . Kemp, Sozen and Siess (18) have proposed  $k = 0.5$ .

TABLE VI-1, shows the average values of the cylinder strength  $f'_c$  as determined by compression tests, the tensile strength  $f'_t$  as determined by split tests and the Modulus of rupture  $f_r$ . Based on overall average values shown in TABLE VI-1, the suitability of the following four Equations was judged by the method of least squares:

$$f'_t = 0.73 (f'_c)^{3/4} \quad (6.2)$$

$$f'_t = 0.74 (f'_c)^{3/4} \quad (6.3)$$

$$f'_t = 5.7 (f'_c)^{1/2} \quad (6.4)$$

$$f'_t = 5.8 (f'_c)^{1/2} \quad (6.5)$$

The graphs for the above four Equations are shown in FIGURE 6.1. Equation (6.4) was considered most suitable because it gave the minimum value of the sum of squared residuals. Since this Equation gave a graph which is practically a straight line, it was replaced by the Equation,

$$f'_t = 0.0457 f'_c + 176.8 \quad (6.6)$$

The graph of this Equation is shown with solid line in FIGURE 6.1. This



graph was used for finding the tensile strength from the compressive strength.

Due to the narrow range of variation of Modulus of rupture  $f_r$ , it was considered adequate to relate it to the tensile strength by the simple Equation:

$$f'_t = 0.56 f_r \quad (6.7)$$

The coefficient 0.56 was calculated from the overall average values of  $f'_t$  and  $f_r$  shown in TABLE VI-1. The graph of Equation (6.7) is shown in FIGURE 6.2.

The values of the tensile strength as determined directly from split test and as derived from values of  $f'_c$  and  $f_r$  are shown in TABLE VI-2. From these values, the weighted average values of the tensile strength, with equal weightage to each control specimen, were calculated and are also shown in TABLE VI-2.

## 6-2 Cracking Torque

The plain concrete specimens, type A, had an average cracking torque (which in this case was also the average ultimate torque) of 5820 lb. in. For most of the reinforced specimens also the cracking torque was close to the above torque for plain concrete specimens. One cause of variation in the cracking torque was the difference in the tensile strength of concrete. The straight line in FIGURE 6.3 represents the cracking torque for plain concrete based on the above torque of 5820 lb. in. and in direct proportion to the tensile strength. The points on FIGURE 6.3(a) represent the actual cracking torques for the various specimens tested.



TABLE VI-1

OVERALL AVERAGE VALUES OF THE COMPRESSIVE STRENGTH  
THE TENSILE STRENGTH AND THE MODULUS OF RUPTURE

	$f'_c$ (psi)	$f'_t$ (psi)	$f_r$ (psi)	Remarks
A	3,370	333	577	The cylinder strength $f'_c$ , the tensile strength $f'_t$ and the Modulus of Rupture $f_r$ were determined by the standard compression test, the split test and the Modulus of Rupture test respectively.
B & C	3,560	361	599	
D & E	4,060	350	632	
F & G	3,710	367	664	
H & I	3,335	325	610	
J & K	4,190	368	648	
L & M	4,105	361	670	
overall average values	26,330	2,465	4,400	
	3,761	352	629	





TABLE VI-2

## WEIGHTED AVERAGE VALUES OF TENSILE STRENGTH

	Type A			Type B & C			Type D & E			Type F & G		
	No. of Sp.	Av. Va- lue (psi)		No. of Sp.	Av. Va- lue (psi)		No. of Sp.	Av. Va- lue (psi)		No. of Sp.	Av. Va- lue (psi)	
Direct from split test	2	333	666	2	361	722	3	350	1050	3	367	1101
From Eq. 6.6	2	331	662	2	340	680	2	363	726	2	347	694
From Eq. 6.7	2	323	646	2	335	670	2	354	708	2	372	744
Total	6	-	1974	6	-	2072	7	-	2484	7	-	2539
Weighted Average	-	-	329	-	-	345	-	-	355	-	-	363

TABLE VI-2 (continued)

	Type H & I			Type J & K			Type L & M			Type N		
	No. of Sp.	Av. Va- lue (psi)		No. of Sp.	Av. Va- lue (psi)		No. of Sp.	Av. Va- lue (psi)		No. of Sp.	Av. Va- lue (psi)	
Direct from split test	3	325	975	3	368	1104	3	361	1083	-	-	-
From Eq. 6.6	2	329	658	2	369	738	2	365	730	3	356	1068
From Eq. 6.7	2	342	684	2	363	726	2	375	750	2	348	696
Total	7	-	2317	7	-	2568	7	-	2563	5	-	1764
Weighted Average	-	-	331	-	-	367	-	-	366	-	-	353



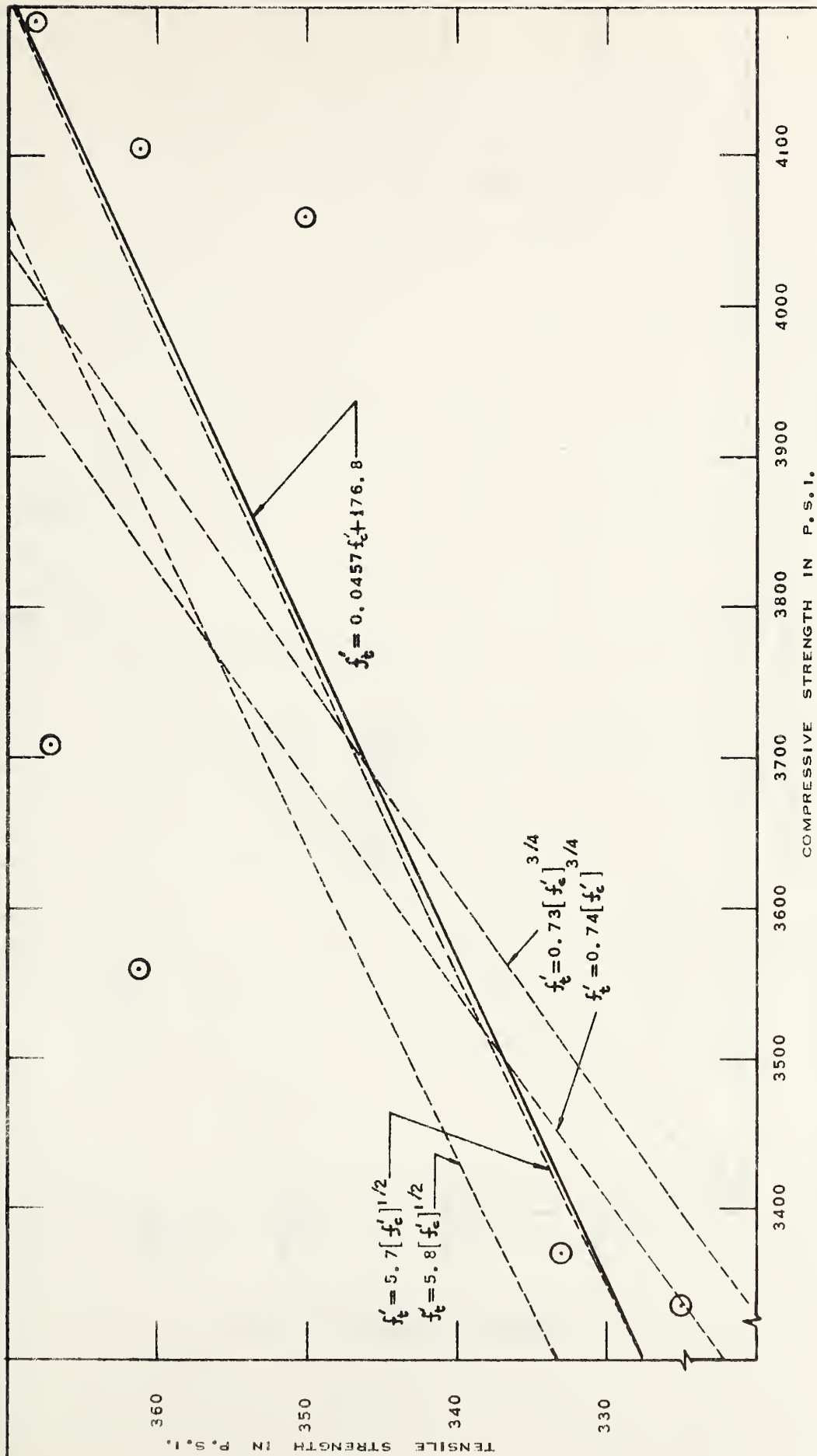


FIGURE 6.1 RELATION BETWEEN COMPRESSIVE AND TENSILE STRENGTH



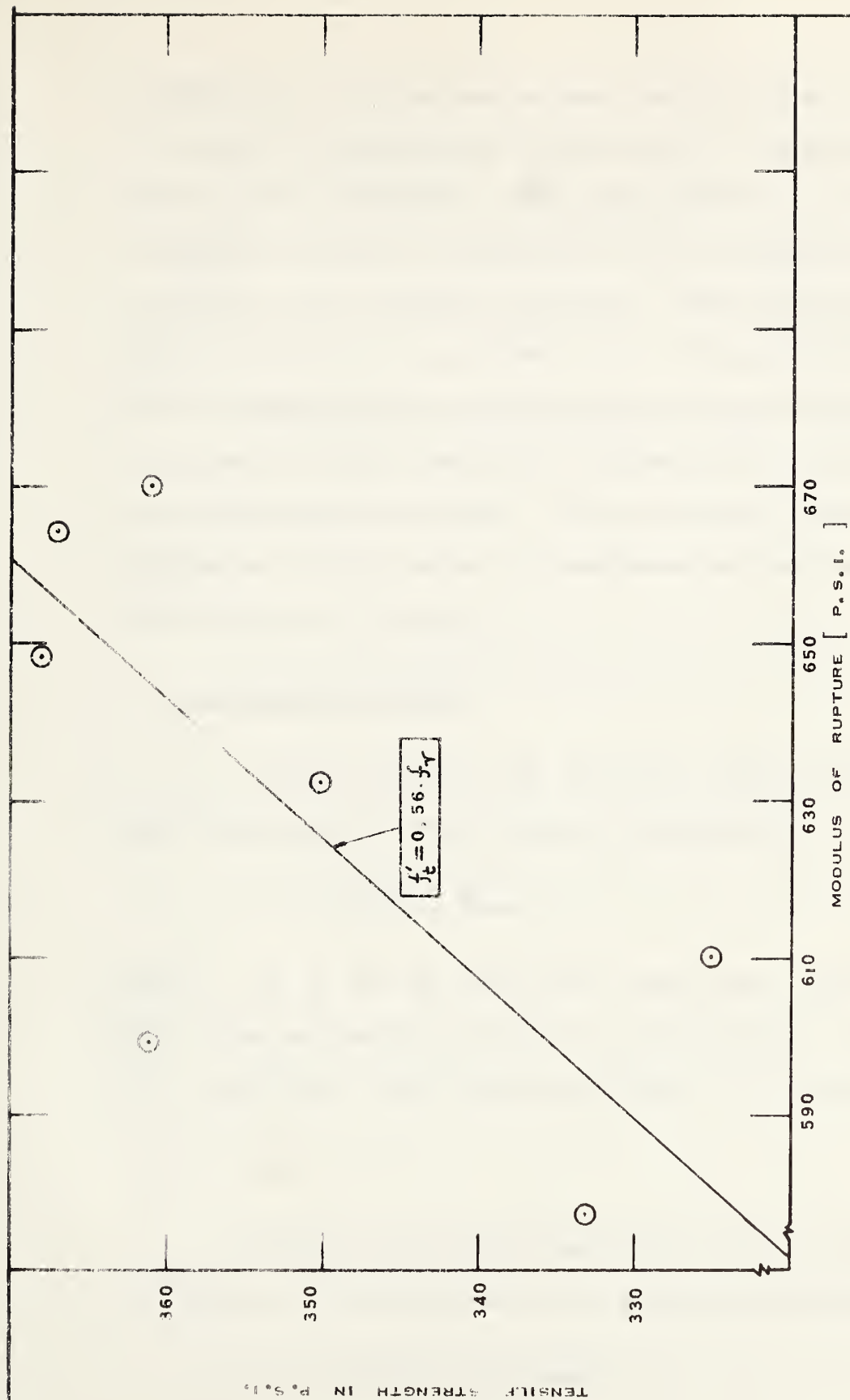


FIGURE 6.2 RELATION BETWEEN MODULUS OF RUPTURE AND TENSILE STRENGTH





In FIGURE 6.3(b), the measured average cracking torques for various types (A through N) of specimens are shown by points. The cracking torques are also given in TABLE VI-3. The average value of the cracking torque for all specimens (except N.3) was 6175 lb. in. The average tensile strength of concrete in all specimens was 352 psi. This corresponds to the cracking torque of 6230 lb. in. (see FIGURE 6.3). A study of FIGURE 6.3 shows that the line representing the cracking torque for plain concrete is almost the regression line for the points representing the cracking torques for plain and reinforced specimens. The reinforcement, therefore, did not increase the cracking torque of a reinforced specimen over that of the corresponding plain specimen.

### 6-3 The Torsional Strength

For plain concrete, the torsional strength according to elastic theory (see Equation A.50) is given by the Equation:

$$T_E = k_2 b^2 d \cdot \tau_{\max} \quad (6.8)$$

where  $b$  and  $d$  are the shorter and longer sides of the rectangle and  $\tau_{\max}$  is the maximum shear induced at ultimate torque. Since  $b = d = 4"$ ,  $k_2 = 0.208$  for a square section and  $\tau_{\max} = f'_t$  for pure torsion,

$$T_E = 13.31 f'_t \quad (6.9)$$

The torsional strength according to plastic theory, assuming full plasticity, (see Equation B.8) is given by the Equation:

$$\begin{aligned} T_p &= \frac{1}{2} b^2 \left(d - \frac{1}{3} b\right) \tau_{\max} \\ &= 21.33 f'_t \end{aligned} \quad (6.10)$$

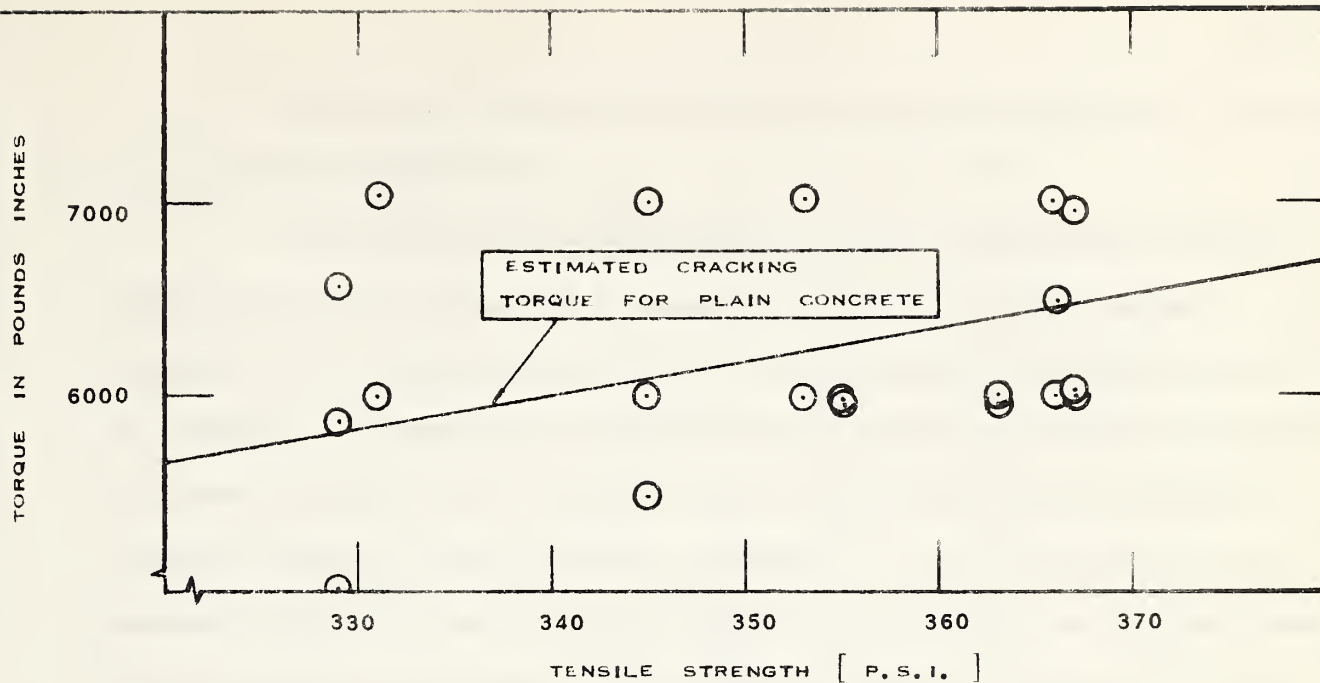


TABLE VI-3  
ROTATIONS, CRACKING TORQUES AND ULTIMATE TORQUES OF SPECIMENS

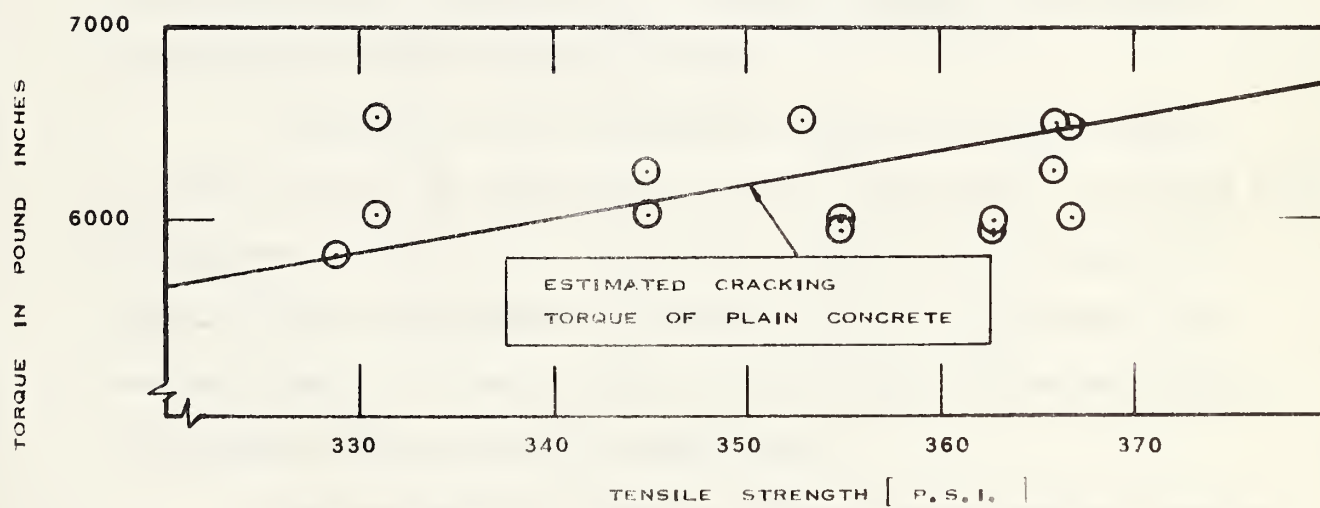
Specimen	Rotation in Radians per inch x 10 <sup>-6</sup>				Cracking Torque		Ultimate Torque		f' <sub>t</sub> (psi)
	at 910 lb.in		at 1910 lb.in		at 2900 lb.in		(lb.in)	Average (lb.in)	
	Average		Average		Average				
A.1	8.8		28.8		57.3		5010	5010	
A.2	11.0	9.6	28.8	28.1	50.4	49.8	5870	5820	329
A.3	8.9		26.7		41.8		6580	6580	
B.1	13.3	12.2	28.9	30.0	48.6	55.3	7020	6260	345
B.2	11.1		31.1		61.9		5500	5500	
C.1	13.2	13.2	28.8	32.2	46.2	54.0	6030	6040	345
C.2	13.2		35.5		61.7		6050	6250	
D.1	15.6	15.6	33.3	34.4	55.2	57.4	6000	6000	355
D.2	15.5		35.5		59.6		6000	6540	
E.1	15.6	14.4	33.4	33.3	59.8	58.6	5970	5985	355
E.2	13.2		33.1		57.4		6000	6540	
F.1	15.6	13.4	30.0	30.6	53.1	53.0	5990	6000	363
F.2	11.1		31.1		52.9		6010	6970	
G.1	15.6	15.6	35.7	36.8	59.9	60.9	5970	5985	363
G.2	15.6		37.8		61.8		6000	7540	
H.1	15.5	15.6	35.3	34.3	57.3	57.4	7050	6525	331
H.2	15.6		33.3		57.5		6000	6000	
I.1	13.3	12.2	33.2	32.2	59.6	60.7	6010	6020	331
I.2	11.1		31.1		61.8		6030	7600	
J.1	8.9	12.2	26.7	32.2	55.3	60.9	6010	6030	367
J.2	15.5		37.7		66.3		6050	7100	
K.1	13.3	12.2	35.6	33.4	64.0	59.7	6000	6490	367
K.2	11.1		31.2		55.4		6980	6980	
L.1	11.0	12.1	28.8	29.9	48.5	49.6	6010	6260	366
L.2	13.2		31.0		50.6		6510	7030	
M.1	11.0	11.0	28.8	29.9	48.5	50.7	7030	6520	366
M.2	11.0		31.0		52.8		6010	9130	
N.1	11.0	15.5	33.2	34.4	55.2	57.4	6000	6525*	353
N.2	19.9		35.5		59.6		7050	8600	
N.3	13.2	13.2	31.0	31.0	57.4	57.4	8070	8100	
								-	-
Total		198.0		482.7		842.8		9820	4936
Average		13.2		32.2		56.2		-	352

\*Specimen N.3 not included in these averages due to its large variation from average values.





[ a ]



[ b ]

FIGURE 6.3 [ a ] ACTUAL CRACKING TORQUES OF SPECIMENS  
 [ b ] MEASURED AVERAGE CRACKING TORQUES  
 OF VARIOUS TYPES OF SPECIMENS





The values of torsional moment based on elastic and plastic theories are tabulated in TABLE VI-4.

It has been seen in section 6-2 that the reinforcement did not add to the cracking torque of a specimen. Hence the cracking torque depended only on the geometry of the cross-section and the tensile strength of concrete. The estimated cracking torques based on the tensile strengths are shown in TABLE VI-4. They were taken from the straight line graph of cracking torque for plain concrete in FIGURE 6.3. The difference of the measured ultimate torque and the estimated cracking torque may be considered as the contribution of steel to the ultimate torque of a specimen. This contribution of steel  $T_s$  is also tabulated in TABLE VI-4.

The points in FIGURE 6.4 represent the measured average ultimate torques for the specimens (types A through N). The ordinate between a point and the line representing the estimated cracking torque gives the contribution of steel to ultimate torque.

In FIGURE 6.5 the contribution of steel to ultimate torque is plotted against the percentage of lateral reinforcement. In FIGURE 6.5(a), the specimen types A, C, D, F and G with 0, 0.17, 0.34, 0.51 and 1.02 percent lateral reinforcement respectively have been represented. The specimen types A, L, N and M with 0, 0.51, 0.77 and 2.72 percent lateral reinforcement have been used in FIGURE 6.5(b).

The contribution of steel to ultimate torque seems to increase in proportion to the percentage of lateral steel. However the rate of increase tends to decrease with higher percentages of reinforcement. The data indicates that there is a certain limit to which the ultimate capacity





TABLE VI-4  
CONTRIBUTION OF STEEL TO THE ULTIMATE TORQUE

Type	$f'_t$ (psi)	$T_E$ $= 13.31 f'_t$ (lb.in)	$T_p$ $= 21.33 f'_t$ (lb.in)	Estimated Cracking Torque $T_{cr}$ (lb.in)	$T_u$ Measured (lb.in)	$T_s =$ $T_u - T_{cr}$ (lb.in)
A	329	4380	7020	5820	5820	0
B	345	4590	7360	6100	6260	160
C	345	4590	7360	6100	6520	420
D	355	4730	7570	6280	6780	500
E	355	4730	7570	6280	6255	-
F	363	4830	7740	6420	7080	660
G	363	4830	7740	6420	7260	840
H	331	4410	7060	5860	6525	665
I	331	4410	7060	5860	7580	1720
J	367	4880	7830	6490	7065	575
K	367	4880	7830	6490	7275	785
L	366	4870	7810	6470	7040	570
M	366	4870	7810	6470	9130	2660
N	353	4700	7530	6240	8350	2110



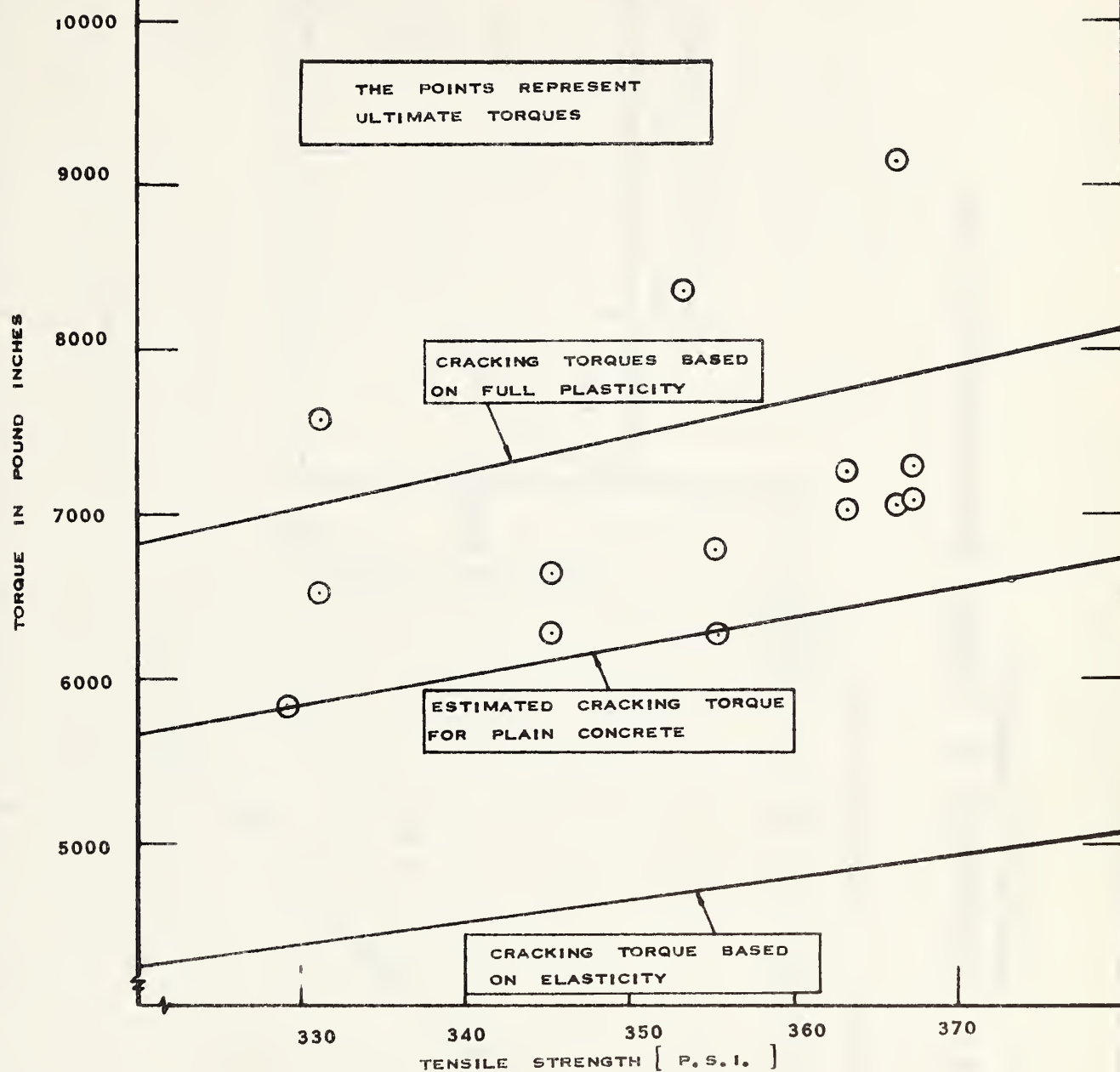


FIGURE 6.4 CRACKING AND ULTIMATE TORQUES



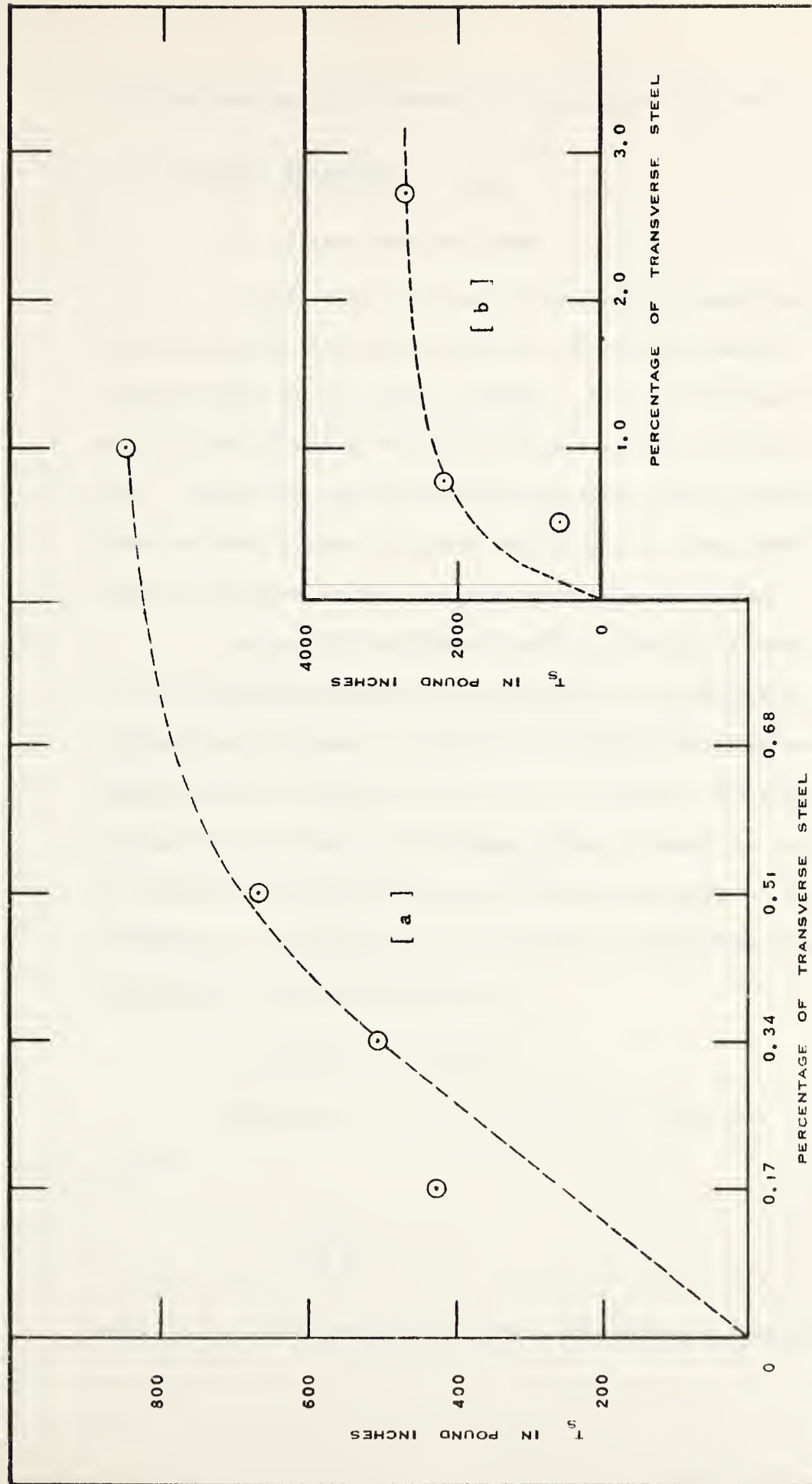


FIGURE 6.5 CONTRIBUTION OF LATERAL REINFORCEMENT TO THE TORSIONAL STRENGTH





of a specimen may be increased by providing reinforcement.

#### 6-4 Torsional Stiffness

##### (a) Torque-Rotation Curves

A study of the torque-rotation curves shows that they were practically straight for lower values of the twisting moment. Here the concrete behaved almost as an elastic material. With increasing torque, inelastic deformations occurred and the rotation tended to increase at a higher rate. Beyond the cracking torque, the shape of the torque-rotation curve depended primarily on the reinforcement. The curves tended to be almost horizontal as the ultimate torque was approached.

The initial portion of the torque-rotation curve corresponding to low torques was practically the same for all specimens. This is evident from a perusal of TABLE VI-3 in which the rotations at twisting moments of 910, 1910 and 2900 lb. in. are given. The rotations for all specimens were close to the average values. Hence the initial stiffness of a specimen did not increase with the reinforcement. It seemed to be a function of the geometry of the section and concrete properties but independent of the reinforcement.

##### (b) Modulus of Rigidity

From Equation (A.49), the Modulus of Rigidity is given by the Equation:

$$G = \frac{T}{K_1 \theta d^4} \quad (6.11)$$

where  $T$  is the torque,  $\theta$  is the corresponding rotation per unit length



and the constant  $K_1$  for a square section (side  $d = 4''$ ) is 0.1406.

Using Equation (6.11) and the rotation of  $13.2 \times 10^{-6}$  radians per inch length at 910 lb. in. torque (TABLE VI-3), the Modulus of Rigidity was found to be  $1.92 \times 10^6$  psi. The Modulus of Rigidity dropped down to  $1.65 \times 10^6$  and  $1.43 \times 10^6$  psi at twisting moments of 1910 and 2900 lb. in. respectively.

#### 6-5 Effect of Longitudinal Reinforcement Only

Specimen types B and H with longitudinal reinforcement only had a brittle and sudden failure as for plain concrete sections. The gain in strength for type B specimens, which had four No. 2 bars, one in each corner, was 160 lb. in. For the H type specimens with nine No. 2 bars, the increase in strength was 665 lb. in. (See TABLE VI-4). This represents an increase of about 3 and 11 percent for types B and H respectively over the estimated cracking torque for the corresponding plain sections. The specimens F and I had the same lateral reinforcement (0.51 percent). The percentages of longitudinal reinforcement for types F and I, however, were 1.23 and 2.75 respectively. The gains in strength for F and I types were 660 and 1720 lb. in. respectively. The difference of 1060 lb. in. between the two gains of torsional strength may be attributed to the increase of longitudinal reinforcement from 1.23 to 2.75 percent. It may also be attributed to more efficient functioning of the lateral reinforcement when more adequate amount of longitudinal steel existed. From the above observations, it appeared that though an increase in the longitudinal reinforcement did not produce any appreciable increase in the torsional strength when the lateral reinforcement was missing, it did so when substantial lateral reinforcement



did exist.

#### 6-6 Effect of Varying Lateral Steel

The effect of increasing the percentage of lateral reinforcement has been discussed in Section 6-3. Though the lateral reinforcement did not seem to affect the cracking torque, it increased the ultimate torque significantly if adequate longitudinal reinforcement was also provided. For M type specimens, the gain in ultimate strength was 2660 lb. in. (see TABLE VI-4). This represents an increase of about 41 percent over the estimated cracking torque for corresponding plain section. The increase in ultimate strength for increasing percentage of lateral reinforcement is plotted in FIGURE 6.5.

#### 6-7 Effect of Position and Size of Longitudinal Bars

Specimens I, J and K had the same percentages of longitudinal (2.75 percent) and transverse (0.51 percent) steel. The transverse steel in all these specimens consisted of 0.144 inch diameter wire at 2 inch spacing. The size and position of longitudinal bars was, however, different (see TABLE IV-7 and FIGURE 4.7).

The ultimate torsional moment for I, J and K types were 7580, 7065 and 7275 lb. in. respectively. Specimens I, in which the longitudinal bars were distributed along the periphery of the cross-section at greater distances from the centroid as compared to those in specimens J, gave greatest ultimate torque. Since the ultimate torque of specimens I was greater than specimens K, it appeared that for the same percentage of longitudinal steel, the smaller size and consequently the closer spacing of



longitudinal bars tended to produce higher torsional strength.

#### 6-8 Effect of Bar Size of Transverse Steel

Specimens K and L had the same percentage of longitudinal steel (2.75 percent) and transverse steel (0.51 percent). The size (No. 3) and arrangement of longitudinal bars was the same in these specimens. While the amount of transverse steel was same in specimens K and L, the specimens K had 0.144 inch diameter ties at 2 inch spacing and specimens L had No. 2 ties at 6 inch spacing. Specimens K had a higher ultimate strength (7275 lb. in.) compared to that of specimens L (7040 lb. in.). The transverse steel in specimens L had a higher yield stress (47,490 psi) compared to that in specimens K (24110 psi). Hence for the same percentage of transverse steel, the smaller size (and consequently closer spacing) of ties gave higher strength.

#### 6-9 Effectiveness of Ties

While all other specimens had P type ties (see FIGURE 4.7) with large overlap, the Q type ties in specimens E were provided with smaller overlap. An inspection of the broken specimens of type E showed that the ties had opened up and hence did not appear to be effective up to the ultimate torque. The higher strength (7580 lb. in.) of I type specimens compared to that of F type specimens (7080 lb. in.) indicated that the ties functioned more efficiently when a larger percentage of longitudinal steel was provided.





#### 6-10 Effect of Steel Strength

Two different grades of steel were used for the ties to see the effect of steel strength on the strength of the specimen. The 0.144 inch diameter wire was of a low grade steel with yield point stress and ultimate stress of 24,110 and 42,330 psi respectively. The No. 2 bar had the yield point stress and ultimate stress of 47,490 and 56,330 psi respectively.

Specimens K and N had the same longitudinal steel (four No. 3 bars, one in each corner). In specimens K, 0.144 inch diameter ties at 2 inch spacing increased the ultimate torque by 785 lb. in. The corresponding increase in specimens N due to No. 2 ties at 4 inch spacing was 2110 lb. in. (see TABLE VI-4). The percentages of transverse steel in specimens K and N were respectively 0.51 and 0.77. This indicated that higher strength steel tended to give a greater increase in the ultimate torque.

#### 6-11 Steel Stresses

A perusal of TABLES V-6 through V-31 and FIGURES 5.3 through 5.21 of CHAPTER V shows that steel had very little, if any, stress up to the cracking torque. After the cracking torque was exceeded, the steel stresses rose rapidly. In most cases when substantial longitudinal and transverse steel existed, the stress in each set of reinforcement reached the yield point stress at the ultimate torque. In some cases, e.g. specimens K.1, M.1 and M.2, the steel stress at ultimate load could not be recorded because the gages were destroyed at collapse of the specimen. It, however, appeared that the steel attained the yield point stress at ultimate torque.



The steel attained the yield point stress only when both longitudinal and transverse steels were provided in substantial amounts. The stress in longitudinal steel in specimen B.2 at ultimate torque was only 5700 psi (TABLE V-6). In specimen H.2, it was only 4200 psi (TABLE V-18). Hence the stress in longitudinal steel at ultimate torque was low if transverse steel was not provided. This indicated that the longitudinal steel was not efficiently used without lateral ties and consequently failed to increase the ultimate torque significantly.

The stresses in both longitudinal and transverse steels at ultimate torque were low (6300 and 7950 psi respectively) in specimen C.1, which had a low percentage (0.17) of transverse steel (TABLE V-7). It appeared that neither the longitudinal nor the transverse steel could be fully utilised unless both sets of reinforcement were adequately provided.

The reinforcement started sharing substantial stresses only when the cracking torque was reached. The steel stress increased at constant torque as the ultimate torque was approached. This indicated substantial creeping and inelastic deformation near the ultimate torque. The yielding of corner bars in specimens K.2 and N.2 and a substantial stress (12,000 psi) in the longitudinal bar at the centroid of the section in specimen J.2 indicated substantial plasticity at ultimate torque because the elastic theory indicated little or no stress in these locations.



## CHAPTER VII

### SUMMARY AND CONCLUSIONS

#### 7-1 Summary

Thirty plain and reinforced concrete specimens were tested in pure torsion. All specimens had a cross-section of 4" x 4" and a length of 4' 6". The same concrete mix was used for all specimens. Three different grades of steel were used. The average yield point stresses for 0.144, 1/4 and 3/8 inch diameter steel were 24,110, 47,490 and 58,860 psi and ultimate stresses of 42,330, 56,330 and 83,460 psi respectively. There were two specimens of each type except types A and N each of which had three specimens. The principal test results are summarized in TABLE VII-1.

#### 7-2 Conclusions

The following are the conclusions drawn from the study of the test results and the behaviour of the specimens in pure torsion:

(1) The plain concrete and longitudinally reinforced specimens failed suddenly with a brittle failure at the formation of the first helical crack.

(2) The longitudinal reinforcement alone did not increase the ultimate strength appreciably. It also did not impart any ductility to the specimen.





TABLE VII-1  
PRINCIPAL TEST RESULTS

Type	Concrete Properties				Reinforcement					
	f' <sub>c</sub> (psi)	f' <sub>t</sub> (psi)	f <sub>r</sub> (psi)	Weighted Av. Tensile Strength (psi)	Longitudinal			Transverse		
					No. and Size	%	Arran- gement*	Diameter and Type*	Spacing (in)	%
A	3370	333	577	329	None	0	-	None	-	0
B	3560	361	599	345	4 #2	1.23	R	"	-	0
C	"	"	"	"	"	"	"	0.144".P	6	0.17
D	4060	350	632	355	"	"	"	" "	3	0.34
E	"	"	"	"	"	"	"	" Q	3	"
F	3710	367	664	363	"	"	"	" P	2	0.51
G	"	"	"	"	"	"	"	" " Double at 2		1.02
H	3335	325	610	331	9 #2	2.75	S	None	-	0
I	"	"	"	"	"	"	"	0.144".P	2	0.51
J	4190	368	648	367	"	"	T	" "	2	"
K	"	"	"	"	4 #3	"	U	" "	2	"
L	4105	361	670	366	"	"	"	1/4" P	6	"
M	"	"	"	"	"	"	"	" " Double at 2-1/4		2.72
N	3910	-	621	353	"	"	"	" "	4	0.77

\* See FIGURE 4.7

continued on next page



TABLE VII-1  
(continued)

PRINCIPAL TEST RESULTS

Type	Observed Strength		Steel Stresses				Ductility
	Cracking Torque (lb.in)	Ultimate Torque (lb.in)	At cracking		At ultimate		
			Longitudinal Steel (psi)	Trans-verse Steel (psi)	Longitudinal Steel (psi)	Trans-verse Steel (psi)	
A	5820	5820	-	-	-	-	None
B	6260	6260	5700	-	5700	-	None
C	6040	6520	0 & 1800	4650	6300 & 12600	7950	Very Little
D	6000	6780	-	-	-	-	A little
E	5985	6255	-	-	-	-	None
F	6000	7080	8100	-	-	-	A little
G	5985	7260	-	-	-	-	Some
H	6525	6525	4200	-	4200	-	None
I	6020	7580	8100;1350 & 300	6750 & 1050	yield & 34200	yield	Appreciable
J	6030	7065	1050;14700 & 9000	-	13950 & 12000	-	Some
K	6490	7275	5850	-	yield	-	Appreciable
L	6260	7040	7050 & 3600	2850 & 1200	-	43500 & yield	Some
M	6520	9130	12150 & 9150	5550 & 2100	-	yield	Much
N	6525**	8350**	0	750 & 15000	yield	yield	Appreciable

\* See FIGURE 4.7

\*\* Specimen N.3 not included in these averages due to its large variation from average values.



(3) The cracking torque was about the same for all specimens.

The reinforcement did not affect the cracking torque.

(4) The ultimate strength was appreciably increased by providing longitudinal and transverse reinforcement in adequate amount.

(5) The cracks were helical and almost at  $45^{\circ}$  to the axis in all specimens.

(6) Though the longitudinal reinforcement alone did not effect any appreciable increase in strength, it was necessary for proper functioning of the transverse reinforcement. If substantial transverse steel did exist, an increase in longitudinal steel resulted in higher ultimate strength.

(7) Adequate amounts of both longitudinal and transverse steel were necessary for full utilisation of either of them. If one of them was missing or was inadequate, the other could not be stressed to the yield point stress.

(8) The actual cracking torque was about midway between that predicted by the elastic and the plastic theories. This indicated that though the sections did not become fully plastic, the inelastic deformation did produce a significant stress redistribution. The elastic theory underestimated and the plastic theory over-estimated the strength of the section.

(9) For low percentages of transverse steel, the increase in ultimate strength was proportional to the increase in transverse steel. However, this rate of increase of ultimate torque decreased for higher per-



centages of transverse steel. There appeared to be a limit up to which the ultimate strength could be increased, which depended upon the geometry of the section and the concrete and steel properties.

(10) The longitudinal bars functioned more effectively and therefore gave higher strength if they were kept away from the centroid of the section. This was because the lever arm for the bars was greater when the bars were placed away from the axis of twist. Also there was greater plastic deformation resulting in higher stress in the outer zone of an elasto-plastic section.

(11) For the same percentage of longitudinal steel, the smaller size and consequently closer spacing of longitudinal bars gave higher strength.

(12) For the same percentage of transverse steel, the smaller size or closer spacing gave higher strength.

(13) An adequate overlap for developing full stress in ties was necessary for effectiveness of the ties.

(14) The higher strength of steel used for the ties gave higher strength to the specimens.

(15) The behaviour of all specimens up to the cracking torque was about the same. The initial stiffness of all specimens was nearly the same since it depended only on the geometry of the section and concrete strength. It was independent of the type, amount or position of the reinforcement.





(16) The torque-rotation curve was practically straight at low values of torque. This indicated that concrete behaved practically as an elastic material for low torques. This linear part of the curve was almost the same for all specimens.

(17) At higher torque, especially above the cracking torque, the torque-rotation curve tended to be flat. The shape of this part of the curve depended primarily on the type, amount and position of reinforcement.

(18) The Modulus of Rigidity decreased with increasing torque. Its value at torques of 910, 1910 and 2900 lb. in. was found respectively as  $1.92 \times 10^6$ ,  $1.65 \times 10^6$  and  $1.43 \times 10^6$  psi.

(19) The steel stress was low up to the cracking torque. The steel stress grew rapidly as the cracking torque was exceeded.

(20) Both longitudinal and transverse steel could be stressed to the yield stress if adequate amount of each was provided. This full utilisation of steel tended to give substantially higher strength. If either the longitudinal or the transverse steel was insufficient, the steel did not attain the yield stress. The stress in steel at ultimate torque was low for specimens with longitudinal steel only.

(21) Torque in excess of the cracking torque was almost entirely carried by the reinforcement.

(22) The steel stress increased at constant torque when it was close to the ultimate torque. This indicated significant stress redistribution



before the specimen collapsed.

(23) None of the reinforcement fractured at the ultimate torque.

(24) The tests helped a better understanding of the behaviour of concrete sections in pure torsion. The tests included some of the variables not previously investigated. Further testing is considered necessary to study the behaviour of rectangular sections and prestressed concrete sections in pure torsion. Due to the dearth of test results, further experimental work in the field of combined bending, torsion and shear is considered extremely useful.



## BIBLIOGRAPHY

1. Andersen, P., "Experiments with Concrete in Torsion" Trans. Am.Soc. of Civil Engineers, 1935, Vol. 100, Paper 1912.
2. Andersen, P., "Rectangular Concrete Sections under Torsion" J.A.C.I., Sept-Oct 1937.
3. Armstrong, S., "The Strength of Concrete Members in Combined Bending and Torsion" Symposium on the Strength of Concrete Structures, London, 1956, Session B, Paper No. 2, Cement and Concrete Association of Great Britain.
4. Bach, C. and Graf, O., "Versuche über die Widerstands fähigkeit Von Beton and Eisenbeton Gegen Verdrehung" Deutscher Ausschuss für Eisenbeton, Heft 16, Wilhelm Ernst, Berlin, 1912.
5. Coulomb, C.A., "Histoire de L'Académie", Paris, 1784.
6. Cowan, H.J., "Elastic Theory for Torsional Strength of Rectangular Reinforced Concrete Beams" Magazine of Concrete Research, Vol. 2, No. 4, July 1950.
7. Cowan, H.J., "Tests of Torsional Strength and Deformation of Rectangular Concrete Beams", Concrete and Constructional Engineering, London, Vol. 46, No. 2, Feb. 1951.
8. Cowan, H.J. and Armstrong, S., "Reinforced Concrete in Combined Bending and Torsion" Fourth Congress of the International Association of Bridge and Structural Engineering, Cambridge and London, 1952.
9. Cowan, H.J., "The Strength of Plain, Reinforced and Prestressed Concrete under Action of Combined Bending and Torsion of Rectangular Sections" Magazine of Concrete Research, Vol. 5, Nov. 14, Dec. 1953.
10. Cowan, H.J., "Torsion of a Rectangular Elastic Isotropic Beam Reinforced with Rectangular Helices of Another Material" Applied Science Res., Vol. 3, Section A, The Hague, 1953.
11. Cowan, H.J., "The Theory of Torsion Applied to Reinforced Concrete Design" Civil Engineering and Public Works Review, London, Vol. 58, No. 567, 568, Sept-Oct 1953.





12. Cowan, H.J. and Armstrong, S., "Deformation of Concrete in Compression and Torsion" Civil Engineering and Public Works Review, London, Vol. 49, No. 580, Oct. 1954.
13. Cowan, H.J. and Armstrong, S., "Experiments on the Strength of Reinforced and Prestressed Concrete Beams and of Concrete Encased Steel Joists in Combined Bending and Torsion" Magazine of Concrete Research, Vol. 7, No. 19, March 1955.
14. Cowan H.J., "Torsion in Reinforced and Prestressed Concrete Beams" J. Inst. of Engineers, Australia, Vol. 28, No. 9., Sept. 1956.
15. Ernst, G.C., "Ultimate Torsional Properties of Rectangular Reinforced Concrete Beams" J. A.C.I., Vol. 29, No. 4, Oct. 1957.
16. Gardner, R.P.M., "The Behaviour of Prestressed Concrete I Beams Under Combined Bending and Torsion" Technical Report TRA 329, Cement and Concrete Association of Great Britain, 1960.
17. Humphreys, R., "Torsional Properties of Prestressed Concrete" The Structural Engineer, London, Vol. XXXV, No. 1, Jan. 1957.
18. Kemp, E.L., Sozen, M.A. and Siess, C.P. "Torsion in Reinforced Concrete" Civil Engineering Studies, Structural Research Series, No. 226, University of Illinois, Sept. 1961.
19. Marshall, W.T., and Tembe, N.R., "Experiments on Plain and Reinforced Concrete in Torsion" Structural Engineer, London, Vol. 19, No. 11, Nov. 1941.
20. Miyamoto, T., "Torsional Strength of Reinforced Concrete" Concrete and Constructional Engineering, Vol. 22, No. 11, Nov. 1927, London.
21. Morsch, E., "Concrete-Steel Construction" Engineering News Publishing Company, New York, 1909 (Originally published in Germany in 1904).
22. Nadai, A., "Plasticity" McGraw-Hill Book Co., New York, 1931.
23. Nylander, H., "Vridning och Vridningsinspanning vid Betongkonstruktioner" Statens Kommitte för Byggnadsforskning, Stockholm, Bulletin No. 3, 1945.
24. Pandit, G.S., "Ultimate Strength of Reinforced Concrete in Torsion" Cement and Concrete, New Delhi, July-Sept 1962. A summary of this paper appeared in the Journal, A.C.I., Proc. Vol. 60, April 1963.
25. Saint-Venant, B.de, Mem. Acad. Sci. Inst. Imperial de France, Series II, 14, 233, Paris, 1856.



26. Sokolnikoff, I.S., "Mathematical Theory of Elasticity" McGraw Hill Book Co., New York, 1956.
27. Southwell, R.V., "Relaxation Methods in Theoretical Physics" First Ed., Vol. 1, Oxford University Press, London, 1946.
28. Timoshenko, S., "Strength of Materials" Part I, D. Van Nostrand Co., New York, 1930.
29. Tomoshenko, S. and Goodier, J.N., "Theory of Elasticity" McGraw Hill Book Co., Second Edition 1951.
30. Turner, L and Davies, V.C., "Plain and Reinforced Concrete in Torsion, with Particular Reference to Reinforced Concrete Beams" The Inst. of Civil Engineers, London, Selected Engineering Papers No. 165, 1934.
31. Young, C.R., Sagar, W.L. and Hughes, C.A., "Torsional Strength of Rectangular Sections of Concrete, Plain and Reinforced" University of Toronto, School of Engineering, Bulletin No. 9, 1922.
32. Zia, P., "Torsional Strength of Prestressed Concrete Members" Journal A.C.I., Vol. 32, No. 10, April 1961.



## APPENDIX A

ELASTIC THEORYA-1 Circular Section

It was Coulomb who first presented correctly the theory of torsion for prismatic members of circular section in the year 1787. This classical solution is quite simple because there is no longitudinal warping of the cross-sections. The stress and consequently the strain are proportional to the distance from the axis of the prism, varying from nothing at the centre to maximum at the surface of the prism. The solution for circular section can be expressed by the Equations:

$$\frac{T}{J} = \frac{\tau}{r} = G.\theta \quad (A.1)$$

where:

T = The twisting moment

J = Polar moment of inertia =  $\frac{\pi R^4}{2}$

$\tau$  = Shear stress at any point distant r from axis

r = Distance from axis

G = Modulus of elasticity in shear

$\theta$  = Angle of twist per unit length of the prism

Equation (A.1) is also applicable to the closed hollow circular prism but the polar moment of inertia of the section is given by:



$$J = \frac{\pi}{2} (R_1^4 - R_2^4) \quad (A.2)$$

where:

$R_1$  = External radius of section

$R_2$  = Internal radius of section

## A-2 Non-circular Section

Following the lead taken by Coulomb, Navier, Poisson and Cauchy investigated the theory of torsion for homogeneous prisms of non-circular section. Assuming that the cross-sections of the bar remain plane and rotate without any distortion, Navier arrived at the erroneous conclusions that, for a given torque the angle of twist of bars is inversely proportional to the centroidal polar moment of inertia of the cross-section and that the maximum shearing stress occurs at the points most remote from the centroid of the cross-section. The above assumption is in contradiction with the boundary conditions. Similarly, Cauchy published a theory of torsion for rectangular sections in 1828. His theory was also incorrect since he failed to consider the warping of cross-sections.

The correct solution of the problem of torsion of prismatic bars by couples applied at the ends was given by Saint Venant. In his so-called 'semi-inverse method', Saint Venant assumed certain deformation of the twisted prism. He then showed that with this assumed deformation, he could satisfy the equations of equilibrium (A.3) and the boundary conditions (A.4) given below:

The Equations of equilibrium of an infinitesimal element, sides  $\delta x$ ,  $\delta y$  and  $\delta z$ , of homogeneous isotropic and elastic material, are: (see FIGURE A.1)





$$\begin{aligned}
\frac{\partial \sigma_x}{\partial x} + \frac{\partial \tau_{xy}}{\partial y} + \frac{\partial \tau_{xz}}{\partial z} + X &= 0 \\
\frac{\partial \sigma_y}{\partial y} + \frac{\partial \tau_{xy}}{\partial x} + \frac{\partial \tau_{yz}}{\partial z} + Y &= 0 \\
\frac{\partial \sigma_z}{\partial z} + \frac{\partial \tau_{xz}}{\partial x} + \frac{\partial \tau_{yz}}{\partial y} + Z &= 0
\end{aligned} \tag{A.3}$$

where

$\sigma_x$ ,  $\sigma_y$  and  $\sigma_z$  are normal stresses in x, y and z co-ordinate directions.

$\tau_{xy}$ ,  $\tau_{yz}$  and  $\tau_{xz}$  are the shears on the faces of the element and

X, Y and Z are the components of the body forces in the three co-ordinate directions.

The boundary conditions are: (see FIGURE A.2)

$$\begin{aligned}
\bar{X} &= \sigma_{x \cdot l} + \tau_{xy \cdot m} + \tau_{xz \cdot n} \\
\bar{Y} &= \sigma_{y \cdot m} + \tau_{yz \cdot n} + \tau_{xy \cdot l} \\
\bar{Z} &= \sigma_{z \cdot n} + \tau_{xz \cdot l} + \tau_{yz \cdot m}
\end{aligned} \tag{A.4}$$

in which,

l, m and n are the direction cosines of the external normal to the surface of the body at the point under consideration and

$\bar{X}$ ,  $\bar{Y}$  and  $\bar{Z}$  are the components of the surface forces per unit area at this point.



Since the assumptions made by Saint Venant satisfy the fundamental Equations of equilibrium and the boundary conditions, then it follows from the uniqueness of the solutions of elasticity Equations that the assumptions made are correct.

Saint Venant assumed that the deformation of twisted prism could be split into two parts:

- (i) Rotations of the cross-sections as for a circular prism.
- (ii) Warping of the cross-sections which is the same for all cross-sections.

Taking the origin of co-ordinates in an end-section (FIGURE A.3), the displacements in the x and y directions respectively are

$$u = -\theta.z.y, \quad v = \theta.z.x. \quad (A.5)$$

where  $\theta z$  is the angle of rotation of the cross-section at a distance  $z$  from the origin.

The longitudinal warping of the cross-sections is defined by the function

$$w = \theta.\psi(x,y) \quad (A.6)$$

where  $w$  is the displacement in the  $z$ -direction and  $\psi$  is a function of  $x$  and  $y$  only.

The unit elongations and the unit shearing strains in the three co-ordinate directions may be expressed by the symbols:  $\epsilon_x$ ,  $\epsilon_y$ ,  $\epsilon_z$ ,  $\gamma_{xy}$ ,  $\gamma_{xz}$  and  $\gamma_{yz}$ . They are related to the displacements  $u$ ,  $v$  and  $w$  by the Equations:



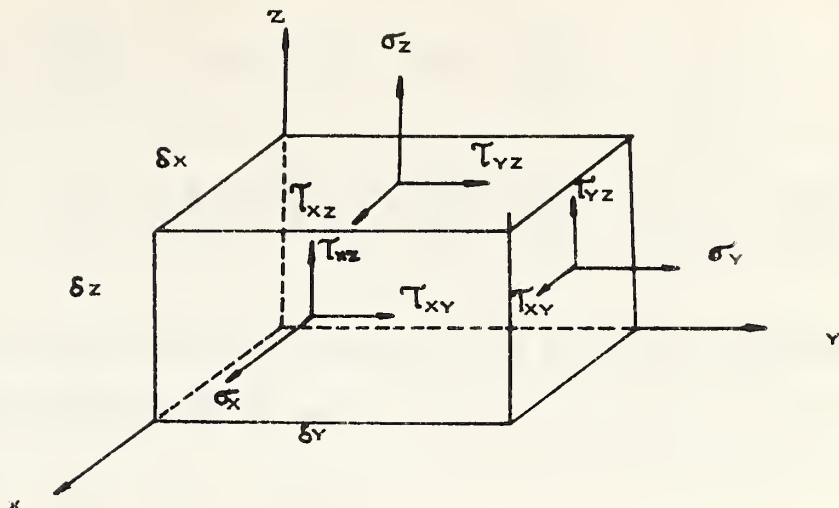


FIGURE A.1. STRESSES ON AN INFINITESIMAL ELEMENT.

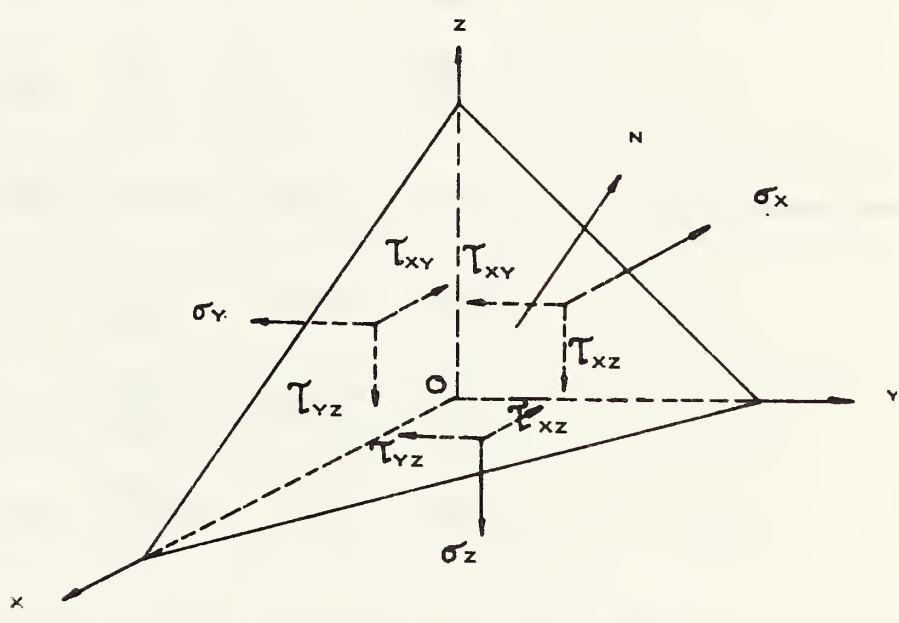


FIGURE A.2 STRESSES ON A TETRAHEDRON.

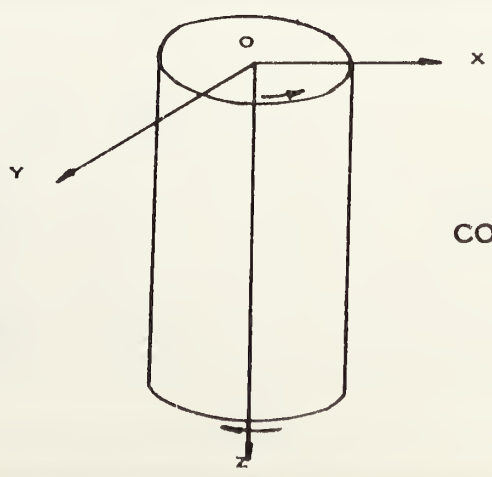


FIGURE A.3  
CO - ORDINATE SYSTEM.





$$\varepsilon_x = \frac{\partial u}{\partial x}, \quad \varepsilon_y = \frac{\partial v}{\partial y}, \quad \varepsilon_z = \frac{\partial w}{\partial z}$$

(A.7)

$$\gamma_{xy} = \frac{\partial u}{\partial y} + \frac{\partial v}{\partial x}, \quad \gamma_{xz} = \frac{\partial u}{\partial z} + \frac{\partial w}{\partial x}, \quad \gamma_{yz} = \frac{\partial v}{\partial z} + \frac{\partial w}{\partial y}$$

From the assumed displacements (A.5) and (A.6), the components of strain from Equations (A.7) are:

$$\varepsilon_x = \varepsilon_y = \varepsilon_z = \gamma_{xy} = 0$$

$$\gamma_{xz} = \frac{\partial w}{\partial x} + \frac{\partial u}{\partial z} = \theta \left( \frac{\partial \psi}{\partial x} - y \right) \quad (\text{A.8})$$

$$\gamma_{yz} = \frac{\partial w}{\partial y} + \frac{\partial v}{\partial z} = \theta \left( \frac{\partial \psi}{\partial y} + x \right)$$

The Equations connecting the strains to the stresses are:

$$\begin{aligned} \varepsilon_x &= \frac{1}{E} \left[ \sigma_x - \mu (\sigma_y + \sigma_z) \right] \\ \varepsilon_y &= \frac{1}{E} \left[ \sigma_y - \mu (\sigma_x + \sigma_z) \right] \\ \varepsilon_z &= \frac{1}{E} \left[ \sigma_z - \mu (\sigma_x + \sigma_y) \right] \end{aligned} \quad (\text{A.9})$$

$$\gamma_{xy} = \frac{1}{G} \tau_{xy}, \quad \gamma_{yz} = \frac{1}{G} \tau_{yz}, \quad \gamma_{xz} = \frac{1}{G} \tau_{xz} \quad (\text{A.10})$$

Using Equations (A.8), (A.9) and (A.10), the stresses are found as:

$$\begin{aligned} \sigma_x &= \sigma_y = \sigma_z = \tau_{xy} = 0 \\ \tau_{xz} &= G\theta \left( \frac{\partial \psi}{\partial x} - y \right) \\ \tau_{yz} &= G\theta \left( \frac{\partial \psi}{\partial y} + x \right) \end{aligned} \quad (\text{A.11})$$



Thus the assumed deformations (A.5) and (A.6) lead to no normal stresses between the longitudinal fibres or along them since all normal stresses vanish. There is also no deformation in the planes of the cross-sections since  $\epsilon_x$ ,  $\epsilon_y$  and  $\gamma_{xy}$  vanish. There is pure shear at each point defined by the components  $\tau_{xz}$  and  $\tau_{yz}$ .

Substituting from Equations (A.11) into Equations of equilibrium (A.3) and ignoring the body forces leads to the two dimensional Laplace Equation:

$$\frac{\partial^2 \psi}{\partial x^2} + \frac{\partial^2 \psi}{\partial y^2} = 0 \quad (\text{A.12})$$

The lateral surface of the bar is free from external forces and has normals perpendicular to the z-axis. Hence for the lateral surface:

$$\bar{X} = \bar{Y} = \bar{Z} = 0 \quad \text{and} \quad \cos(N_z) = n = 0 \quad (\text{A.13})$$

Using Equations (A.13), the first two of the boundary conditions (A.4) are identically satisfied. The third condition gives:

$$\tau_{xz} \cdot l + \tau_{yz} \cdot m = 0 \quad (\text{A.14})$$

From Equation (A.14) it follows that the resultant shearing stress at the boundary is directed along the tangent to the boundary (FIGURE A.4). Considering an infinitesimal element ABC at the boundary and assuming that s is increasing in the direction from C to A

$$\begin{aligned} l &= \cos(N_x) = \frac{dy}{ds} \\ m &= \cos(N_y) = -\frac{dx}{ds} \end{aligned} \quad (\text{A.15})$$



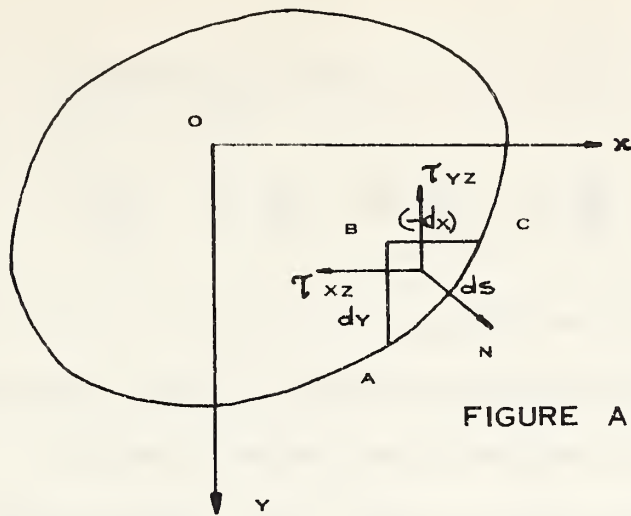


FIGURE A.4. BOUNDARY ELEMENT.

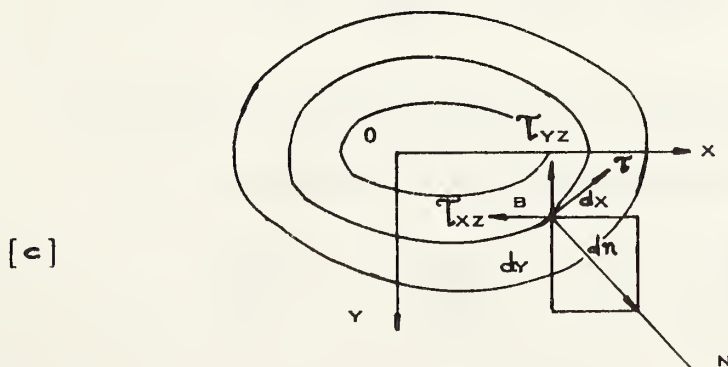
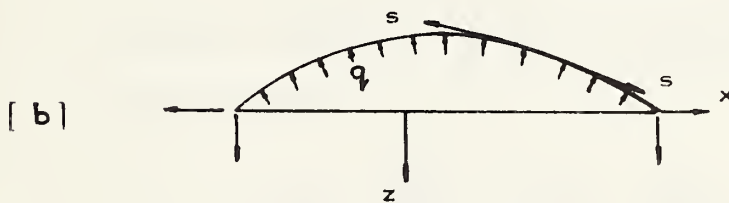
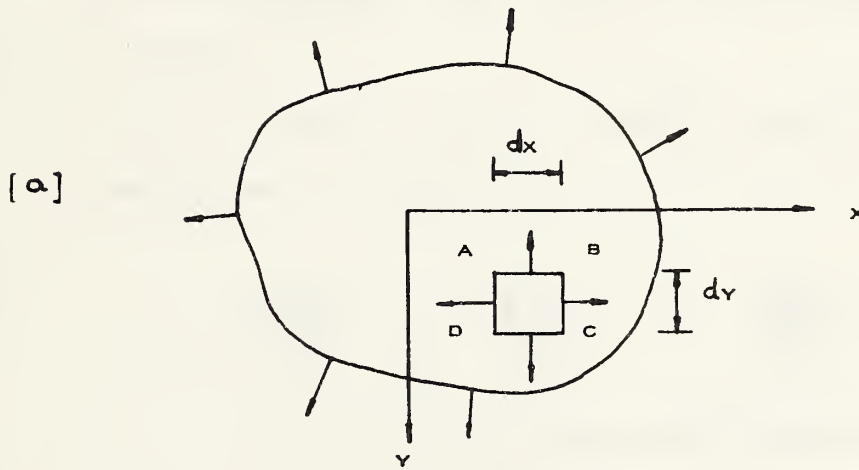
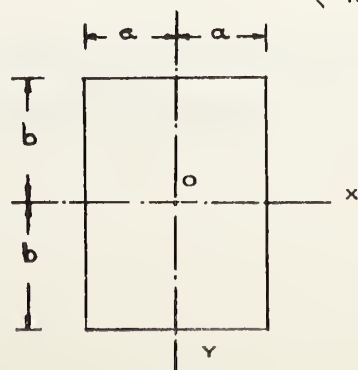


FIGURE A.5 MEMBRANE ANALOGY.

FIGURE A.6  
RECTANGULAR SECTION.



Substituting from (A.11) and (A.15), the Equation (A.14)

gives:

$$\left( \frac{\partial \psi}{\partial x} - y \right) \frac{dy}{ds} - \left( \frac{\partial \psi}{\partial y} + x \right) \frac{dx}{ds} = 0 \quad (\text{A.16})$$

Thus any solution of the torsion problem must satisfy the two-dimensional Laplace Equation (A.12) and the boundary condition (A.16).

It was L. Prandtl who introduced the stress function  $\phi$  into the torsion problem. This leads to simpler boundary condition as compared to (A.16).

Since  $\sigma_x$ ,  $\sigma_y$ ,  $\sigma_z$  and  $\tau_{xy}$  vanish, the Equations of equilibrium (A.3) reduce to:

$$\frac{\partial \tau_{xz}}{\partial z} = 0, \quad \frac{\partial \tau_{yz}}{\partial z} = 0, \quad \frac{\partial \tau_{xz}}{\partial x} + \frac{\partial \tau_{yz}}{\partial y} = 0 \quad (\text{A.17})$$

The first two are identically satisfied since  $\tau_{xz}$  and  $\tau_{yz}$ , as given by Equations (A.11), are independent of  $z$ . The third Equation is satisfied if

$$\tau_{xz} = \frac{\partial \phi}{\partial y} \quad \text{and} \quad \tau_{yz} = -\frac{\partial \phi}{\partial x} \quad (\text{A.18})$$

where  $\phi$ , the stress function, is a function of  $x$  and  $y$ .

From Equations (A.11), Equations (A.18) give:

$$\frac{\partial \phi}{\partial y} = G\theta \left( \frac{\partial \psi}{\partial x} - y \right), \quad -\frac{\partial \phi}{\partial x} = G\theta \left( \frac{\partial \psi}{\partial y} + x \right) \quad (\text{A.19})$$

Eliminating  $\psi$  from Equations (A.19) leads to the second order partial differential Equation:





$$\frac{\partial^2 \phi}{\partial x^2} + \frac{\partial^2 \phi}{\partial y^2} = -2G \cdot \theta \quad (\text{A.20})$$

The boundary condition (A.14) gives on substituting from (A.15) and (A.18)

$$\frac{\partial \phi}{\partial y} \cdot \frac{dy}{ds} + \frac{\partial \phi}{\partial x} \cdot \frac{dx}{ds} = \frac{d\phi}{ds} = 0 \quad (\text{A.21})$$

Equations (A.21) show that the stress function  $\phi$  must be constant along the boundary of the cross-section. In the case of singly connected boundaries, this constant can be chosen arbitrarily and is generally assumed zero. Then the solution of the torsion problem reduces to finding the stress function  $\phi$  which satisfies equation (A.20) and is zero everywhere on the boundary.

The normals to the end cross-sections are parallel to the z-axis, hence for any point on the end cross-section,

$$l = m = 0, \quad n = \pm 1 \quad (\text{A.22})$$

Hence Equations (A.4) become:

$$\bar{X} = \pm \tau_{xz}, \quad \bar{Y} = \pm \tau_{yz} \quad (\text{A.23})$$

in which the positive sign refers to the end of the bar on which the external normal points in the positive z direction, i.e. lower face in FIGURE A.3. Hence on the end sections, the shearing forces are distributed in the same manner as the shearing stresses over any other cross-section of the bar. These shearing forces give rise to a torque. Substituting from Equations (A.18) into Equations (A.23) and noting that  $\phi$  is zero over



the boundary:

$$\iint \bar{X} \, dx dy = \iint \tau_{xz} \, dx dy = \iint \frac{\partial \phi}{\partial y} \, dx dy = \int dx \int \frac{\partial \phi}{\partial y} \, dy = 0 \quad (\text{A.24})$$

$$\iint \bar{Y} \, dx dy = \iint \tau_{yz} \, dx dy = -\iint \frac{\partial \phi}{\partial x} \, dx dy = -\int dy \int \frac{\partial \phi}{\partial x} \, dx = 0$$

Thus the resultant of forces over the ends of the bar is zero. The forces actually form a couple:

$$T = \iint (\bar{Y}x - \bar{X}y) \, dx \, dy = -\iint \frac{\partial \phi}{\partial x} x \, dx dy - \iint \frac{\partial \phi}{\partial y} y \, dx dy \quad (\text{A.25})$$

Integrating (A.25) by parts leads to, since  $\phi = 0$  at boundary

$$T = 2 \iint \phi \, dx dy \quad (\text{A.26})$$

Each term of the last member of Equations (A.25) contributes one half of the torque. One half of the torque is due to  $\tau_{xz}$  and the other half due to  $\tau_{yz}$ .

The assumed displacements (A.5) lead to a stress distribution which satisfies the equations of equilibrium (A.3), leaves the lateral surface of the bar free from external forces and produces end torque given by (A.26). The compatibility conditions need not be considered since the stresses have been derived from the displacements (A.5). The solution is exact, since all Equations of elasticity are satisfied.

The solution is rigorous only if the forces at ends of bar are distributed in a definite manner. From Saint Venant's principle, the stresses in a long twisted bar at a sufficient distance from the ends depend only on the resultant torque  $T$  and are practically independent of the mode of distribution of end forces.



The foregoing results of the elastic theory can be summarised as follows:

Corresponding to the simple Equation for circular section:

$$\frac{M}{J} = \frac{\tau}{r} = G.\theta$$

the Equation for non-circular section is:

$$\frac{T}{K} = \frac{\tau}{R} = G.\theta \quad (\text{A.27})$$

where  $K$  called the Torsion-constant replaces the polar moment of inertia  $J$  and  $R$  called the stress-factor replaces  $r$ , the distance from the axis of the circular section. The torsion constant  $K$  is given by the Equation:

$$K = 2 \iint \xi \, dx dy \quad (\text{A.28})$$

and the stress-factor  $R$  is given by the Equations:

$$R = \frac{\partial \xi}{\partial n} = \text{grad } \xi \quad (\text{A.29})$$

where

$$\xi = \frac{\phi}{G.\theta} \quad (\text{A.30})$$

$\phi$  being the stress-function.

The torsion problem leads to the partial differential Equation:

$$\frac{\partial^2 \phi}{\partial x^2} + \frac{\partial^2 \phi}{\partial y^2} = -2 G\theta \quad (\text{A.31})$$

or

$$\frac{\partial^2 \xi}{\partial x^2} + \frac{\partial^2 \xi}{\partial y^2} = -2$$



and the component shear stresses are given by:

$$\tau_{xz} = G\theta \cdot \frac{\partial \xi}{\partial y} = \frac{\partial \phi}{\partial y} \quad (\text{A.32})$$

$$\tau_{yz} = -G\theta \cdot \frac{\partial \xi}{\partial x} = -\frac{\partial \phi}{\partial x}$$

The boundary condition for  $\phi$  or  $\xi$  is:

$$\frac{d\phi}{ds} = \frac{d\xi}{ds} = 0 \quad (\text{A.33})$$

i.e. the functions  $\phi$  and  $\xi$  are constants along the boundary.

Using Equations (A.27) and (A.28)

$$T = G\theta K = 2 G\theta \iint \xi \, dx dy = 2 \iint \phi \, dx dy \quad (\text{A.34})$$

### A.3 Membrane Analogy

This analogy was introduced by L. Prandtl. FIGURE A.5 shows a homogeneous membrane supported at the edges of an opening of exactly the same shape as the cross-section of the twisted bar. The membrane is inflated slightly by a small pressure differential. The equilibrium is maintained by uniform tensile stresses throughout the membrane.

If  $S$  is the uniform tension per unit length of the boundary, the downward component of the tensile forces on the sides AD and BC of an infinitesimal element ABCD is  $-S(\frac{\partial^2 z}{\partial x^2}) dx dy$ . The other two sides of the element similarly give a downward component  $-S(\frac{\partial^2 z}{\partial y^2}) dx dy$ . Hence if  $q$  is the pressure differential, the Equation of equilibrium of the element is:

$$S \frac{\partial^2 z}{\partial x^2} dx dy + S \frac{\partial^2 z}{\partial y^2} dx dy + q \cdot dx dy = 0$$

$$\text{hence} \quad \frac{\partial^2 z}{\partial x^2} + \frac{\partial^2 z}{\partial y^2} = -\frac{q}{S} \quad (\text{A.35})$$





This Equation is of the same form as Equation (A.20) for the torsion problem. The elevation of the membrane  $z$  is analogous to the stress function  $\phi$  if the quantity  $q/S$  is replaced by  $2G\theta$ . The elevation of the membrane at the boundary is zero. This is analogous to the boundary condition (A.21).

The deflection surface of the membrane can be represented by contours. The deflection is same along any one contour:

$$\frac{\partial z}{\partial s} = 0 \quad (\text{A.36})$$

The corresponding Equation for the stress function  $\phi$  is:

$$\frac{\partial \phi}{\partial s} = \left( \frac{\partial \phi}{\partial y} \cdot \frac{dy}{ds} + \frac{\partial \phi}{\partial x} \cdot \frac{dx}{ds} \right) = \tau_{xz} \cdot \frac{dy}{ds} - \tau_{yz} \cdot \frac{dx}{ds} = 0 \quad (\text{A.37})$$

Equations (A.37) indicate that the projection of the resultant shearing stress at a point  $A$  on the normal  $N$  to the contour passing through  $A$  is zero. It means that the shearing stress at the point  $A$  is in the direction of the tangent to the contour through this point. Curves whose tangents point in the direction of resultant shear are called lines of shearing stress. Hence the contours of the membrane are lines of shearing stress.

The resultant shear stress  $\tau$  at  $A$  is obtained by projecting the stress components  $\tau_{xz}$  and  $\tau_{yz}$  on the tangent to the contour:

$$\tau = \tau_{yz} \cos (Nx) - \tau_{xz} \cos (Ny)$$

Substituting

$$\tau_{xz} = \frac{\partial \phi}{\partial y}, \quad \tau_{yz} = -\frac{\partial \phi}{\partial x}, \quad \cos (Nx) = \frac{dx}{dn}, \quad \cos (Ny) = \frac{dy}{dn}$$

$$\tau = - \left( \frac{\partial \phi}{\partial x} \cdot \frac{dx}{dn} + \frac{\partial \phi}{\partial y} \cdot \frac{dy}{dn} \right) = - \frac{d\phi}{dn} \quad (\text{A.38})$$



Hence the resultant shear stress at any point is given by the maximum slope of the membrane at this point.

Quantitative results can be obtained from direct measurements of the geometry of the membrane. Since exact solution for the circular section is known, the results for non-circular section can be obtained by comparison of membranes over a circular and non-circular opening when both membranes are submitted to the same pressure differential. The membrane analogy is also extremely useful for obtaining quick qualitative results.

The important conclusions of the membrane analogy are:

- (i) The stress function  $\phi$  is analogous to the elevation of the membrane  $z$ .
- (ii) The lines of shearing stress are the same as the contours of the membrane.
- (iii) The magnitude of resultant shear is analogous to the maximum slope of the membrane. The maximum shear acts at points where the contour lines are closest.
- (iv) From Equation (A.26), it can be concluded that double the volume under the membrane represents the twisting moment if  $q/s$  is replaced by  $2G\theta$ .

#### A.4 Rectangular Section

Using the membrane analogy, the deflections of the uniformly loaded rectangular membrane, shown in FIGURE A.6 must satisfy the differential Equation:

$$\frac{\partial^2 z}{\partial x^2} + \frac{\partial^2 z}{\partial y^2} = -q/s \quad (\text{A.35})$$



and should be zero at the boundary.

The series function:

$$z = \sum_{n=1,3,5,\dots}^{\infty} b_n \cos \frac{n\pi x}{2a} Y_n \quad (\text{A.39})$$

in which  $b_1, b_3, \dots$  are constants and  $Y_1, Y_2, \dots$  are functions of  $y$  only, satisfies the condition of symmetry with respect to  $y$ -axis and vanishes on the sides  $x = \pm a$ .

Substituting from (A.39) into (A.35) and expanding the right member of (A.35) into an infinite series, the condition of symmetry with respect to  $x$ -axis and the boundary condition on the edges  $y = \pm b$  give:

$$Y_n = \frac{16qa^2}{s \cdot n^3 \pi^3 b_n} (-1)^{\frac{n-1}{2}} \left[ 1 - \frac{\cosh (n\pi y/2a)}{\cosh (n\pi b/2a)} \right] \quad (\text{A.40})$$

Substituting in (A.39), the general expression for deflection becomes:

$$z = \frac{16qa^2}{s\pi^3} \sum_{n=1,3,5,\dots}^{\infty} \frac{1}{n^3} (-1)^{\frac{n-1}{2}} \left[ 1 - \frac{\cosh (n\pi y/2a)}{\cosh (n\pi b/2a)} \right]$$

$$\cos \frac{n\pi x}{2a} \quad (\text{A.41})$$

Replacing  $q/s$  by  $2G\theta$ , the stress function  $\phi$  is obtained:

THE UNIVERSITY OF CHICAGO  
LIBRARY

THE UNIVERSITY OF CHICAGO  
LIBRARY  
1207 EAST 58TH STREET  
CHICAGO, ILL. 60637  
TEL. 773-936-5000  
FAX 773-936-5001  
WWW.CHICAGO.LIBRARY.EDU

THE UNIVERSITY OF CHICAGO  
LIBRARY  
1207 EAST 58TH STREET  
CHICAGO, ILL. 60637  
TEL. 773-936-5000  
FAX 773-936-5001  
WWW.CHICAGO.LIBRARY.EDU

THE UNIVERSITY OF CHICAGO  
LIBRARY  
1207 EAST 58TH STREET  
CHICAGO, ILL. 60637  
TEL. 773-936-5000  
FAX 773-936-5001  
WWW.CHICAGO.LIBRARY.EDU

$$\phi = \frac{32G\theta a^2}{\pi^3} \sum_{n=1,3,5,\dots}^{\infty} \frac{1}{n^3} (-1)^{\frac{n-1}{2}} \left[ 1 - \frac{\cosh (n\pi y/2a)}{\cosh (n\pi b/2a)} \right] \cos \frac{n\pi x}{2a} \quad (\text{A.42})$$

The stress components are obtained by differentiation:

$$\tau_{yz} = -\frac{\partial \phi}{\partial x} = \frac{16G\theta a}{\pi^2} \sum_{n=1,3,5,\dots}^{\infty} \frac{1}{n^2} (-1)^{\frac{n-1}{2}} \left[ 1 - \frac{\cosh (n\pi y/2a)}{\cosh (n\pi b/2a)} \right] \sin \frac{n\pi x}{2a} \quad (\text{A.43})$$

For  $b > a$ , the maximum shear stress occurs at the middle of the long sides

$x = \pm a$ . Putting  $x = a$ ,  $y = 0$  in Equation (A.43) gives:

$$\tau_{\max} = 2G\theta a - \frac{16G\theta a}{\pi^2} \sum_{n=1,3,5,\dots}^{\infty} \frac{1}{n^2 \cosh (n\pi b/2a)} \quad (\text{A.44})$$

The infinite series on the right is rapidly convergent. For the square section, ( $a=b$ ):

$$\tau_{\max} = 1.351 G \cdot \theta \cdot a \quad (\text{A.45})$$

In general,

$$\tau_{\max} = k \cdot 2G\theta a \quad (\text{A.46})$$

in which  $k$  is a number whose value depends upon the ratio  $b/a$

(see TABLE A.1).





The twisting moment is obtained by integration of the stress function  $\phi$ :

$$\begin{aligned}
 T &= 2 \int_{-a}^a \int_{-b}^b \phi \, dx dy. \\
 &= \frac{1}{3} G\theta (2a)^3 (2b) \left[ 1 - \frac{192}{\pi^5} \frac{a}{b} \sum_{n=1,3,5}^{\infty} \frac{1}{n^5} \tanh \frac{n\pi b}{2a} \right] \quad (A.47)
 \end{aligned}$$

The series on the right converges rapidly. For a square section, ( $a=b$ ):

$$T = 0.1406 G\theta (2a)^4 \quad (A.48)$$

In general, the torque can be represented by the Equation:

$$T = k_1 G\theta (2a)^3 (2b) \quad (A.49)$$

where  $k_1$  is a number whose value depends upon the ratio  $b/a$  (see TABLE A.1).

Eliminating  $\theta$  from Equations (A.46) and (A.49):

$$\tau_{\max} = \frac{T}{k_2 (2a)^2 (2b)} \quad (A.50)$$

where  $k_2 = k_1/k$ . (see TABLE A.1).

THE UNIVERSITY OF CHICAGO

1917

John C. ...

...

...

...

...

...

...

...

...

TABLE A.1  
TABLE OF CONSTANTS

b/a	k	k <sub>1</sub>	k <sub>2</sub>	b/a	k	k <sub>1</sub>	k <sub>2</sub>
1.0	0.675	0.1406	0.208	3	0.985	0.263	0.267
1.2	0.759	0.166	0.219	4	0.997	0.281	0.282
1.5	0.848	0.196	0.231	5	0.999	0.291	0.291
2.0	0.930	0.229	0.246	10	1.000	0.312	0.312
2.5	0.968	0.249	0.258	$\infty$	1.000	0.333	0.333

From the above theory or by considering the Geometry of the analogous membrane, some interesting conclusions may be drawn. For example, it may be seen that for a given cross-sectional area, the square section has the greatest torsional stiffness and that the torsional stiffness of a 'T' or 'L' section is approximately equal to the sum of the torsional stiffnesses of the component rectangles.



## APPENDIX B

PLASTIC THEORYB-1 Circular Section

The elastic torsional resistance moment of a circular section of radius  $R$  is:

$$T_E = \int_0^R 2\pi r \cdot \tau_{\max} \left( \frac{r}{R} \right) r \, dr = \frac{1}{2} \pi R^3 \cdot \tau_{\max} \quad (B.1)$$

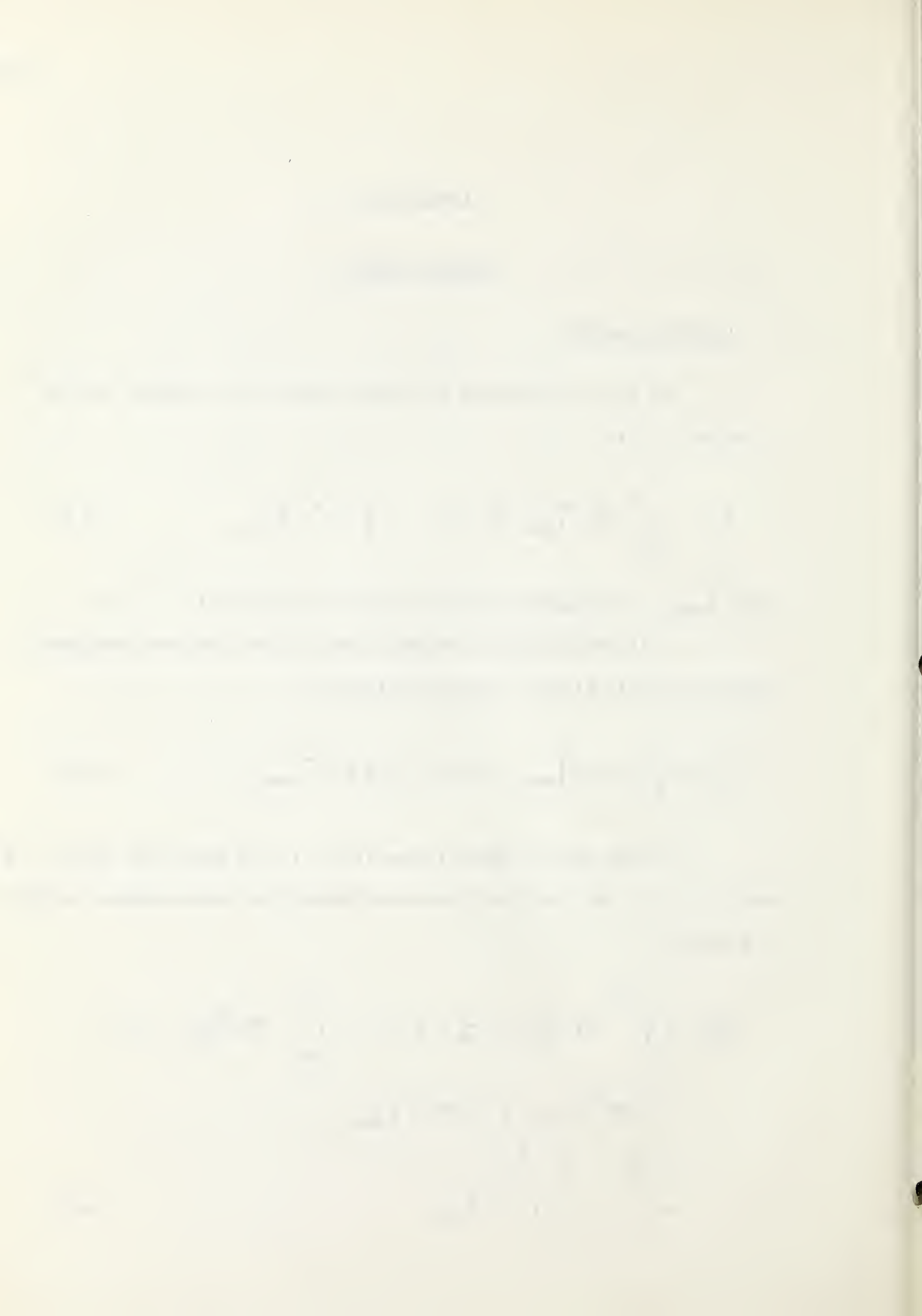
where  $\tau_{\max}$  is the maximum shear stress in the material.

If the whole section becomes plastic, the torsional resistance moment of a fully plastic circular section is:

$$T_P = \int_0^R 2\pi r \cdot \tau_{\max} \cdot r \, dr = \frac{2}{3} \pi R^3 \cdot \tau_{\max} \quad (B.2)$$

For the case of partial plasticity, if the plasticity ratio  $= \epsilon$  and  $e = 1 - \epsilon$ , the torsional resistance moment for elasto-plastic section is given by:

$$\begin{aligned} T_{EP} &= \int_0^{eR} 2\pi r \cdot \tau_{\max} \left( \frac{r}{eR} \right) r \, dr + \int_{eR}^R 2\pi r \tau_{\max} \cdot r \, dr \\ &= \frac{2}{3} \pi R^3 \tau_{\max} - \frac{1}{6} \pi (eR)^3 \cdot \tau_{\max} \\ &= T_P - \frac{1}{4} e^3 T_P \\ &= T_P - \frac{1}{4} (1 - \epsilon)^3 T_P \end{aligned} \quad (B.3)$$



From Equation (B.3), it is noted that for plasticity ratio greater than  $1/2$ , the resisting torque of the partially plastic section  $T_{EP}$  is of the same order as fully plastic resisting torque  $T_p$ . For  $\epsilon = 1/2$ ,  $T_{EP} = \frac{31}{32} T_p$ . Also see TABLE B.1.

TABLE B.1

RATIO OF ELASTO-PLASTIC TO PLASTIC RESISTING  
TORQUE FOR VARIOUS VALUES OF PLASTICITY RATIO

$\epsilon$	0	0.1	0.2	0.3	0.4	0.5	0.6	0.7	0.8	0.9	1.0
$\frac{T_{EP}}{T_p}$	0.75	0.818	0.872	0.914	0.946	0.969	0.984	0.994	0.998	1.0	1.0

## B-2 Non-circular Section

The assumption of full plasticity implies constant shear stress throughout the section. Thus:

$$\sqrt{[\tau_{xz}^2 + \tau_{yz}^2]} = \text{Constant} \quad (\text{B.4})$$

Also,

$$\begin{aligned} \tau_{xz} &= \partial \phi_p / \partial y \\ \tau_{yz} &= -\partial \phi_p / \partial x \end{aligned} \quad (\text{B.5})$$

where  $\phi_p$  is the plastic stress function. From Equations (B.4) and (B.5):

$$\sqrt{\left[\left(\frac{\partial \phi_p}{\partial x}\right)^2 + \left(\frac{\partial \phi_p}{\partial y}\right)^2\right]} = \left| \text{Grad } \phi_p \right| = \text{Constant} \quad (\text{B.6})$$

which indicates that the plastic stress function  $\phi_p$  has constant slope.





### B-3 Sand Heap Analogy

From Equation (B.6), it is evident that the plastic stress function  $\phi_p$  can be represented by a surface of constant slope. Nadai suggested the analogy of sand heap. Since,

$$T_p = 2 \iint \phi_p \, dx dy \quad (B.7)$$

the volume of sand, that may be heaped on a level plate of the same shape as the cross-section under consideration, will represent the ultimate torque. For a rectangular section of width  $b$  and depth  $d$ , the volume of sand heap is  $\frac{1}{4} s b^2 (d - \frac{1}{3} b)$  where  $s$  is the constant slope of the sand heap. Replacing  $s$  by the maximum shear stress  $\tau_{\max}$ , the ultimate torque:

$$T_p = \frac{1}{2} b^2 (d - \frac{1}{3} b) \tau_{\max} \quad (B.8)$$

There is no simple analytical solution for the problem of partial plasticity of non-circular sections. The membrane analogy may, however, be extended to the case of partial plasticity. The portion of the membrane corresponding to the plastic zone of the cross-section should have constant slope. This may be done by erecting a roof of constant slope over an opening representing the cross-section and inflating the membrane till it touches the roof to the desired extent. The portion of the membrane which touches the roof corresponds to the plastic zone whereas the remaining portion near the axis represents the elastic zone of the cross-section. Nadai performed some interesting experiments illustrating this theory.









Property of:  
DEPARTMENT OF CIVIL ENGINEERING  
UNIVERSITY of ALBERTA.



**B29812**